CHAPTER IV

RESULTS AND DISCUSSION

4.1 Physical Characteristic Study

The physical characteristics of bagasse (B) and bagasse fly ash (BFA) should be evaluated to determine the possibility of utilization. Many key parameters were determined in this study using material samples form local sugar factory in Saraburi province, Thailand. Selected constituents of materials used in theses investigations are presented as follow:

4.1.1 Bulk Specific Gravity

Bulk specific gravity can be used to preliminarily evaluate chemical compositions, noncombustible material, voids and fineness of the material. Moreover, it is significant in designing the mix proportion and unit weight of concrete. In Table 4.1, a comparison of bulk specific gravities of bagasse, bagasse fly ash, Portland cement, sand and crushed stone are tabulated. As Table 4.1 shows, the bulk specific gravity of bagasse was less than that of bagasse fly ash, 0.34 and 1.85 for bagasse and bagasse fly ash, respectively. The bulk specific gravity values of these materials are much lower than those of Portland cement, sand and crushed stone.

As Table 4.1 shows, the difference between materials may be due to chemical compositions. Bulk specific gravity of each constituent was different that is, Portland cement contains high CaO, Al_2O_3, and Fe_2O_3, which have high bulk specific gravity. On the other hand, SiO_2 with its low bulk specific gravity is the main component in bagasse and bagasse fly ash. The chemical compositions were shown in Table 4.4. In addition, it may be due to particle size, Rachakornkij (2000) revealed that the finer particle size was, the higher bulk specific gravity was for the material. The particle size of bagasse fly ash was smaller than that of bagasse as discussed in section 4.1.3.

Table 4.1 Bulk Specific Gravities of Bagasse, Bagasse Fly Ash, Portland Cement, Sand and Crushed Stone

Material	Bulk specific gravity
Bagasse	0.34
Bagasse fly ash	1.85
Portland cement	3.12-3.15
Sand	2.65
Crushed stone	2.70

4.1.2 Pore size, Porosity, and Specific Pore Volume

The pore sizes of bagasse and bagasse fly ash are shown in Table 4.2, that is 2031 Å (203 nm) and 774 Å (77 nm), respectively. The pores of material are generally classified into three groups; micropore (pore size < 2 nm), mesopore (2-50 nm), and macropore (> 50 nm) (Juang, et al., 2002). The pore sizes of the sampled bagasse and bagasse fly ash mostly lie in the macropore range.

Table 4.2 Pore size, Porosity, and Pore specific volume of Bagasse and Bagasse Fly Ash

Parameter	Bagasse	Bagasse Fly Ash
Pore size (Å)	2031.437	774.960
Porosity (%)	1.09	3.97
Pore specific volume (cm^3/g)	0.0222	0.0897

It can be seen in Table 4.2 that the porosity and specific pore volume of bagasse fly ash were higher than those of bagasse. Gupta and Ali (2000) treated bagasse fly ash from local sugar factory in India with hydrogen peroxide at 60°C for

24 h and washed with double-distilled water three times, after that they washed it with deionized water and dried at 100°C. They found that porosity of bagasse fly ash was 36%; which is more than that of the bagasse fly ash used in this study. However, the treatment process should take a lot of time and budget.

4.1.3 Particle Size Distribution

As mentioned in Sections 3.1.1 and 3.1.2, bagasse was ground to 200 μm fineness while bagasse fly ash was sieved to the desired particle size of 150 μm. The particle size distributions of bagasse and bagasse fly ash were shown in Figures 4.1 and 4.2, respectively. Table 4.3 showing particle size of materials, indicated that the fineness of material was available size according to designed.

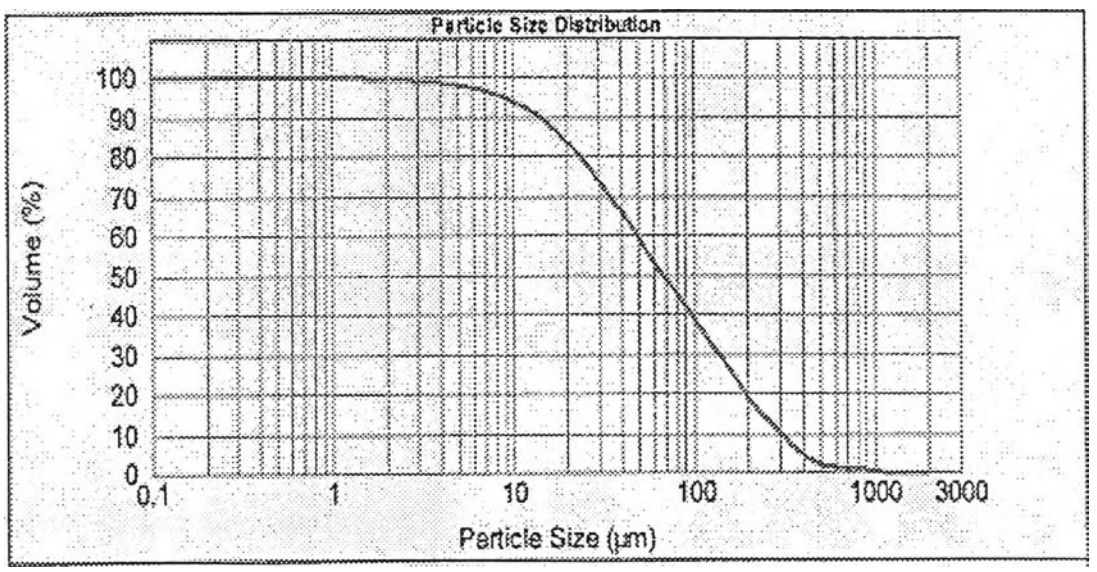

Figure 4.1 Particle Size Distribution of Bagasse

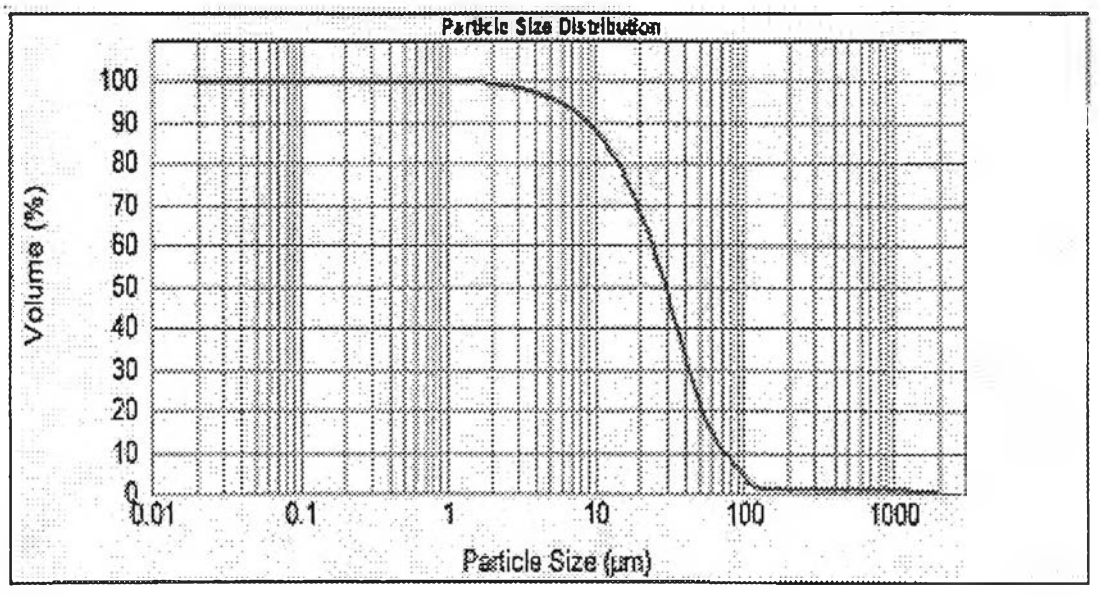

Figure 4.2 Particle Size Distribution of Bagasse Fly Ash

Table 4.3 Particle Sizes of Bagasse and Bagasse Fly Ash

Material	**$d_{50\%}$ (microns)**	**$d_{90\%}$ (microns)**
Bagasse	65.730	301.003
Bagasse fly ash	30.586	69.135

4.1.4 Specific Surface Area

Form BET analysis results, the surface area of bagasse fly ash is higher than that of bagasse, 52.80 and 4.81 m^2/g for bagasse fly ash and bagasse, respectively. Thus, it is expected that the adsorption of Pb(II) and Cr(VI) will be higher on bagasse fly ash than that of bagasse.

4.1.5 Morphology

Figure 4.3 showing SEM photographs clearly revealed the surface texture and different levels of porosity of the material under study. It was evident that the particles of both materials are in the form of non-spherical particles. For bagasse, SEM photograph showed that the acidic condition treatment can developed porosity on the surface. Untreated bagasse is shown in Figure 4.4, pore on surface was lower than that of treated bagasse.

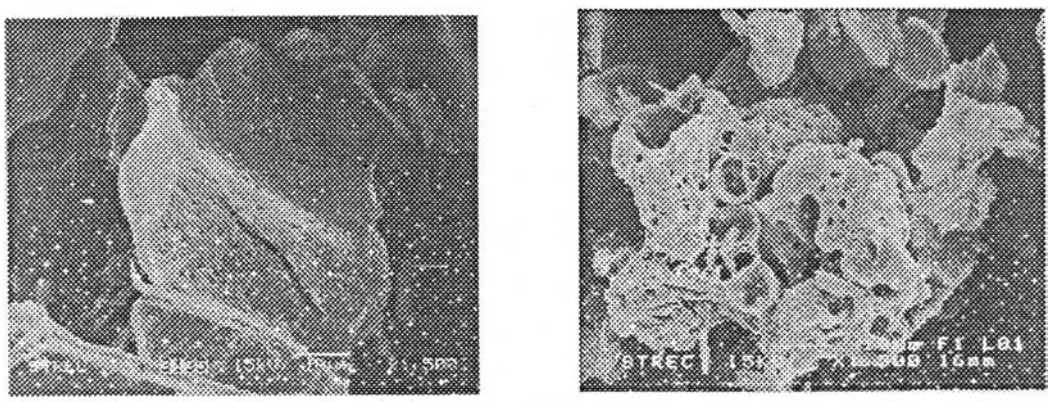

(a) (b)

Figure 4.3 Scanning Electron Micrograph of (a) Bagasse and (b) Bagasse Fly Ash (1500x Magnification)

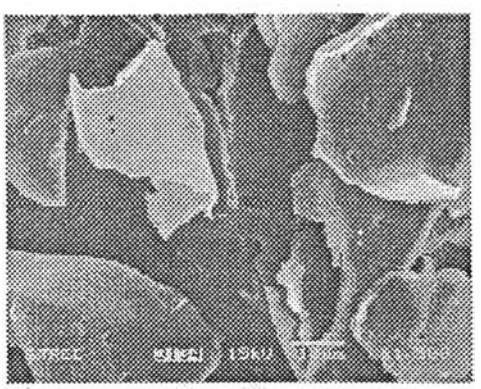

Figure 4.4 Scanning Electron Micrograph of Untreated Bagasse (1500x Magnification)

4.2 Chemical Characteristic Study

Many key parameters of chemical characteristic were determined in this study using material samples form local sugar factory in Saraburi province, Thailand.

4.2.1 Bulk Chemical Composition

Chemical composition of material can be used to predict the behavior of the material in the environment as well as in its applications. For example, high chloride content in the material would have an adverse effect on reinforced steel in concrete. It also reflects the ability of soluble chloride salts of metal to metal to be leached into the environment (Rachakornkij, 2000).

The composition of bagasse is shown in Table 4.4. The main fractions of bagasse, cellulose, were in the same range as other herbaceous materials, such as rice, barley straw and sorghum straw (Aguilar, et al., 2002). Cellulose is the first most abundant of organic substance in the cell wall of plants. The cellulose is a polymer of glucose molecules condensed and linked together linearly by 1,4-β-glycosidic bonds, as shown in Figure 4.5. Cellulose's properties are three dimensions like net, many pores, insolubility, and unbroken. It contains various functional groups, such as carboxyl group and hydroxyl group.

The metal ions of bagasse were measured using XRF which reported them in their respective oxide forms, as shown in Table 4.5. After burning in boiler bagasse become bagasse fly ash. Most components of bagasse were burned and volatized, so the main components of bagasse fly ash were mainly metal ions. The results show the major constituent, Silica, measured at 1.36 % and 51.96 % by weight of bagasse and bagasse fly ash, respectively. In addition, the chemical compositions of cement were summarizes in Table 4.5 for comparison.

A comparison with Portland cement is also made in the same table. It was seen that the silica content of Portland cement was lower than that of bagasse fly ash but

more than that of bagasse. Alumina, calcium and sulfate content were much higher than bagasse and bagasse fly ash. Magnesium and iron contents were about same as those of bagasse fly ash but much higher than bagasse.

Table 4.4 Main Components of Bagasse

Components	Percentage dry weight		
	Kosayothin, 2002	Rao, et al., 2002	Katyal, et al., 2003
Cellulose	44-45	70	26.6-54.3
Organic mater (sugar, pentasan, peptose, proteins, etc.)	25	10	NR
Lignin	20	20	14.3-24.45
Others (metal ions)	10	1	NR

NR referred to not reported

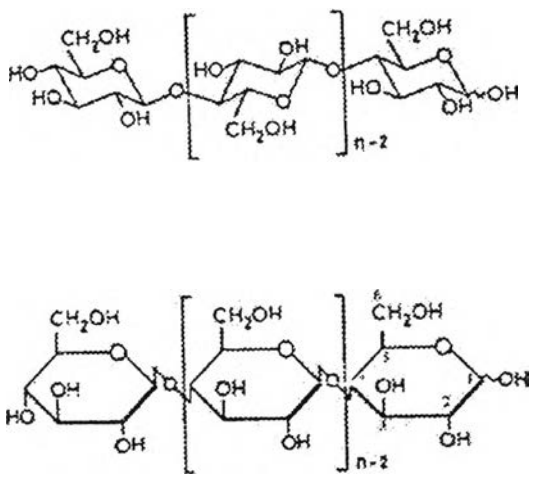

Figure 4.5 Structure of Cellulose (http://www.fibersource.com/f-tutor/cellulose.html)

Table 4.5 Chemical Composition (w/w; %) of Bagasse, Bagasse Fly Ash and Portland Cement

Constituents	Bagasse	Bagasse fly ash	Portland cement [a]
Na_2O	<<	0.43	NR
MgO	<<	1.74	0.1-4.0
Al_2O_3	0.083	1.37	3-8
SiO_2	1.358	51.96	17-25
P_2O_5	0.07	1.43	NR
SO_3	0.169	0.11	1-3
Cl	0.853	<<	NR
K_2O	0.108	1.32	NR
CaO	0.194	7.26	60-67
TiO_2	<<	0.22	NR
MnO	<<	0.14	NR
Fe_2O_3	<<	0.82	0.5-6.0

[a] Neville and Brooks, 1994

<< referred to less than 0.05%

NR referred to not reported

Bagasse fly ash generated from the burning process of bagasse in boiler that the burning conditions may differ from one factory to another. Then the chemical composition of bagasse fly ash from any factories may vary. The comparison with the previous studies is thus necessary. Table 4.6 summarizes the chemical composition of bagasse fly ash from this study as well as from previous studies for comparison. From the Table, the results show the similar values for each constituents, it indicated that the difference in burning conditions of boilers did not significantly affect to chemical compositions of bagasse fly ash.

Table 4.6 Chemical Composition (w/w; %) of Bagasse Fly Ash

Constituents	Alum, 1987	Gupta and Ali, 2001	Jarutawai, 2002	This study
SiO_2	65.8	60.5	67.94	51.96
K_2O	7.5	NR	2.19	1.32
Al_2O_3	5.5	15.4	4.75	1.37
CaO	4.2	2.9	3.63	7.26
Fe_2O_3	3.3	4.9	1.61	0.82
MgO	NR	0.81	1.23	1.74
SO_3	2.0	NR	0.12	0.11

NR referred to not reported

Based on ASTM C618-96, classification of bagasse and bagasse fly ash as a pozzolan, is shown in Table 4.7. It is seen that both of bagasse and bagasse fly ash do not strictly fall in to any of the classes set by ASTM standards. Although SO_3, MgO, and Na_2O contents met the standards for all classes, but the main property, $SiO_2+Al_2O_3+Fe_2O_3$ content, is lower than the minimum standard value. However, trying to make use of the materials, one should also consider the other properties such as relative compressive strength with Portland cement at 28 days which will be discussed in section 4.4.

Table 4.7 Comparison of Chemical Properties of Bagasse and Bagasse Fly Ash with ASTM Requirement for a Pozzolan.

Property (%)	Pozzolan class			B	BFA
	N	F	C		
$SiO_2+Al_2O_3+Fe_2O_3$, min	70.0	70.0	50.0	1.441	54.15
SO_3, max	4.0	5.0	5.0	0.169	0.11
MgO, max	5.0	5.0	5.0	<0.05	1.74
Na_2O,max	1.50	1.50	1.50	<0.05	0.43

4.2.2 Mineralogical Compositions

The information on bulk chemical compositions only gives a coarse idea as to how much each element is in the materials. But information on compound those elements constitute are really important for the prediction of chemical reactions that will occur in Pb(II) and Cr(VI) removal process and reaction in cement.

Figure 4.6 illustrate the XRD patterns of bagasse and bagasse fly ash. Most of X-ray spectra of the bagasse did not show any peak thereby indicating the amorphous nature of the material. This should not cause a surprise since the information on components of bagasse, as discussed in section 4.2.1, indicated that main component of bagasse was cellulose which is amorphous. XRD examination of bagasse reveals that the possible main components of the crystalline phases were $Ca_3SiO_4Cl_2$, $C_2H_{17}O_5Si_{46}O_{92}$, and $Al_2Si_4O_{10}$.

Bagasse fly ash, X-ray spectra showed that most peaks of SiO_2 were in form of crystalline phases. Generally, silica will be responsible for increase compressive strength from the pozzolanic reaction between calcium hydroxide and silica and the hydration of silica itself in the alkaline environment (Singh, et al., 2000) but only silica is in an amorphous state (Rachakornkij, 2000; and Hernandez, et al., 1998).

The identity of other phases is very difficult to find because the patterns are characterized by a large number of small, overlapping peaks and the sample contains high quantities of poorly crystalline of amorphous materials.

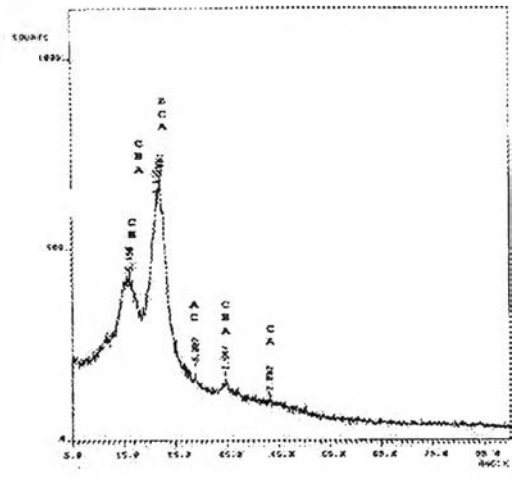

(a)

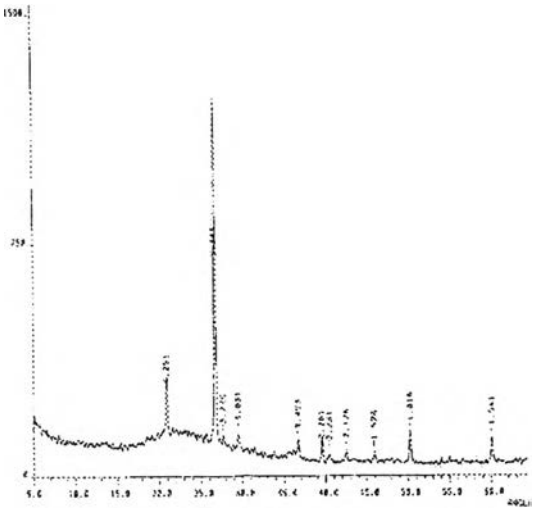

(b)

Figure 4.6 XRD Patterns of (a) Bagasse and (b) Bagasse Fly Ash

4.2.3 Loss on Ignition (LOI)

LOI value of bagasse and bagasse fly ash was 97.17 and 33.17%, respectively. As discussed earlier, LOI is mainly used to determine the carbon content in the sample. LOI value of more than 6% in coal fly ash will reduce the air entrainment in the concrete, thus negatively affecting workability, strength, and durability of

concrete (Rachakornkij, 2000). In addition, high carbon content will cause absorption of chemical additive and low compressive strength of concrete.

Based on ASTM C618-96, classification for pozzolanic material, the maximum LOI value was 10, 6, and 6% for pozzolanic class N, F, and C, respectively. It is seen that both of bagasse and bagasse fly ash dose not strictly fall in to any of the classes given by ASTM standards. These results were according to information on percent of SiO_2+Al_2O_3+Fe_2O_3, as discussed above.

4.2.4 pH

pH value of bagasse and bagasse fly ash, was 5.8 and 11.6, respectively. The pH of material is an indication of how its leachate would behave in the real environmental as well as in the leaching test. Normally, high pH which contributes to high alkalinity would make it pass the regulatory LP-No.6 test. Because most regulated metals remain insoluble at high pH solution (Rachakornkij, 2000).

4.2.5 Water Absorption Capacity

The results showed that absorption capacity of bagasse and bagasse fly ash was 353 and 65%, respectively. Absorption capacity of material is defined as the ability of an oven-dried material to absorb moisture in a 100% relative humidity environment. As mention above, absorption capacity value may be used as an indication of how much the material would take up water in the mix.

4.2.6 Functional Group

The FT-IR spectra of bagasse and bagasse fly ash recorded in the 4000 to 400 cm^{-1} are shown in Figure 4.7. The possible functional group of bagasse was alkyl group (hydroxyl or amino substituent), hydroxy or amino compound, aliphatic alcohol (primary or secondary or cyclic hydroxyl), and carbonyl compound. Inorganic compound (silica or silicate) was possible functional group of bagasse fly ash.

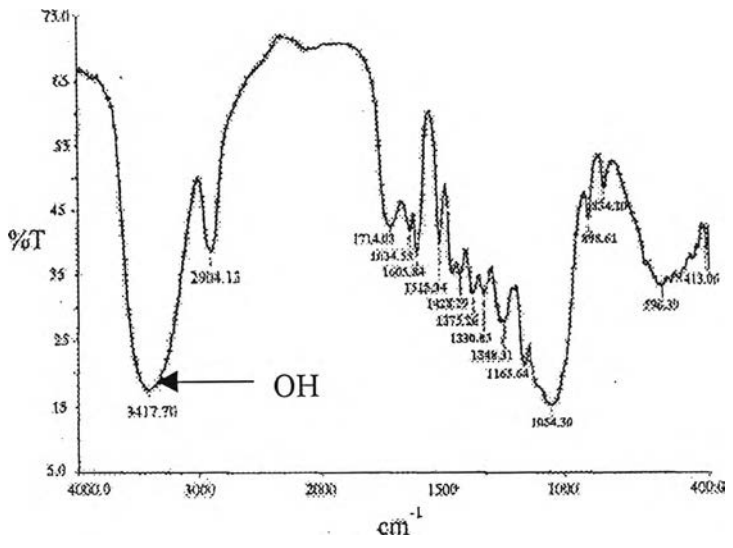

(a)

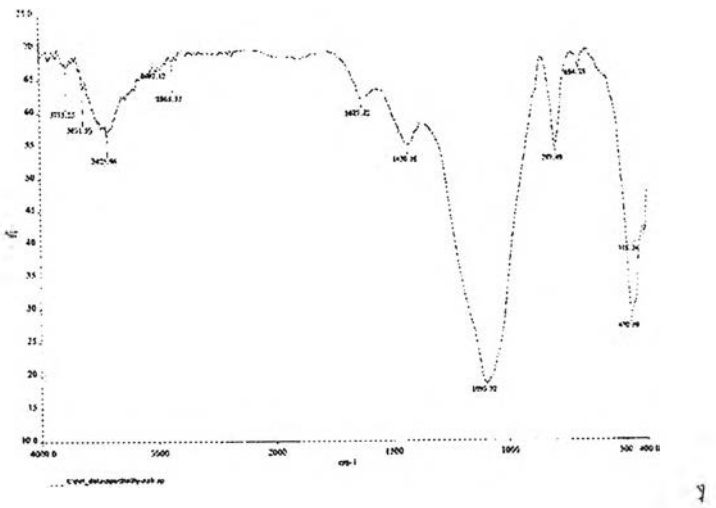

(b)

Figure 4.7 FT-IR spectra of (a) Bagasse and (b) Bagasse Fly Ash

4.3 Removal Study

All experiments were carried out in triplicate and means are given. The experimental results are as follows:

4.3.1 Removal of Lead

4.3.1.1 Effect of contact time

The time-dependent behavior of lead removal between adsorbate and adsorbent was measured using the conditions that were previously described in Table 3.3. The results are plotted in Figure 4.8. The removal of lead was found to increase with increasing contact time, but it became almost constant after 15 and 45 minutes for bagasse and bagasse fly ash, respectively. The rate of removal is higher in the beginning due to a larger surface area of the materials available for the adsorption of the Pb(II). After the adsorbed material forms a one-molecule thick layer, the capacity of the adsorbent gets exhausted and then the uptake rate is controlled by the rate at which the sorbate is transported from the exterior to the interior sites of the adsorbent particle (Yu, et al., 2003). From the results, therefore, contact periods of 60 minutes was finally selected for all of the next equilibrium experiments.

Bagasse was shorter equilibrium contact time comparing to bagasse fly ash, it may be due to pore size on surface of material. The adsorption is fast in relative large pores, and slow entries into small micropores due to the diffusion effect (Hu, et al., 2003). From Table 4.2, it was shown that pore size of bagasse (2031 Å) was larger than that of bagasse fly ash (774 Å).

The percentage of Pb removal and amount of Pb adsorbed for bagasse (67.07%, 0.669 mg/g) was lower than that of bagasse fly ash (96.70%, 0.965 mg/g). It may be due to porosity and pore specific volume of material. The adsorption capacity is high in relative high porosity and pore specific volume due to high adsorption site.

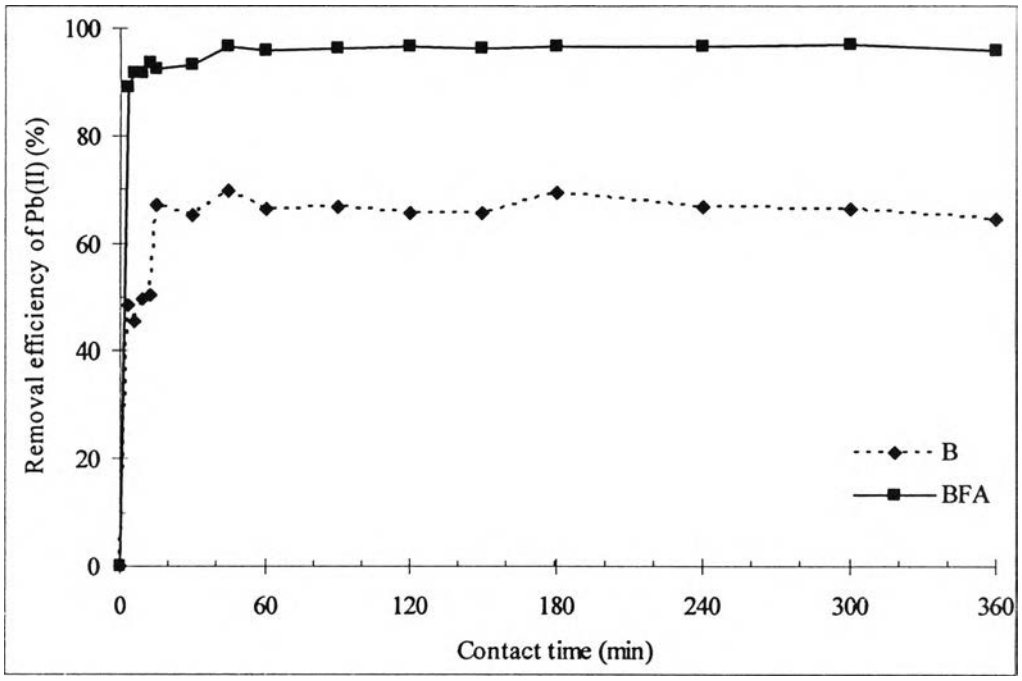

(a)

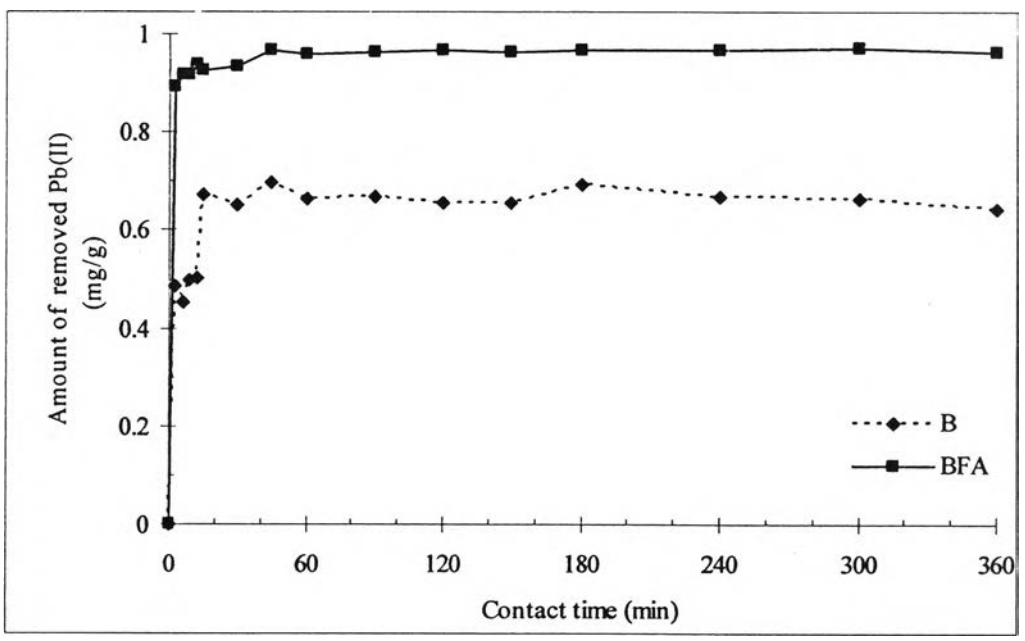

(b)

Figure 4.8 Effect of Contact Time on (a) Removal of Pb(II) and (b) Amount Removed of Pb(II) (solution pH 4, initial concentration 10 mg/L, dose 10 g/L)

4.3.1.2 Effect of initial concentration

The removal experiments were carried out at the conditions explained in Table 3.3. The results are given in Figures 4.9 and 4.10 for removal on bagasse and bagasse fly ash, respectively. The figures showed the removal efficiency of Pb(II) as a function of initial concentration at different solution pH values. It was observed that, bagasse reduced Pb(II) from 95.63% (0.467 mg/g) to 66.30% (4.055 mg/g) with the initial Pb(II) ion concentration varied from 5 to 80 mg/L with a constant adsorbent dose at pH 6. In the case for bagasse fly ash, the removal efficiencies were 99.54% (1.971 mg/g) and 99.46% (7.914 mg/g) at an initial concentration of Pb(II) ion 20 and 80 mg/L at pH 6, respectively. For bagasse fly ash, at initial concentration less than 20 mg/L, the equilibrium concentration was less than detection limit of the AAS used in the study (0.05 mg/L).

It can be observed that the removal of Pb(II) on bagasse and bagasse fly ash exhibited similar trend; that is, it decreased with increasing initial Pb(II) ion concentration. On the other hand, the adsorption capacity increased with increasing initial concentration at all solution pH values. Similar observations have also been reported by other researchers who investigated adsorption of Pb(II) by using bentonite (Naseem and Tahir, 2001). The adsorption isotherm of Pb(II), as shown in Figure 4.14 in section 4.3.1.5, it showed that the maximum adsorptions were approximately 90 and 230 mg/g for bagasse and bagasse fly ash, respectively. It means that adsorbents have available adsorption sites in very large amount when compared with sorbate. High initial concentration of Pb, therefore, was high adsorption capacity because large available amount of sorbate can attract and retain in an immobilized form onto surface of adsorbent. On the other hand, low initial concentration of Pb, little available amount of sorbate was adsorbed then adsorption capacity was low. But it was high difference level between initial concentration and final concentration of Pb. Then the percent removal was high in case of low initial concentration. Comparing to the low initial concentration, the results for high initial concentration were opposite.

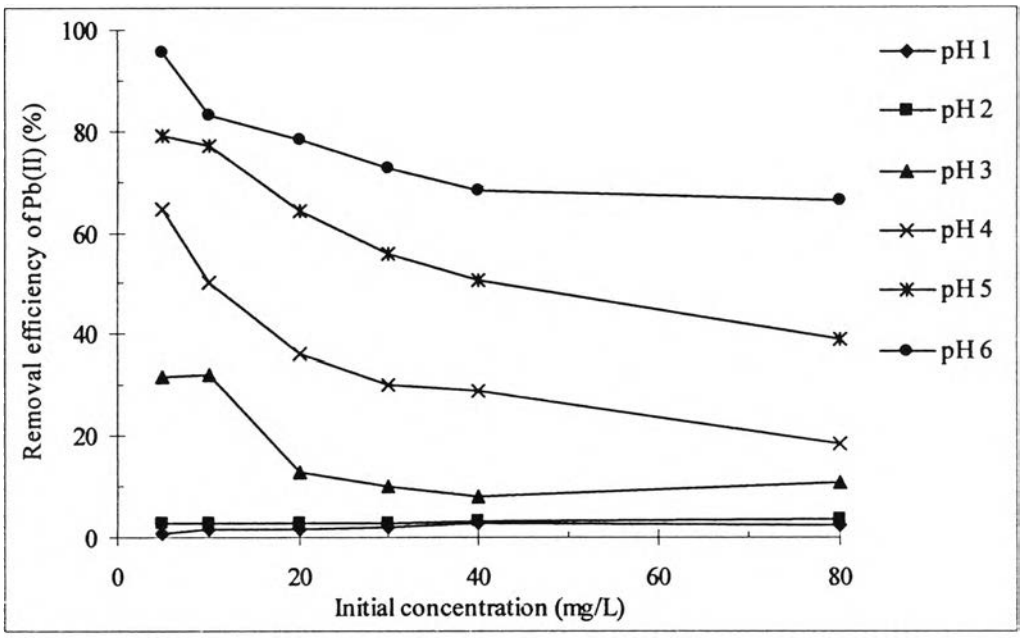

(a)

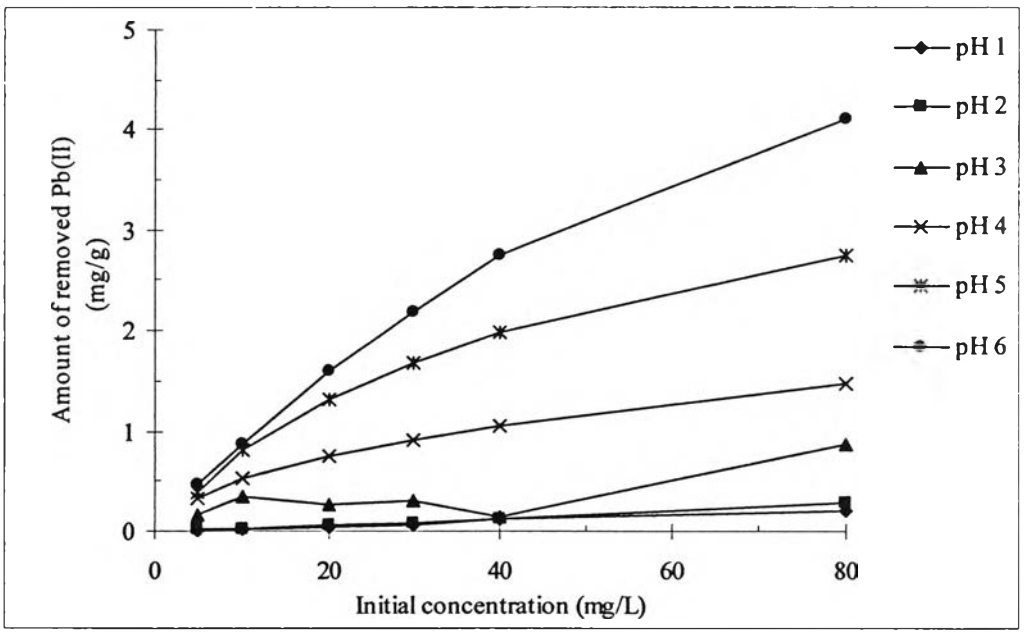

(b)

Figure 4.9 Effect of Initial Concentration on (a) Removal of Pb(II) and (b) Amount Removed of Pb(II) by Bagasse at Difference Solution pH (contact time 60 min, dose 10 g/L)

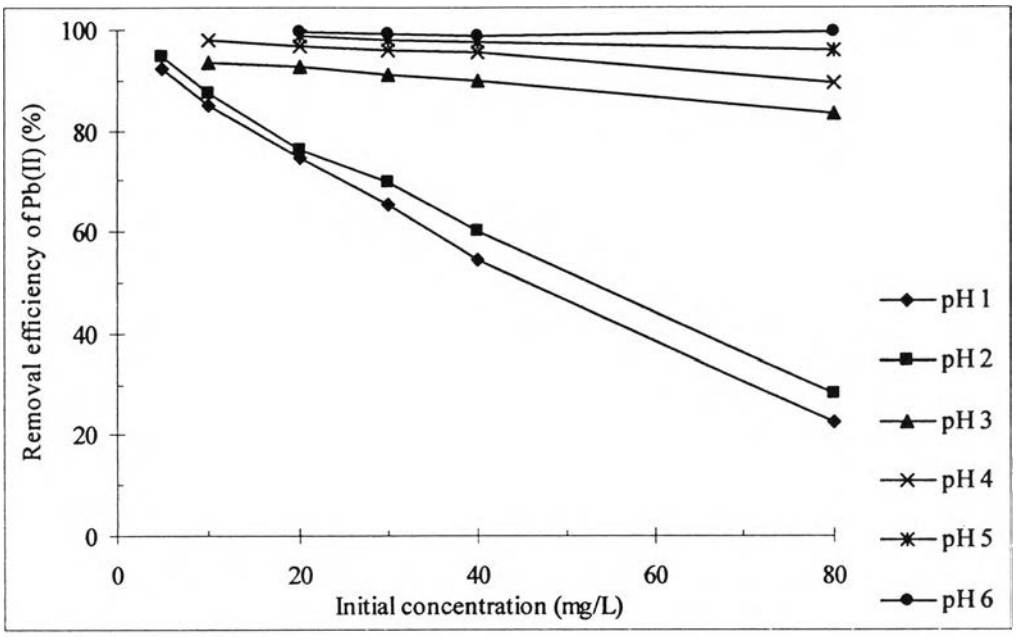

(a)

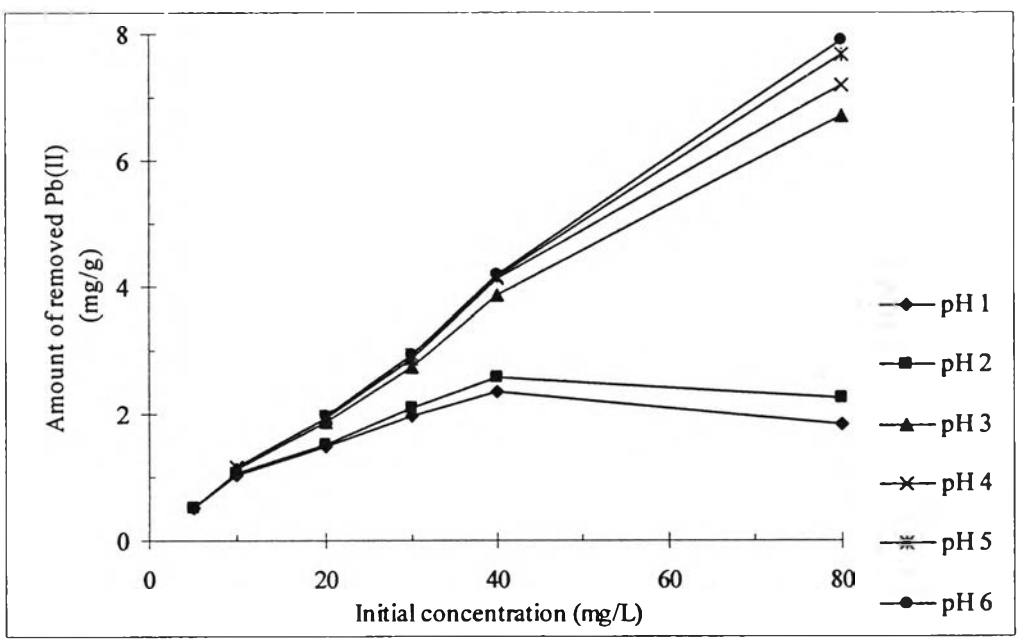

(b)

Figure 4.10 Effect of Initial Concentration on (a) Removal of Pb(II) and (b) Amount Removed of Pb(II) by Bagasse Fly Ash at Difference Solution pH (contact time 60 min, dose 10 g/L)

4.3.1.3 Effect of solution pH

The results can be observed that the removal of Pb(II) on bagasse and bagasse fly ash exhibited similar trend; that is, it increased with increasing solution pH, from its minimum at lower pH to its maximum at a higher pH range, at all initial concentrations (Figure 4.11 and 4.12). They were apparent that removal efficiency rose from 1.77 to 98.19% for bagasse and from 74.42 to 99.54% for bagasse fly ash when pH was increased from pH 1 to pH 6.0 (at initial concentration was 20 mg/L). Similar observations have also been reported by other investigators that using various adsorbent materials (Yu, et al., 2001; Zhan and Zhao, 2003; Herrera-Urbina and Fuerstenau, 1995; Naseem and Tahir, 2001; Namasivayam and Ranganathan, 1998; Wu, et al., 2003).

The maximum removal of Pb(II) by bagasse and bagasse fly ash occurred at a pH of about 6.0. The measured solution pH values were fairly consistent with less than 0.65 pH unit difference between the initial and final pH values.

Further experiments at a solution pH of above 6 were not conducted due to high precipitation of lead in the solution (more than 50% at solution pH 7). This is advantageous for Pb(II) removal and recovery from wastewater because wastewater containing lead is already kept acidic by the plants in order to avoid lead precipitation (Zhan and Zhao, 2003).

From the results, it can be seen that pH is an important factor in lead adsorption onto these adsorbent materials under investigation. Several studies have been published on the adsorption of Pb(II) onto different oxides and hydroxides. These investigations only reported the pH-dependence of adsorption up to completion of metal uptake. The adsorption edge was found to lie between pH 5 and 7 for silica, and between pH 4.5 and 7 for alumina (Herrera-Urbina and Fuerstenau, 1995).

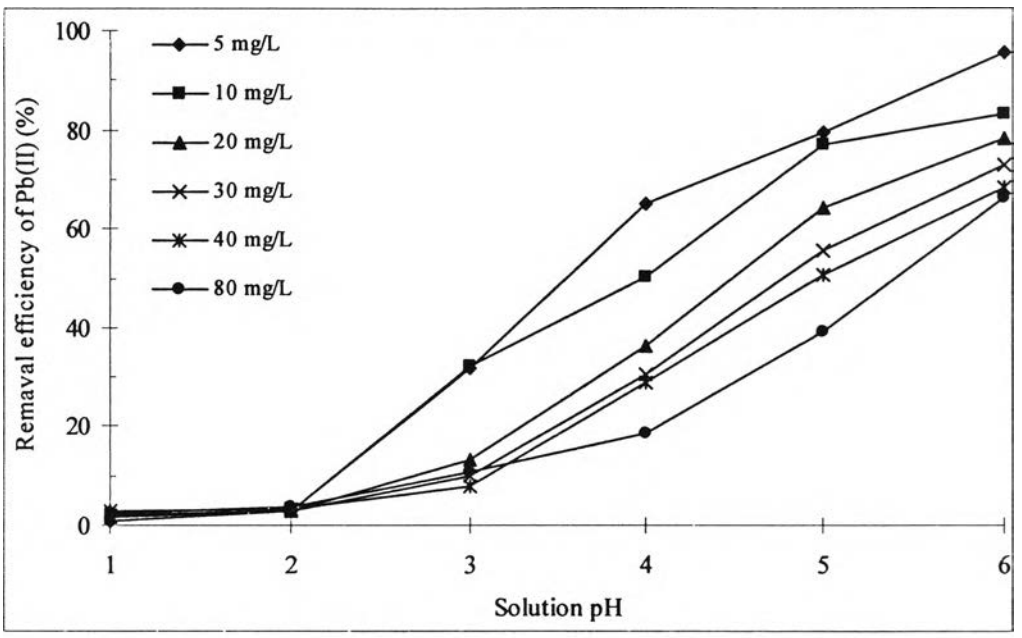

(a)

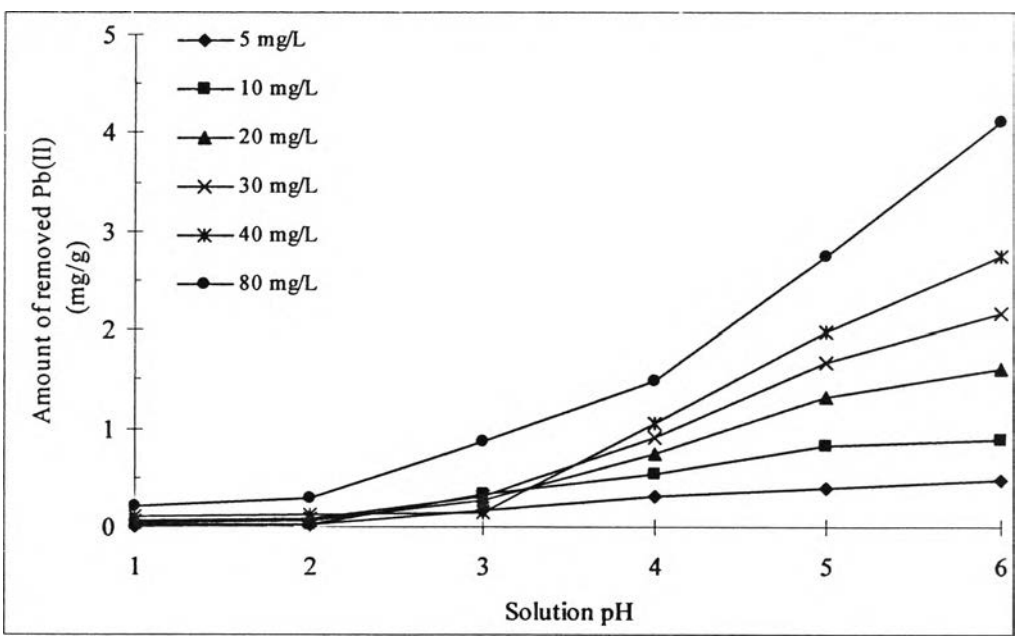

(b)

Figure 4.11 Effect of Solution pH on (a) Removal of Pb(II) and (b) Amount Removed of Pb(II) by Bagasse at Difference Initial Concentrations (contact time 60 min, dose 10 g/L)

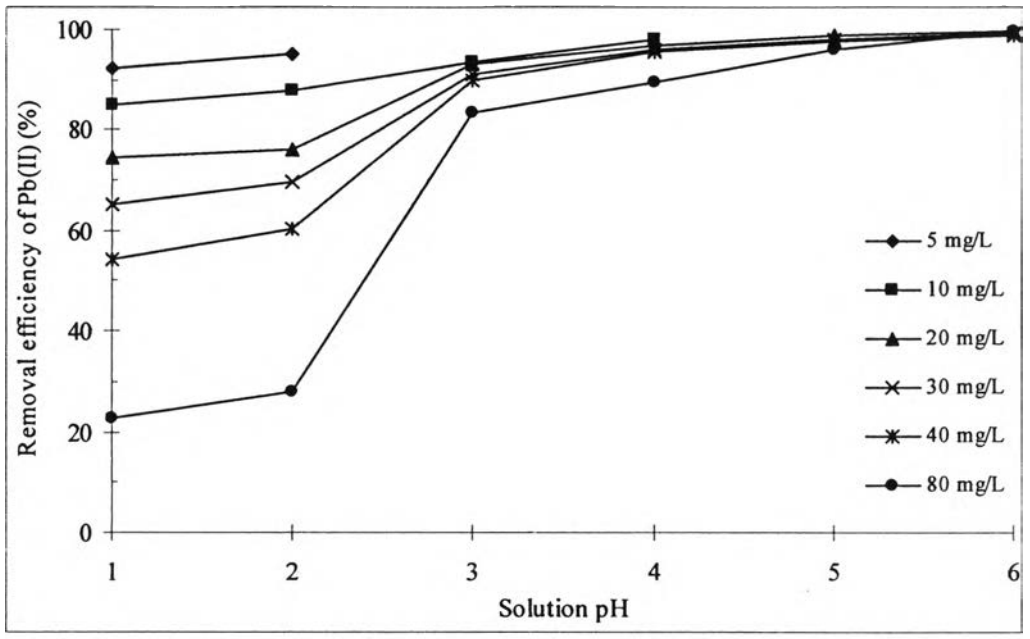

(a)

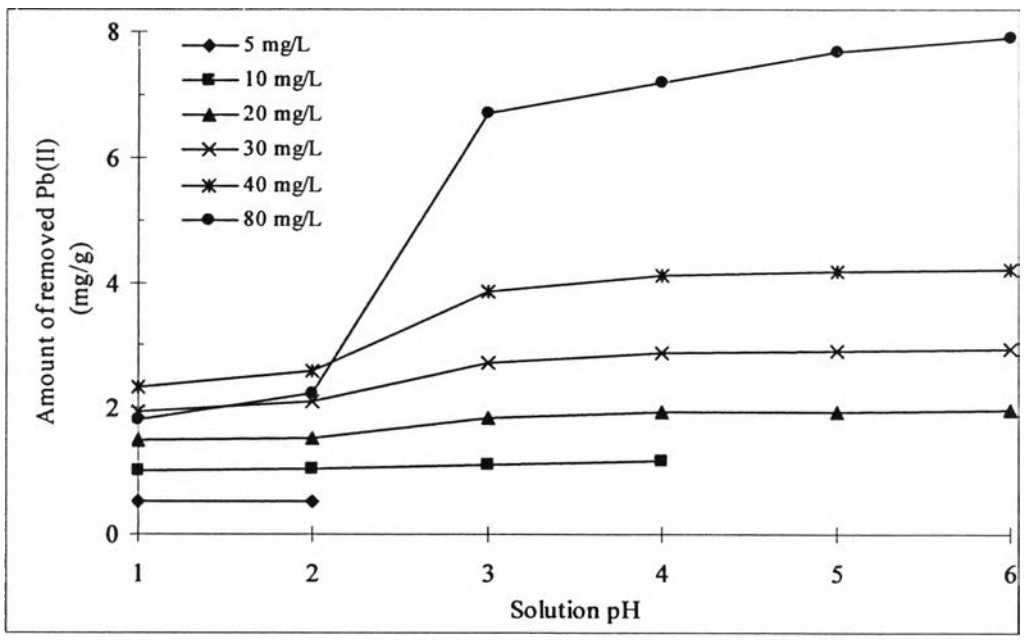

(b)

Figure 4.12 Effect of Solution pH on (a) Removal of Pb(II) and (b) Amount Removed of Pb(II) by Bagasse Fly Ash at Difference Initial Concentrations (contact time 60 min, dose 10 g/L)

In addition, these results of pH-dependence can be explained by considering the point of zero charge of the materials. The pH at the point of zero charge (pH_{PZC}) is reported at 8.2 and 2.3 for alumina and silica, respectively (Mohan, et al., 2002). In addition, Herrera-Urbina and Fuerstenau (1995) reported that quartz surface carried a negative charge at all pH values above about 2. Since the main composition of these materials was silica (51.96%) then their pH_{PZC} should be near 2.3. That means, when pH value is above 2.3, the negative charge density on the surface of the adsorbent increases, thus increasing available sites for the adsorption of Pb(II) ion. At low pH, a competition between hydrogen ions adsorption and Pb(II) removal exists. Therefore, increasing the initial concentration of proton in aqueous solutions may result in the decrease of Pb(II) removal.

From FT-IR spectra, as mentioned above, the possible functional groups of bagasse was alkyl group (hydroxyl or amino substitute), hydroxyl or amino compound, aliphatic alcohol (primary or secondary or cyclic hydroxyl), and carbonyl compound. The alkyl chains which contain a wide variety of functional groups (-COOH, -OH, -NH2, etc.) can bind strongly to metals (Wu, et al., 2003) as follows:

$$R\text{-}COOH + Pb^{2+} \Leftrightarrow R\text{-}COOPb^{+} + H^{+}$$

$$R\text{-}OH + Pb^{2+} \Leftrightarrow R\text{-}OPb^{+} + H^{+}$$

As mentioned above, at higher pH value, protons combine with OH^- to form H_2O and more Pb can be adsorbed via above reaction equation.

In addition, ion exchange may be a principle mechanism for the removal of Pb(II) ions onto bagasse. The major components of the polymeric material in bagasse are lignin, tannins or other phenolic compounds. These kinds of material possess the capability of capturing heavy metal ions (Yu, et al., 2001). It can be speculated that lignin, tannins or other phenolic compounds are the active ion exchange compounds. As it is well known, Pb(II) exist in acidic solution as cations. It

may be concluded that at low pH values ion-exchange reaction involving metals are in competition with the high concentrations of H^+ in the solution.

4.3.1.4 Effect of dosage

The results are plotted in Figure 4.13. It was found that the removal efficiency of Pb(II) increased with increasing adsorbent dose. Similar observations have also been reported by other investigators which adsorbed Pb(II) by using sawdust and bentonite (Yu, et al., 2001; Naseem and Tahir, 2001). In the case of bagasse, the removal efficiency increased from 24.330% at 0.2 g/L to 63.81% at 20 g/L. While, for bagasse fly ash, the removal increased from 58.93% at 0.2 g/L to 99.97% at 20 g/L. Moreover, in both cases, the removal efficiency became almost constant at 10 g/L dose.

It was apparent that the removal of lead increased rapidly with increase in the amount of the adsorbent due to the greater availability of the exchangeable sites or surface areas at higher concentrations of the adsorbent.

4.3.1.5 Adsorption Isotherm

Isotherms for the removal of Pb(II) onto bagasse and bagasse fly ash are shown in Figure 4.14. The linearized Langmuir and Freundlich isotherms for the removal of lead onto bagasse and bagasse fly ash are shown in Figure 4.15. A detailed analysis of the regression coefficients (R^2) in Table 4.8 showed that Langmuir and Freundlich models adequately described the adsortption data, but the data are better fitted by the Freundlich isotherm for both adsorbent. Although the Freundlich and Langmuir constants K_f and Q_o have different meanings, they led to the same conclusion about the correlation of the experimental data with the sorption model. The basic difference between K_f and Q_o is that Langmuir isotherm assumes adsorption-free energy independent of both the surface coverage and the formation of monolayer whereas the solid surface reaches saturation.

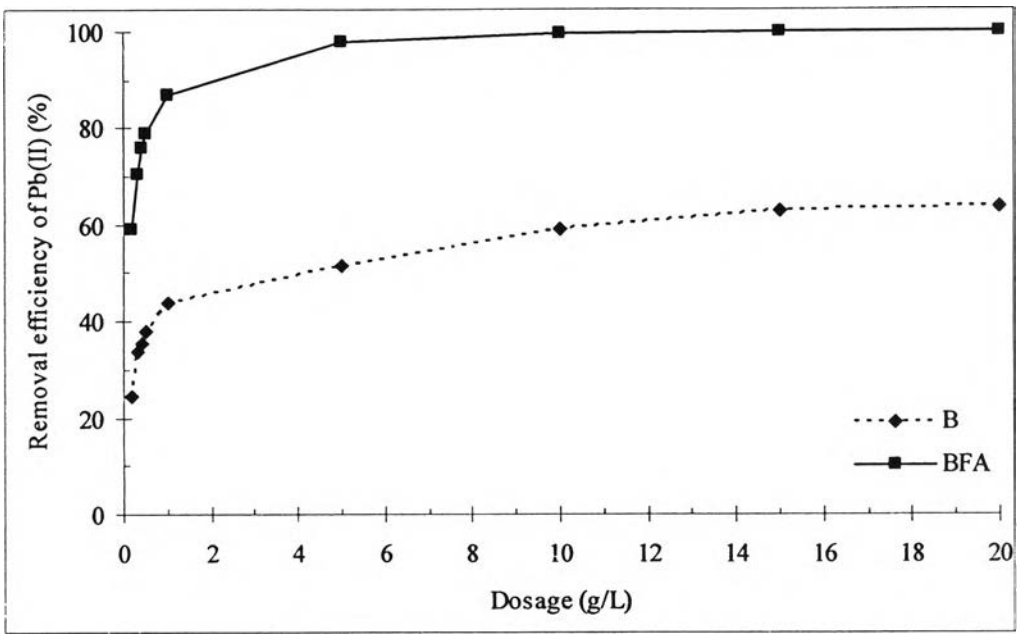

(a)

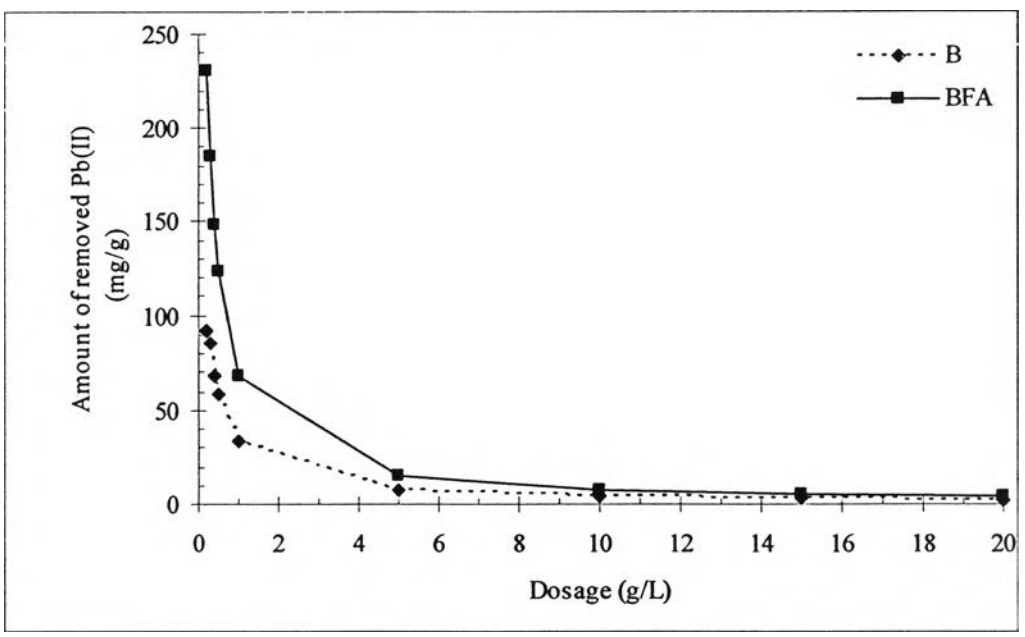

(b)

Figure 4.13 Effect of Dosage on (a) Removal of Pb(II) and (b) Amount Removed of Pb(II) (contact time 60 min, initial concentration 80 mg/L, solution pH 6)

While as, the Freundlich isotherm does not predict saturation of the solid surface by the adsorbate, and therefore, the surface covering being mathematically unlimited. In conclusion, Q_o is the monolayer adsorption capacity while K_f is the relative adsorption capacity or adsorption power.

Adsorption isotherm of Pb onto bagasse and bagasse fly ash fitted well by Freundlich, it may be due to characteristic of surface of materials. As mentioned in section 2.3.6, the Fruendlich isotherm equation assumes that the adsorbent has a heterogeneous surface composed of adsorption site with different adsorption potentials. From scanning electron micrograph in Figure 4.3, it showed that bagasse and bagasse fly ash were heterogeneous surface material.

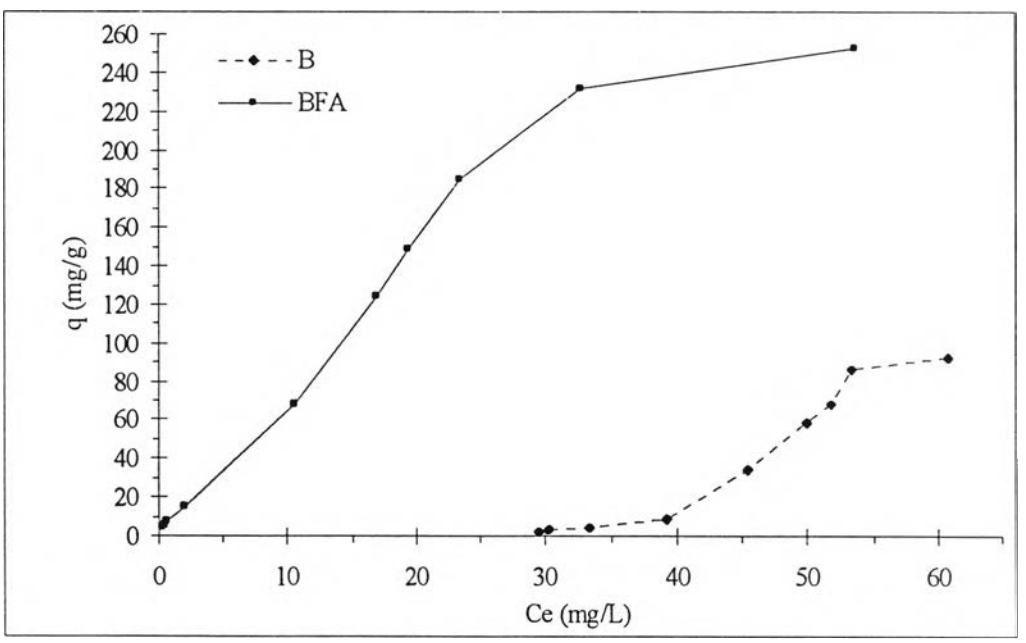

Figure 4.14 Isotherms for Removal of Pb(II) onto Bagasse and Bagasse Fly Ash (contact time 60 min, initial concentration 80 mg/L, solution pH 6)

Table 4.8 Equation and Regression Values of Langmiur and Frundlich Isotherm

Materials	Bagasse (B)		Bagasse Fly Ash (BFA)	
Isotherm	**Equation**	**R^2**	**Equation**	**R^2**
Langmiur	y = 21.952x - 0.4074	0.9325	y = 0.0805x + 0.0042	0.9827
Frundlich	y = 5.4333x - 7.5262	0.9728	y = 0.849x + 1.0297	0.9914

Using the slope and the intercept of the line, the constant K_f and n were found to be $2.97*10^{-8}$ and 0.18, respectively for bagasse and 10.71 and 1.18, respectively for bagasse fly ash as shown in Table 4.9. As mentioned above, the K_f values which are related to relative adsorption capacity indicated that bagasse fly ash had more adsorption capacity than bagasse for Pb(II) removal. Like K_f, bagasse fly ash had adsorption intensity, n, more than that of bagasse. Since n > 1, the adsorption is favorable (Daneshvar, et al., 2002). It was according to the adsorption experimental results as mentioned above. The Table 4.10 was showed the recommended isotherm equations.

Table 4.9 Constants Values of Langmuir and Freundlich Isotherm

Material	Langmuir constants			Freundlich constants	
	Q_o	**b**	**r**	**K_f**	**n**
B	-2.455	-0.019	-2.063	$2.977*10^{-8}$	0.184
BFA	238.095	0.052	0.193	10.707	1.178

Table 4.10 Recommended Isotherm Equation of Bagasse and Bagasse Fly Ash

Material	Recommended isotherm equation
B	Log (x/m) = 5.4333 log Ce - 7.5262
BFA	Log (x/m) = 0.849 log Ce+ 1.0297

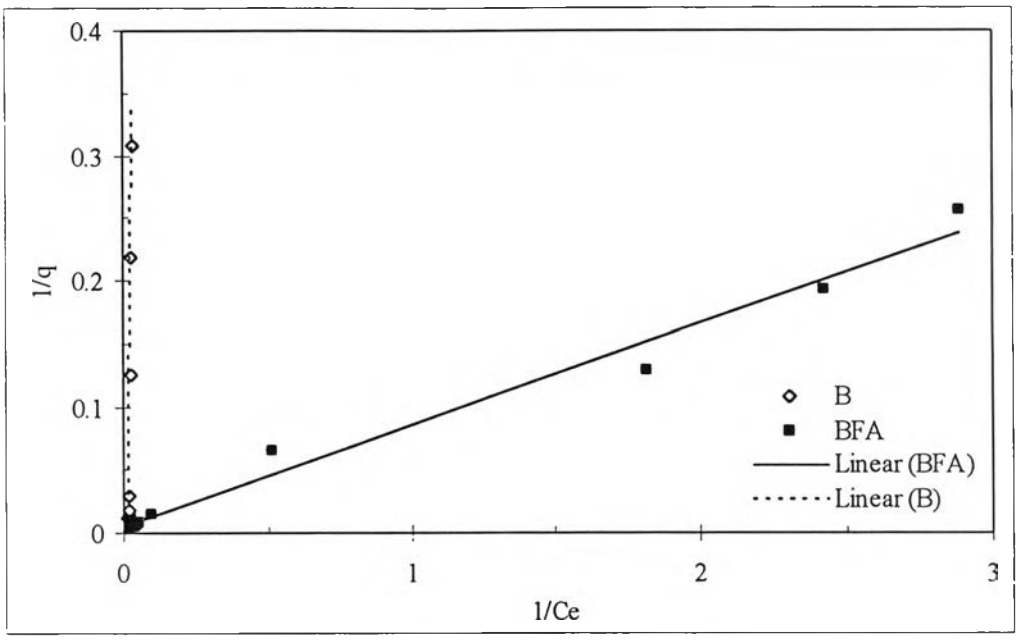

(a)

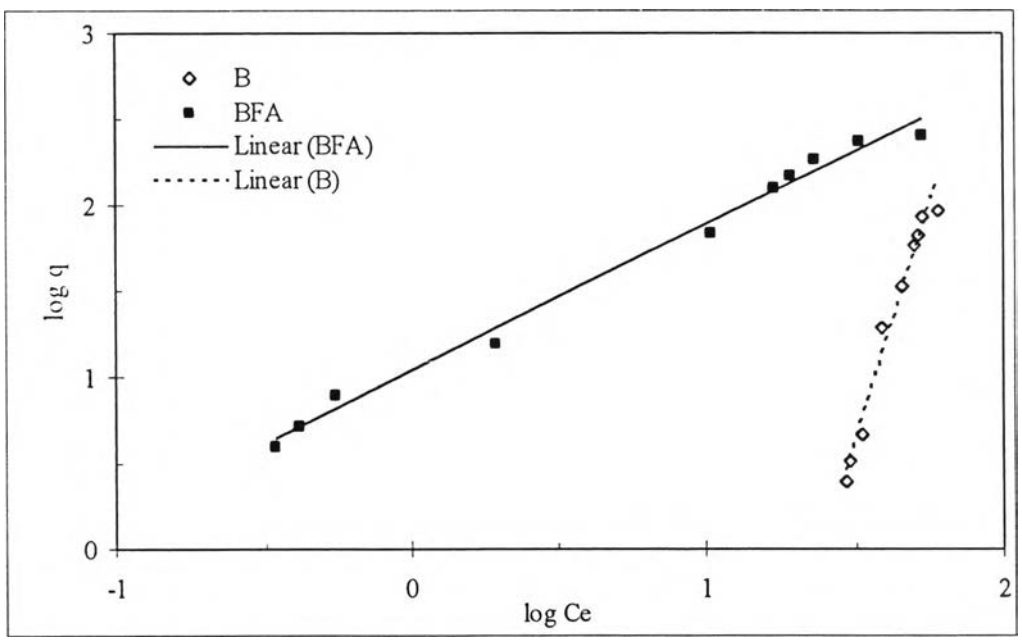

(b)

Figure 4.15 Linearized (a) Langmuir and (b) Freundlich Isotherms

4.3.2 Removal of Hexavalent Chromium

Chromium exists in two stable oxidation states, Cr(III) and Cr(VI). Although, this study was considered of Cr(VI) concentration, but reduction reaction can transform Cr(VI) to Cr(III). Thus, the solution sample is contained both Cr(VI) from input and Cr(III) from reduction. Therefore, this study presents the experiment data in terms of removal of total Cr (Cr(VI)+Cr(III)) and Cr(VI). Data of concentration of total Cr were determined by atomic absorption spectrophotometer, but concentrations of Cr(VI) were measured by UV spectrophotometer, and concentration of Cr(III) which calculated from the difference in concentrations between the total Cr and Cr (VI).

4.3.2.1 Effect of Contact Time

Time dependent experiments were preformed and the results are shown in Figure 4.16 and 4.17. In case of bagasse, the Cr(VI) concentration was found to sharply decrease and was reduced to below the detection limit of the analytical equipment. Meanwhile, the Cr(III), which was not initially present, appeared in the solution and increased in proportion to the amount of Cr(VI) depleted. In addition, for bagasse fly ash, the similar trend was observed.

Decrease in Cr(VI) concentration and increase in Cr(III) concentration were found almost constant from 30 minutes onwards for both materials. The maximum removal efficiency was stated from 30 minutes of contact time. Therefore, contact period 60 minutes was finally selected for all of the next equilibrium tests.

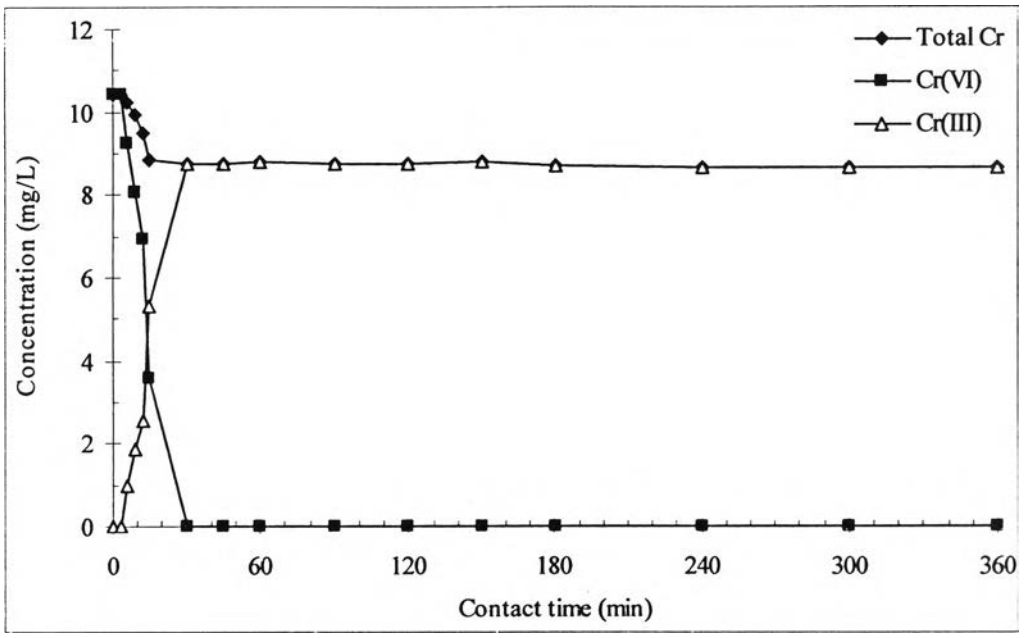

(a)

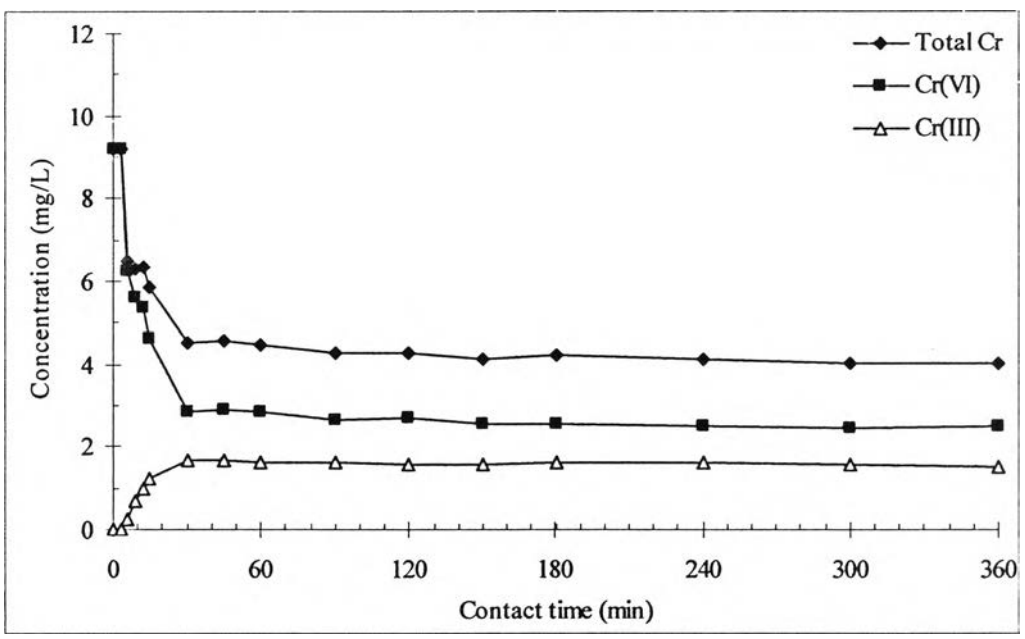

(b)

Figure 4.16 Effect of Contact Time on Concentration of Total Cr, Cr(VI) and Cr(III) by (a) Bagasse and (b) Bagasse Fly Ash (solution pH 2, initial concentration 10 mg/L, dose 20 g/L)

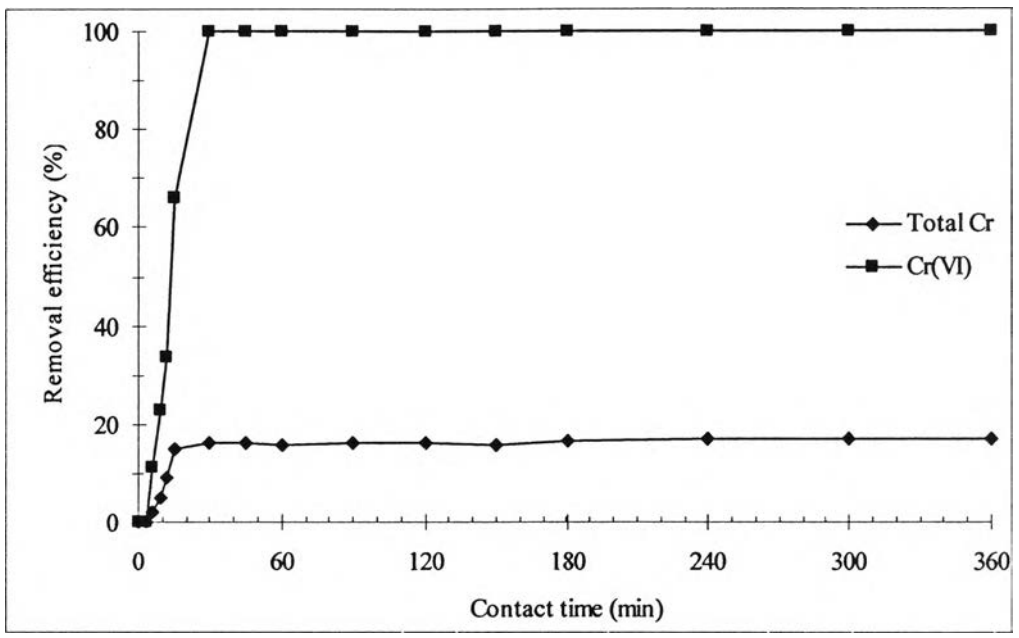

(a)

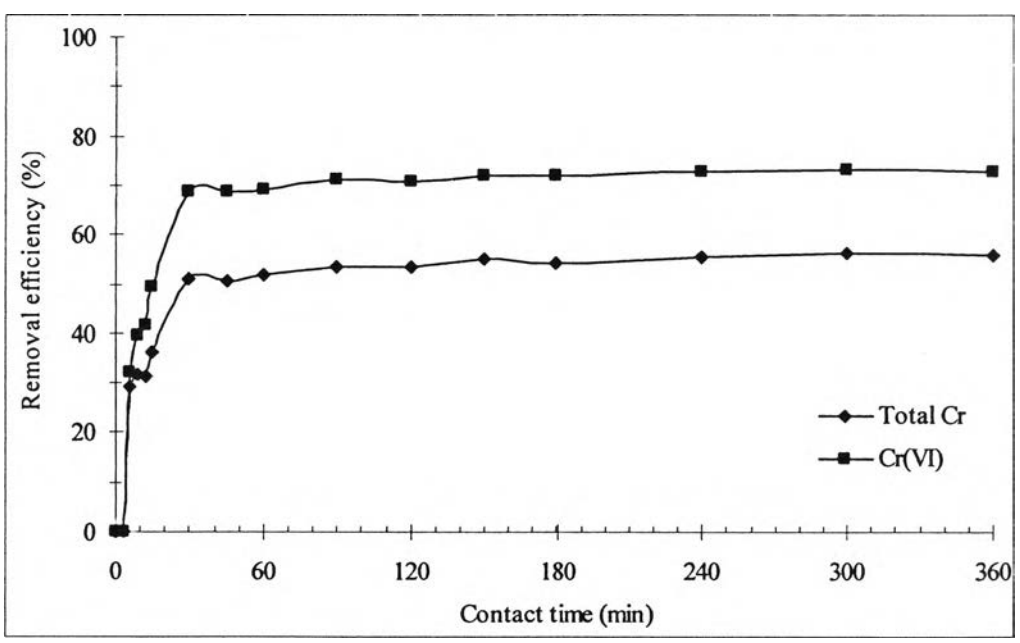

(b)

Figure 4.17 Effect of Contact Time on Removal Efficiency of Total Cr and Cr(VI) by (a) Bagasse and (b) Bagasse Fly Ash (solution pH 2, initial concentration 10 mg/L, dose 20 g/L)

The equilibrium time was found to be relatively shorter than many other materials such as rice husk carbon, cow dung carbon (Das, et al., 2000), coconut shells carbon, peach stones (Guo, et al., 2002), and high-performance activated carbons (Hu, et al., 2003). It may be due to the large pores, the adsorption is fast in relative large pores, and slow entries into small micropores due to the diffusion effect (Hu, et al., 2003). As shown in Table 4.2, the pore sizes of bagasse and bagasse fly ash are 2031 Å and 774 Å, respectively, which are larger than other adsorbents.

However, the Cr(III) quantity was detected always lower than the amount of Cr(VI) removed. Explanations are possible: a fraction of non-reduced Cr (VI) could be bound onto the sorbent because of its positive surface or the missing Cr (III) quantity remained adsorbed onto the material after Cr(VI) reduction (Reddad, et al., 2003). Therefore, the removal of Cr(VI) may involve two processes, namely, reduction of Cr(VI) to Cr(III) and adsorption of Cr(VI) and Cr(III). Bagasse can remove Cr(VI) more than bagasse fly ash, but, it can remove total Cr less than bagasse fly ash.

Figure 4.18 showing the percentage of minimal reduction, it is Cr(III) concentration which detected in solution sample. As mentioned above, Cr(III) may adsorbed on surface of material and suspended in solution. Thus, Cr(III) concentration that detected in solution sample may be not the total Cr(III). Cr(III) concentration in solution sample was present in term of minimal reduction. Figure 4.18 showed higher efficiency of bagasse in reduction Cr(VI) to Cr(III) comparing to bagasse fly ash. These results indicated that bagasse can remove Cr(VI) via reduction more than adsorption. On the other hand, bagasse fly ash can remove Cr(VI) by adsorption more than reduction.

For reduction process, Cr(VI) in acidic solution demonstrates a very high positive redox potential which signifies that it is strongly oxidizing and unstable in the attendance of electron donors. Hydroxyl and carboxylic groups probably play a role as electron donors (Reddad, et al., 2003). FTIR analysis indicated that bagasse contained many hydroxyl groups at frequency of 3400-3200 cm^{-1}, meanwhile, bagasse

fly ash did not contained this functional group. In addition Figure 4.5 showed structure of cellulose, it is a polymer of glucose molecules condensed and linked together linearly by means of 1,4-β-glycosidic bonds. This Figure showed that cellulose consisted with a lot of hydroxyl group, it is according to FTIR analysis results and the cellulose may burned and disappear under 1,400 °C of boiler in sugar factory. Then bagasse fly ash was not contained hydroxyl groups. Therefore, bagasse may act as electron donors in the experiments and can reduce Cr(VI) higher than bagasse fly ash.

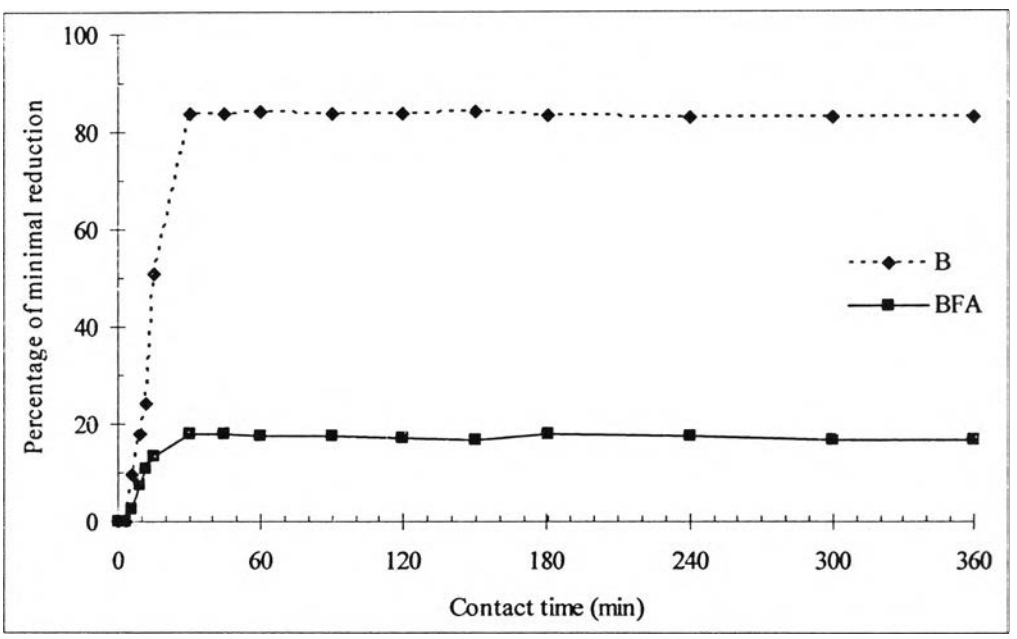

Figure 4.18 Effect of Contact Time on Percentage of Minimal Reduction by Bagasse (B) and Bagasse Fly Ash (BFA) (solution pH 2, initial concentration 10 mg/L, dose 20 g/L)

For the adsorption process, bagasse basically contains lignin and cellulose. The polar functional groups of lignin-like aldehydes, ketones, alcohols, acids and phenolic hydroxides are involved in the formation of bonds with anions species (Ajmal, et al., 1996). For bagasse fly ash, SiO_2 was the main adsorption site on surface of bagasse fly ash. As a result, bagasse fly ash can adsorbed Cr(VI) and Cr(III), that was present in term of total Cr, higher than bagasse. The adsorption capacity was found to increase with BET surface area and pore volume (Guo, et al.,

BET surface area and pore volume analysis indicated that surface area and pore volume of bagasse were lower than bagasse fly ash.

4.3.2.2 Effect of Initial Concentration

Figures 4.19 and 4.20 showed the experimental data of removal of total Cr and Cr(VI), respectively, versus initial concentration of Cr(VI) at various solution pHs. These results indicated that, total Cr and Cr(VI) removal were higher under low initial Cr(VI) concentration within all various solution pHs in the experiments (1-6). These experiment data indicated that the removal efficiency for total Cr and Cr(VI) decrease with increasing the initial concentration. Similar sorption studies were reported earlier by several workers (Guo, et al., 2002; Das, et al., 2000; Yu, et al., 2003). Though the percentage removal was decreased with increase in Cr(VI) concentration but the actual amount of Cr(VI) removed per unit mass of the materials was increased as shown in Table F (Appendix F). This accord well with the findings of other investigators (Garg, et al., 2004; and Cimino, et al., 2000).

In case of bagasse, almost complete Cr(VI) removals were achieved by reduction reaction at low initial concentration. From these data, it indicated that the conversion of Cr(VI) decrease with increasing the initial concentration. Because, for the solution containing lower initial Cr(VI), the amount of electron donors or bagasse in the solution was sufficient. On the contrary, when the solutions having high Cr(VI) concentrations were used, electron donors might become insufficient.

As same trend, in lower concentration, the adsorbate could occupy the active sites on the material surface sufficiently. But with the increase in adsorbate concentration, the number of active adsorption sites is not enough to accommodate adsorbate ions. In addition, the limit of pore size dimension and the electrostatic repulsion between negative charge of adsorbate ions results in the decrease of adsorption percentage (Guo, et al., 2002).

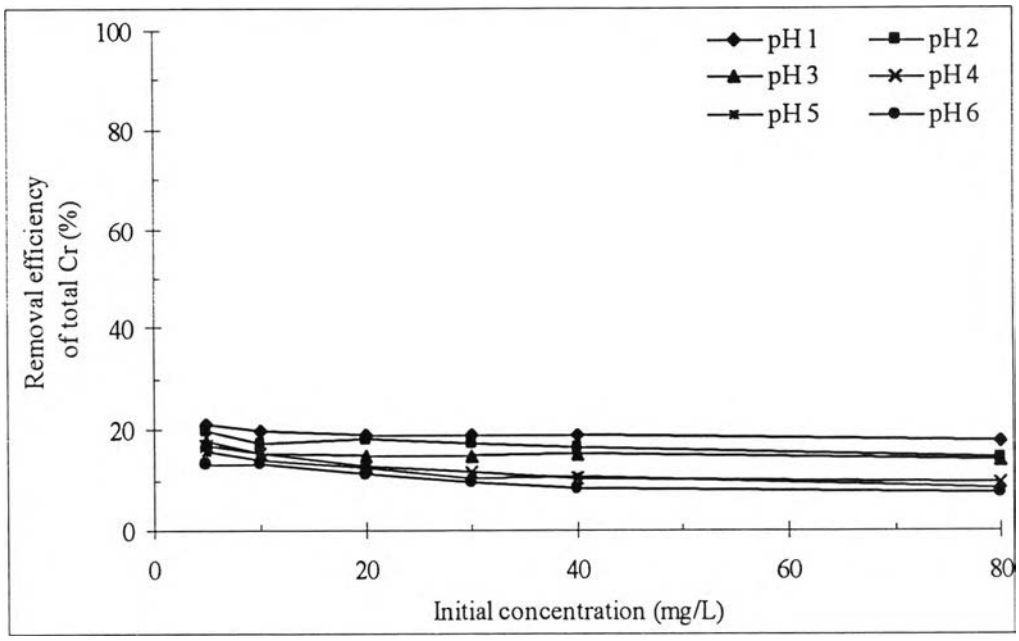

(a)

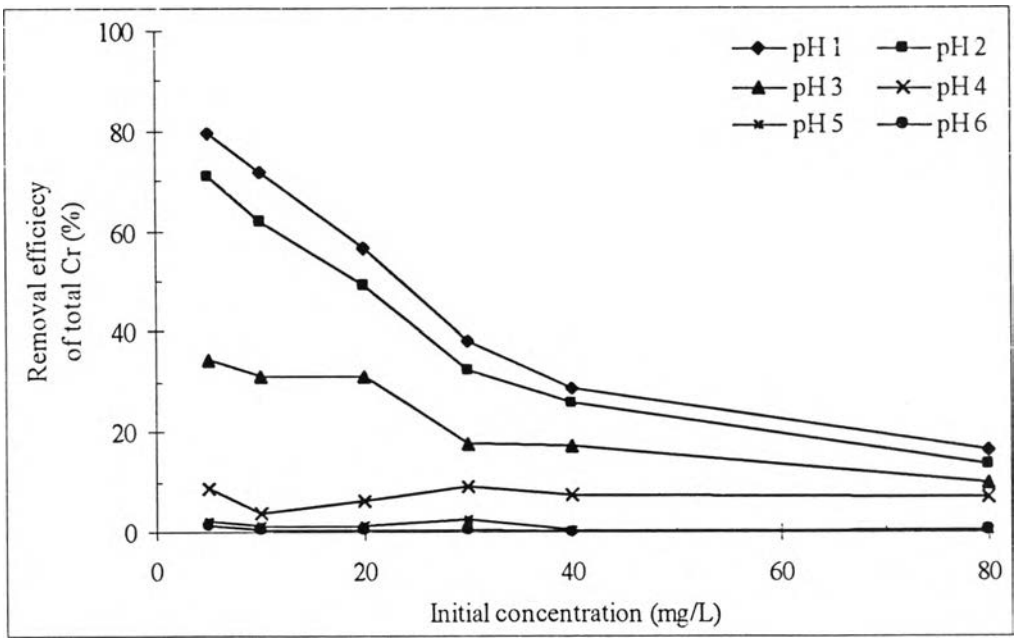

(b)

Figure 4.19 Effect of Solution pH and Initial Concentration on Removal of Total Cr by (a) Bagasse and (b) Bagasse Fly Ash (contact time 60 min, dose 20 g/L)

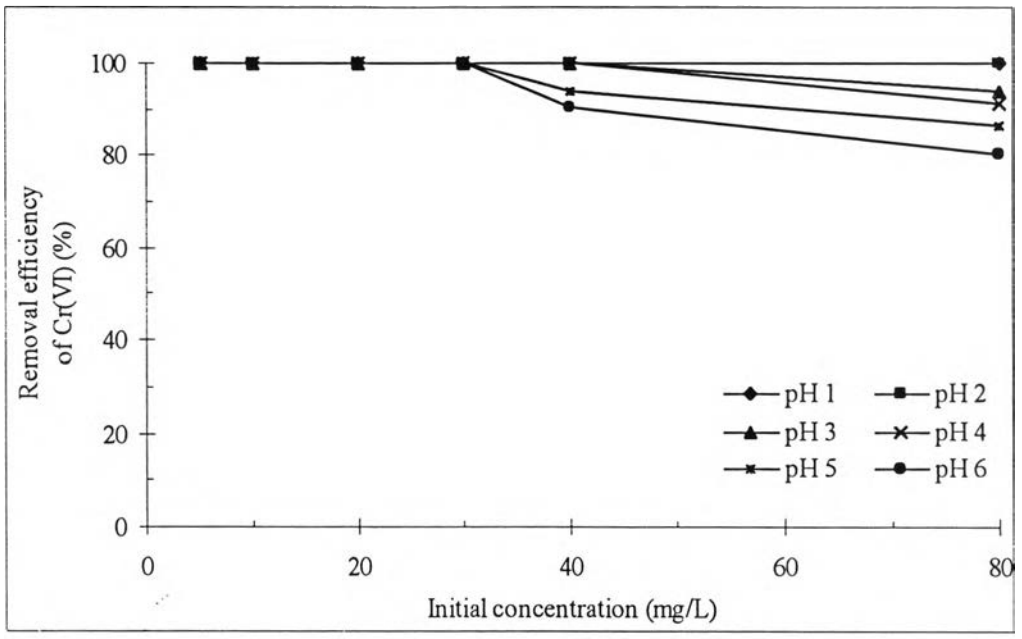

(a)

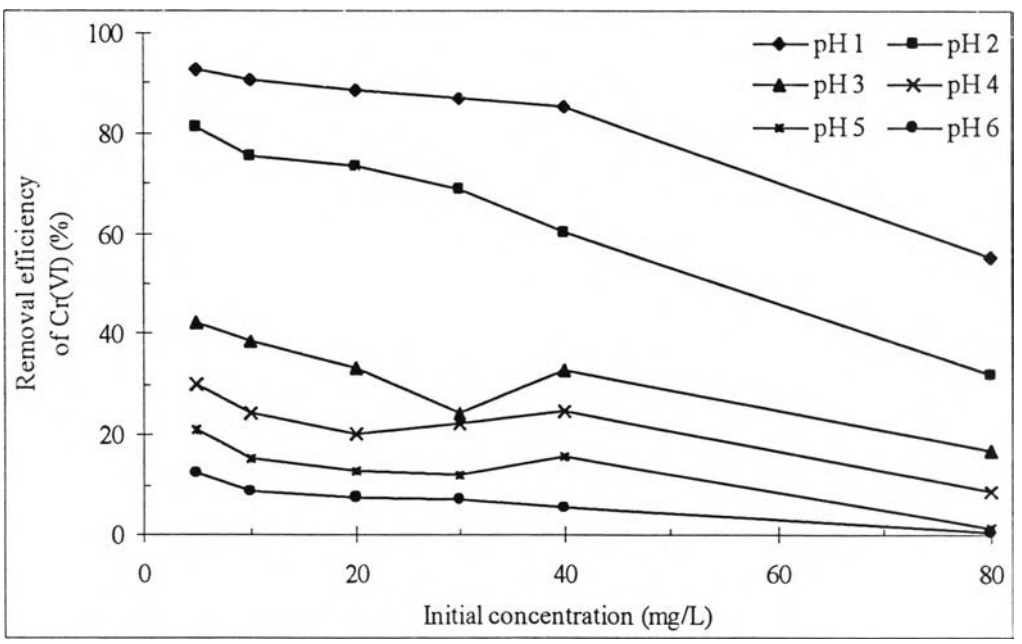

(b)

Figure 4.20 Effect of Solution pH and Initial Concentration on Removal of Cr(VI) by (a) Bagasse and (b) Bagasse Fly Ash (contact time 60 min, dose 20 g/L)

4.3.2.3 Effect of Solution pH

The influence of pH on chromium removal for several initial Cr(VI) concentrations is presented in Figures 4.19 and 4.20. The total Cr removal and Cr(VI) conversion were found to be greatly dependent on pH. The total Cr and Cr(VI) removal were better under acidic conditions and amount of Cr(III) appearing in solution was contemporaneously increased in the same way. These results indicated that the total Cr and Cr(VI) removal decreased with increasing solution pH and reduction and adsorption of Cr(VI) were highly efficient in acidic condition. Similar result was observed by several workers (Selvaraj, et al., 2003; Guo, et al., 2002; Das, et al., 2000; Ajmal. et al., 1996; Bayat, 2002; Pradhan, et al., 1999; Bishnoi, et al., 2004; Daneshvar, et al., 2002).

In case of adsorption, the high adsorption of Cr(VI) at low pH can be explained by considering the point of zero charge of the materials and the species of chromium. At acidic pH, the predominant species of Cr(VI) are dichromates ($Cr_2O_7^{2-}$), acid chromates ($HCrO_4^-$), and chromates (CrO_4^{2-}) as shown in Figure 2.4. As mentioned above, under acidic conditions, the positive charge density on the surface of the materials increases, it become protonated. The electrostatic force of attraction between the sorbent surface and the anionic species of Cr(VI) were increased, thereby increasing available sites for the adsorption of Cr(VI) ions. As the pH is increased above the zeta potential of the adsorbent, there is a reduction in the electrostatic attraction between the Cr(VI) species and the adsorbent surface, with a consequent decrease in percentage adsorption (Selvaraj, et al., 2003). In addition, the decrease in adsorption at higher pH values maybe due to the competitiveness of the oxyanions of chromium and OH^- ions in the solution (Das, et al., 2000; and Pradhan, et al., 1999)

As mentioned above, adsorption was the main mechanism for removal of Cr(VI) by bagasse fly ash. FT-IR spectra showed that inorganic compounds (silica or silicate) were possible functional groups of bagasse fly ash. SiO_2 could adsorb either positive or negative contaminants depending on the pH of the solution (Bayat,

2002). The central ion of silicates has an electron affinity, giving the oxygen atoms bound to it low basicity. This condition allows the silica surface to act as a weak acid, which can react with water, forming surface silanol (SiOH) groups. As a result, at low pH the silica surface is positively charged and at high pH values it is negatively charged. This condition indicates that the maximum Cr(VI) adsorption capacity of the bagasse fly ash can be attributed to the electrostatic interaction of the adsorbate with surface silica sites. This consideration also explains why bagasse fly ash with high SiO_2 content is more effective adsorbent than the bagasse at equilibrium conditions for Cr(VI) ions.

The Cr(VI) removal is opposite from Pb(II) removal may by due to the characteristic of ion in solution. Namely, Pb(II) is cation in solution, meanwhile, Cr (VI) is anion in solution, as mentioned in section 2.2.

In case of reduction process, it was found that in some studies dealing with Cr(VI) reduction, it has been reported that the Cr(VI) reduction efficiency of reducing agent depends largely on amount of acid and that reduction reaction rapidly occurs at low pHs (Erdem, et al, 2004). It is because of the fact that protons are consumed during the reduction of Cr(VI) as follows (Park, et al, 2004):

$$Cr_2O_7^{2-} + 14H^+ + 6e^- \Leftrightarrow 2Cr^{3+} + 7H_2O$$

$$CrO_4^{2-} + 8H^+ + 3e^- \Leftrightarrow Cr^{3+} + 4H_2O$$

$$HCrO_4^- + 7H^+ + 3e^- \Leftrightarrow Cr^{3+} + 4H_2O$$

$$H_2CrO_4 + 6H^+ + 3e^- \Leftrightarrow Cr^{3+} + 4H_2O$$

Thus, in the strong acidic condition in which there are high amount of protons, the reduction efficiencies were more than those of the weaker ones. This equation explains and confirms the important role played by pH in the removal of Cr (VI).

From the results, the removal process of Cr(VI) is enhanced in the highly acidic pH range. Taking into explanation that the Cr(VI) bearing wastewaters are often highly acidic (even below pH 1) (Zouboulis, et al., 1994). It becomes apparent that the reduction step could be carried out even more effectively at these acidic media.

4.3.2.4 Effect of Dosage

The effect of the quantity of materials on the total Cr and Cr(VI) removal were determined as shown in Figures 4.21 and 4.22. It was found that, increase in both materials from 1 to 40 g/L led to an expected increase in total Cr and Cr(VI) removals. In the meantime, the amount of Cr(III) increased. Nevertheless, bagasse doses of more than 20 g/L were enough to complete the removal of Cr(VI) within 60 min. It should be noted that a further increase in bagasse dosage higher than 20 g/L had a negligible effect on the Cr(VI) conversion. However, bagasse fly ash was unable to remove Cr(VI) completely and more than 25 g/L dosage was required. Bagasse had higher partial reduction efficiency than bagasse fly ash and was required in the lower dosage as shown in Figure 4.23. The increase in the removal with increase in the material dosage is due to the increase in the number of reaction sites or active sites. Similar trend has been observed for the removal of Cr(VI) by other materials (Selvaraj, et al., 2003; Das, et al., 2000; Raji and Anirudhan, 1998; Bishnoi, et al., 2004).

Generally, the addition of 10-25 g/L of bagasse, followed by a 60 min mixing step in the equilibrium pH around of 2, was found to be sufficient for 90-100% removal of Cr(VI) from a solution containing initially 80 mg/L Cr(VI).

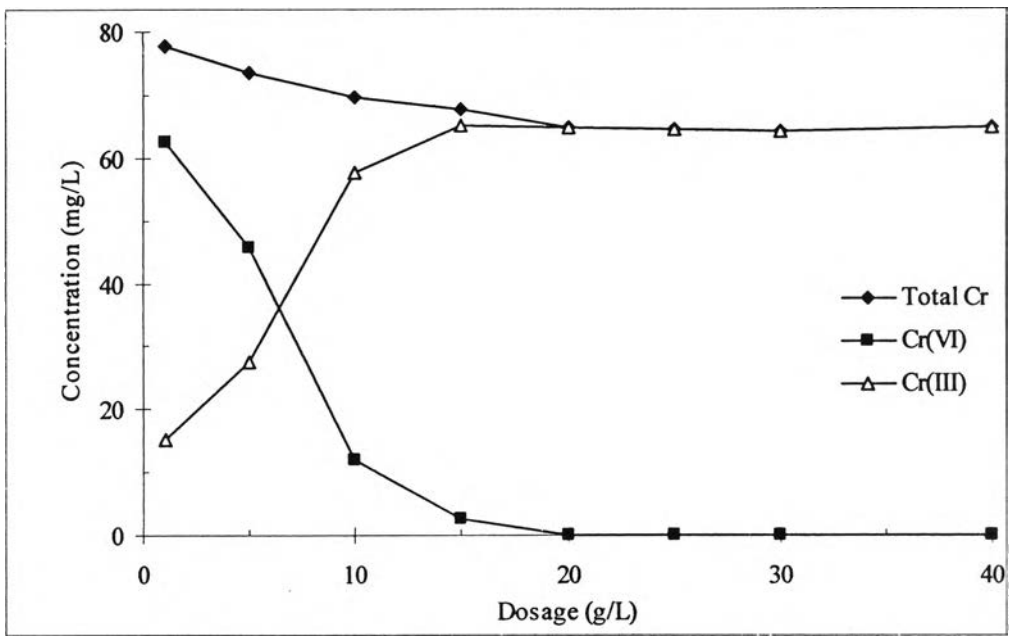

(a)

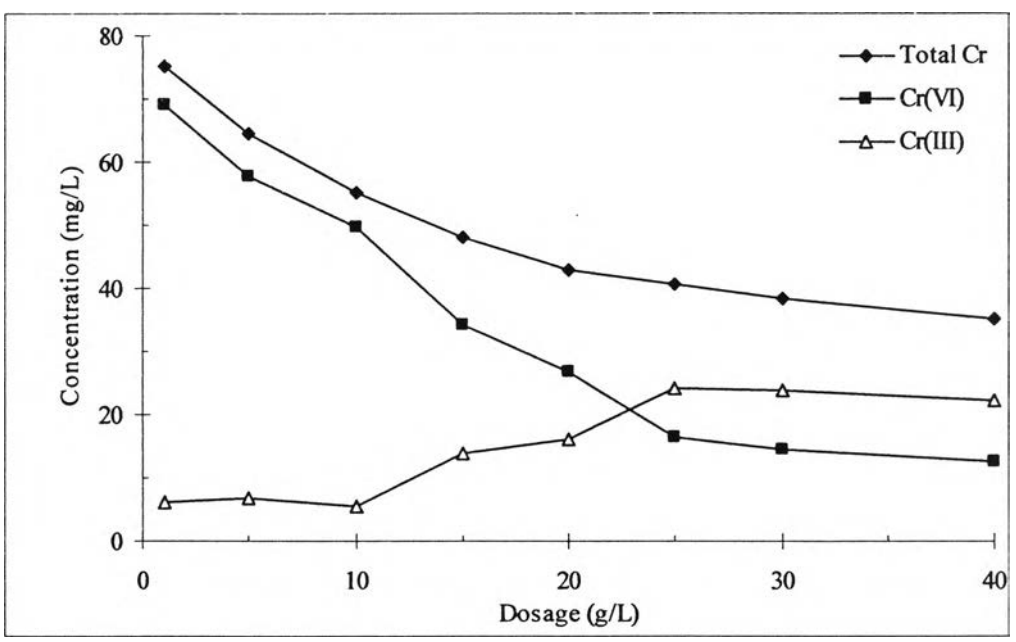

(b)

Figure 4.21 Effect of Dosage on Final Concentration by (a) Bagasse and (b) Bagasse Fly Ash (contact time 60 min, initial concentration 80 mg/L, solution pH 1)

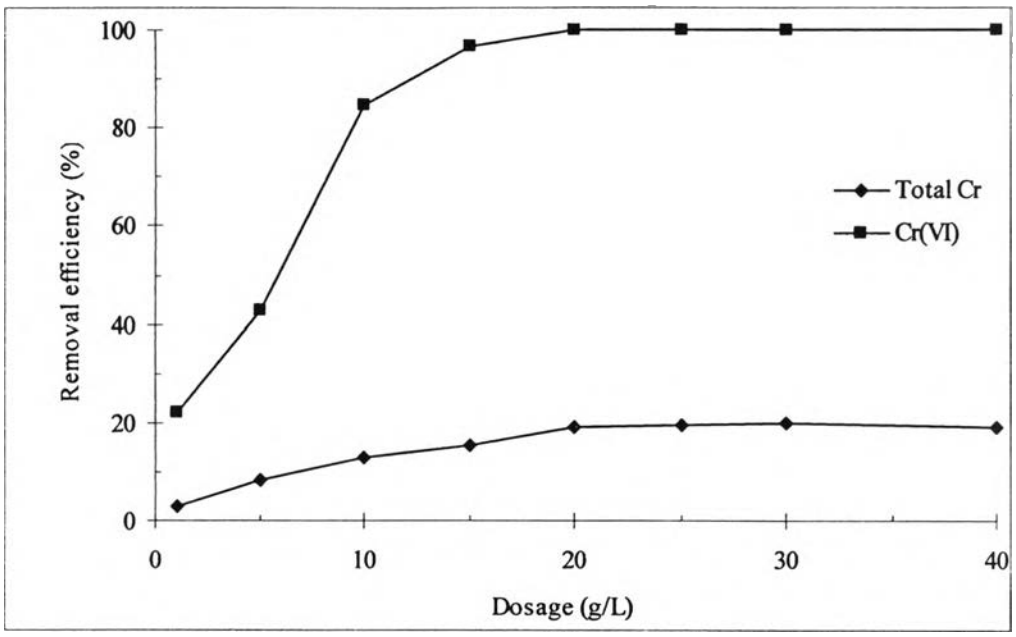

(a)

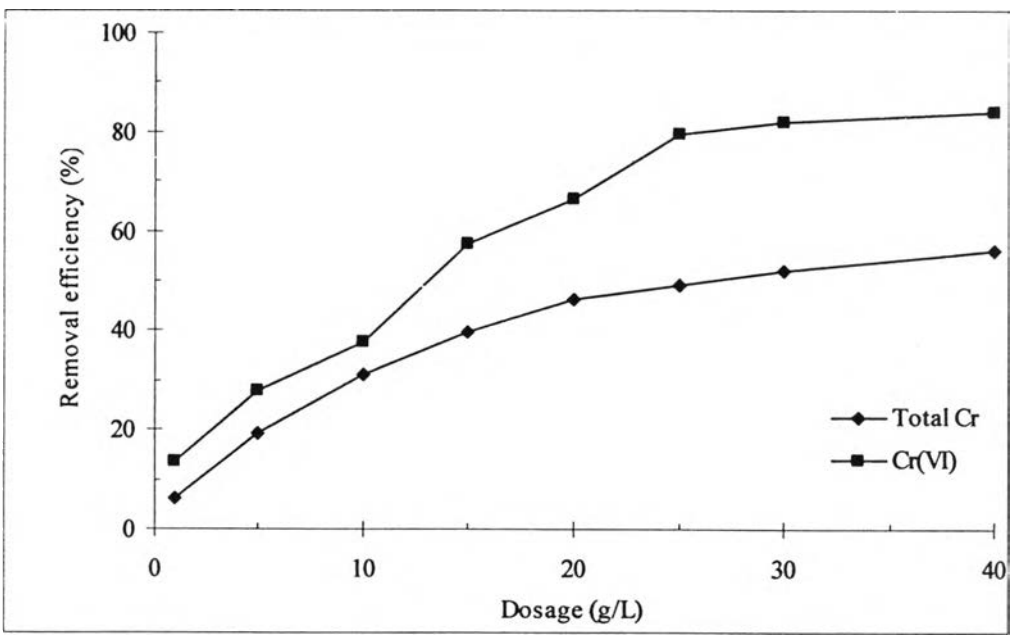

(b)

Figure 4.22 Effect of Dosage on Removal Efficiency by (a) Bagasse and (b) Bagasse Fly Ash (contact time 60 min, initial concentration 80 mg/L, solution pH 1)

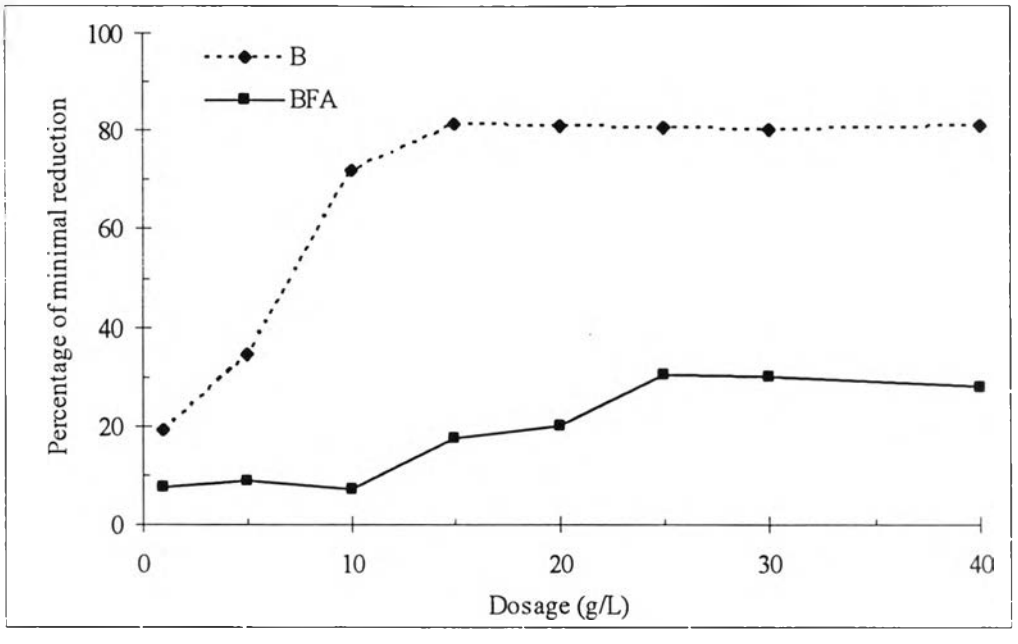

Figure 4.23 Effect of Dosage on Percentage of Minimal Reduction by (a) Bagasse and (b) Bagasse Fly Ash (contact time 60 min, initial concentration 80 mg/L, solution pH 1)

4.3.2.5 Kinetics Analysis

Correlations of rate data may be sought for any of several purposes. Process engineer may wish to develop a model for a specific reaction so as to be able to predict the effect of reactor operating changes on performance (Satterfield, 1980). The models of removal kinetics correlate the solute uptake rate, so these models are important in water treatment process design (Selvaraj, et al., 2003). The rate constant for remove of Cr(VI) by bagasse and bagasse fly ash was studied using the zero-order, first-order, second-order, and Langmuir-Hinshelwood (L-H) model.

The experimental conditions, equation and related statistic parameters are reported in Table 4.11. The identification of kinetic model, among the mentioned four, which best fitted the experimental results has been evaluated using the correlation coefficient (R^2). Form this Table, the L-H models present good fit to the

experimental data. Figure 4.24 (a) and (b) show the results of the kinetic study of bagasse and bagasse fly ash, respectively. L-H model are generally recognized mathematical relationships developed to describe the distribution of a substance that are adsorbed on surface of adsorbent and then reacted to form products. Rate expressions can be derived for any type of postulated mechanism. The form and complexity of the expression depend on the assumptions made concerning this mechanism. A few cases are presented in Appendix.

Table 4.11 Kinetic Analysis Data of Bagasse and Bagasse Fly Ash

Conditions	Type of Model	Equation	R^2
B-Cr(VI)	Zero-order	y = 0.3815x - 0.6075	0.9495
	First-order	y = -0.064x + 2.5162	0.7854
	Second-order	y = 0.0103x + 0.064	0.6737
	Langmiur-Hinshelwood	y = 0.2035x - 0.023	**0.9871**
BFA-Cr(VI)	Zero-order	y = 0.2141x + 0.7505	0.8298
	First-order	y = -0.0396x + 2.1767	0.9429
	Second-order	y = 0.0084x + 0.0946	0.9803
	Langmiur-Hinshelwood	y = 0.1315x + 0.0037	**0.9804**

According to the L-H model, the reaction rate (r) is proportional to the fraction of surface covered by the substrate. In each case the following expression can be obtained:

$$r = kKC / 1+KC$$

where K is the apparent equilibrium of adsorption constant, k the apparent reaction rate constant, and C is the concentration at any time.

Table 4.12 Langmiur-Hinshelwood Parameters for Cr(VI) Removal by Bagasse and Bagasse Fly Ash

Condition	K (L/mg)	k (mg/L min)	Reaction rate (r)
B	-0.2035	0.1130	-0.0230 C / 1-0.2035 C
BFA	-0.1315	-0.0281	0.0037 C / 1-0.1315 C

The L-H isotherm serves to describe the rate of transformation, and may be used for reactor optimization, but they have no physical meaning, and may not be used to identify surface processes (Galve and Rodriguez).

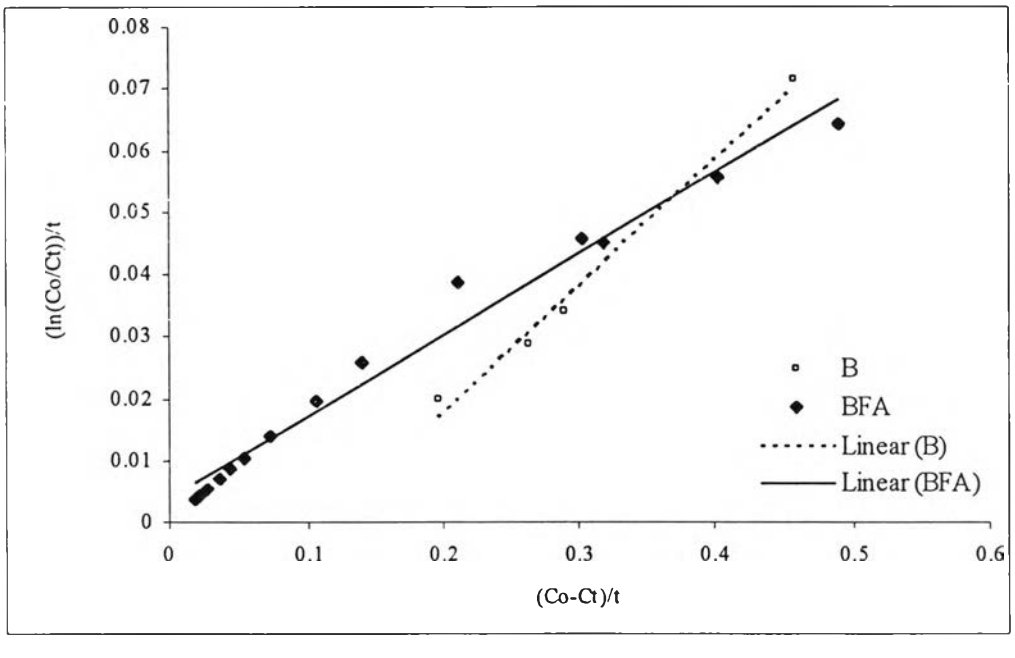

Figure 4.24 Test of Langmiur-Hinshelwood Model for Cr(VI) Removal by Bagasse and Bagasse Fly Ash (contact time 60 min, initial concentration 80 mg/L, solution pH 1)

Bagasse and bagasse fly ash after use as an adsorbent can be employed as a filling material in pavement linings, in soil stabilization, in cement and concrete industries, or can be disposed off in a landfill. For this study, after heavy metal removal process, both of materials were investigated the feasibility to be disposed off in landfill and the feasibility to replace cement in concrete blocks.

4.4 Solidification and Stabilization (S/S) Study

Compressive strength of a concrete is a property that provides a good indicator of its quality. Therefore, in this part, the results were presented in ksc (kg/cm^3) unit of compressive strength and relative compressive strength in percent unit. In S/S system, the interested binders involved 6 materials namely; bagasse (B), lead adsorbed bagasse (B-Pb), chromium adsorbed bagasse (B-Cr), bagasse fly ash (BFA), lead adsorbed bagasse fly ash (BFA-Pb), and chromium adsorbed bagasse fly ash (BFA-Cr).

4.4.1 Bagasse

From the removal study results, it was found that the maximum adsorption capacity of bagasse adsorbing lead occured at the following condition; solution pH 6, initial concentration approximately 80 mg/L, and bagasse dose 10 g/L. Adsorption capacity of bagasse in these condition was 4.0552 mg/g. In case of chromium, maximum adsorption capacity was 0.7114 mg/g at solution pH 1, initial concentration approximately 80 mg/L, and bagasse dose 20 g/L. These conditions were used for the works in this part because they should represent worst case scenario for leachability study.

4.4.1.1 Effect of replacement percentage

The experiments were measured using the conditions that were previously described in Table 3.4. The experimental results are summarized in Table 4.13 for four water-to-cement ratio (0.40, 0.50, 0.60, and 0.70) and three replacement percentages (5, 10, and 15%). Figure 4.25 showed mortar specimens which had cement replaced by bagasse at 0 to 15% and mortar specimens after unconfined compressive strength test. This figure showed that at 15% cement replacement, the mortars were unable to remain as cubes. Thus, the experiments with 15% replacement should be rejected.

In all cases of the specimens, the compressive strength was dependent on the amount of B, B-Pb, or B-Cr added in the binder system. It was observed that when B, B-Pb, or B-Cr substituted aggregates, compressive strength lower than the controls were obtained. The compressive strength and relative compressive strength decreased as the percentage of B, B-Pb or B-Cr in the mix was increased. Therefore, replacement of 5%, which yielded the best strength performance, was finally selected for curing time tests.

XRD analysis results as shown in Figures 4.26 (a) and (b), indicated that bagasse inhibited cement hydration. At 5% cement substitution with bagasse, the hydration product, $Ca(OH)_2$, is only detected at final setting times at very low concentrations (The hydration reaction as mentioned in equation 2.8-2.10). The distinct diffraction peak of $Ca(OH)_2$ is at 18.08° 2θ and 34.16° 2θ, and for C_3S, at 29.44° 2θ and 50.84° 2θ. Most detected components were raw components of Portland cement; C_2S and C_3S. The Portland cement hydration was inhibited by the increasing amount of bagasse. The reasons for the poor compressive strength for the specimens containing bagasse may be due to very low bulk specific gravity of bagasse as mentioned in Section 4.1.1. This result in, porosity of mortar and low compressive strength, as a results. In addition, the poor contact between the portlandite may occur when mortar containing bagasse. They may be interrupt dissolution-precipitation reaction of hydration reaction as mentioned in Section 2.5.2.

The analysis of variance (ANOVA) was shown in Table 4.14. The P-value is the probability of being wrong in concluding that there is an association between dependent and independent variables. The smaller the P-value, the greater the probability that there is an association (Bayat, 2002). Using the ANOVA at a 99.50 % confidence level, it was found that there was significant difference ($p<0.005$) among the w/c ratios and replacement percentage, while there was no significant difference ($p>0.005$) among the types of bagasse (B, B-Pb, and B-Cr). Traditionally, it is concluded that type of bagasse did not have and influence on compressive strength. While, the varied w/c ratios and replacement percentages had an effect on compressive strength.

Table 4.13 Compressive Strength and Relative Compressive Strength at Difference Percent Replacements and Water-to-Cement Ratios of B, B-Pb and B-Cr at 7-day Curing Time

Percent replacement	w/c ratio	Compressive strength (ksc)			Relative compressive strength (%)		
0	0.40	230.20			100.00		
	0.50	229.36			100.00		
	0.60	185.20			100.00		
	0.70	144.48			100.00		
		B	**B-Pb**	**B-Cr**	**B**	**B-Pb**	**B-Cr**
5	0.40	73.70	77.47	70.58	32.01	33.65	30.66
	0.50	69.63	66.70	68.38	30.36	29.08	29.81
	0.60	19.33	24.46	25.02	10.44	13.21	13.51
	0.70	9.57	12.23	10.84	6.62	8.46	7.51
10	0.40	4.00	4.06	4.11	1.74	1.76	1.78
	0.50	4.74	4.12	4.90	2.07	1.80	2.14
	0.60	1.68	2.07	1.90	0.91	1.12	1.03
	0.70	0.81	1.06	0.93	0.56	0.73	0.64

Table 4.14 The two-way ANOVA Results of Bagasse at 99.50% Confidence Level

w/c ratio	Between type of B		Between percent replacement	
	P-value	**meaning**	**P-value**	**meaning**
0.40	0.199	No difference	1.02E-06	Difference
0.50	0.152	No difference	1.62E-08	Difference
0.60	0.478	No difference	1.5E-05	Difference
0.70	0.674	No difference	3.56E-07	Difference
Percent replacement	**Between type of B**		**Between w/c ratio**	
	P-value	**meaning**	**P-value**	**meaning**
0	0.676	No difference	5.55E-05	Difference
5	0.529	No difference	2.07E-07	Difference
10	0.686	No difference	6.57E-06	Difference

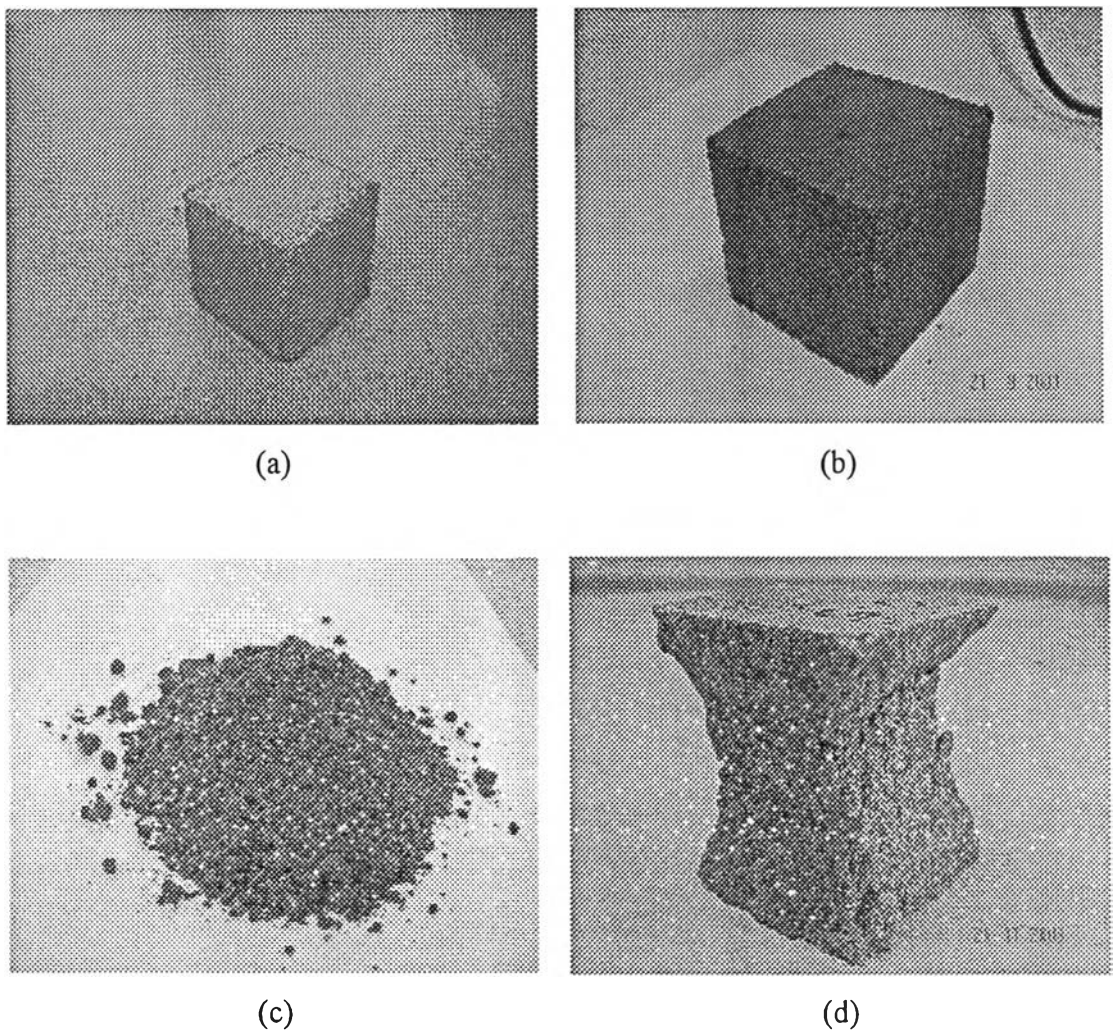

Figure 4.25 Mortar Specimens with Cement Replaced by Bagasse at (a) 0%, (b) 10%, (c) 15% and (d) after Compressive Strength Test

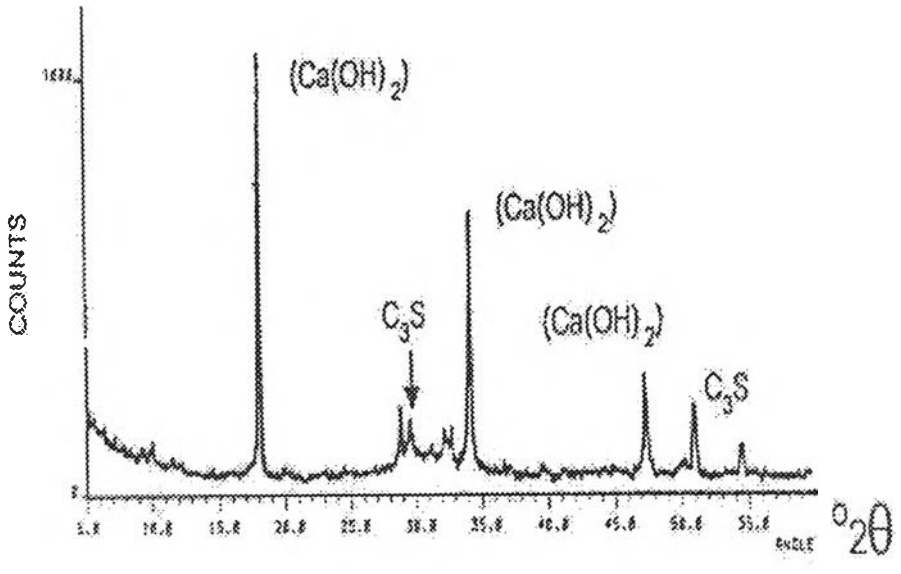

(a)

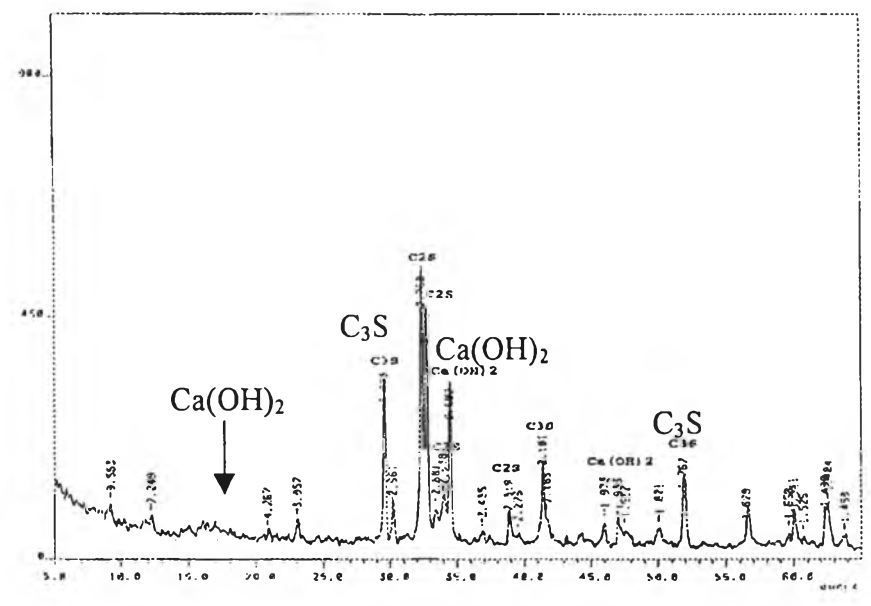

(b)

Figure 4.26 XRD Spectra of Mortars with (a) 0% replacement and (b) 5% replacement with Bagasse at w/c ratio of 0.45 and 7-day Curing Time.

4.4.1.2 Effect of water-to-cement ratio

Figures 4.27, 4.28, and 4.29 demonstrate that the compressive strength of mortar is affected by water-to-cement ratio at 0-10% replacement of B, B-Pb and B-Cr. Based on the results, the compressive strength of specimens with water-to-cement ratio of 0.40, and 0.50 was almost level. The w/c ratio of 0.50 was finally selected for curing time tests.

Water is essential to initiate the hydration reactions but a broad range of w/c ratio can be sustained (Glasser, 1997). In the w/c ratio more than 0.50, the compressive strength decreased. In the study, therefore, the optimum value of w/c ratio was set at 0.40-0.50. It is also well known that strength decreases as matrix porosity increases, and that porosity increases as the w/c ratio increases above an optimal value (Stegemann and Buenfeld, 2002). Then, more than 0.50 w/c ratio is above an optimal value.

4.4.1.3 Effect of curing time

Figure 4.30 shows the change in compressive strength and relative compressive strength with age at w/c ratio of 0.50, 0 and 5% replacement. It is observed that, for all specimens, the compressive strength increased with curing time, but sample specimens notable increases the compressive strength of concrete compared to control concrete at all ages (up to 28 days). However, in all cases, the values of compressive strengths of specimens after a 3-day curing were enough to meet the landfilling standard (3.5 kg/cm^2) established by the Ministry of Industry No.6, B.E. 2540 (1997).

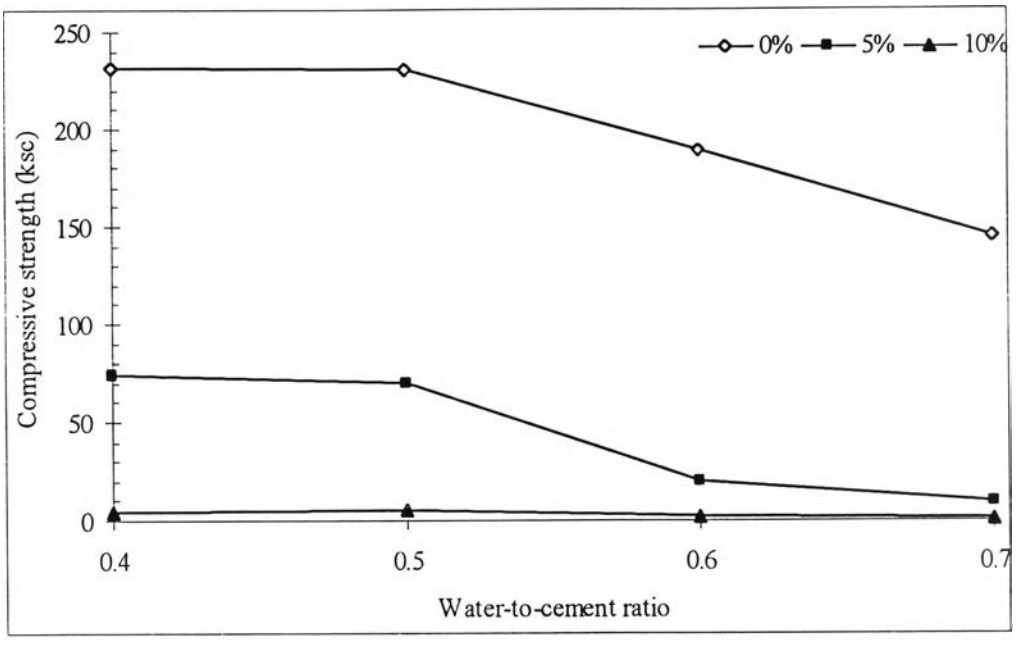

(a)

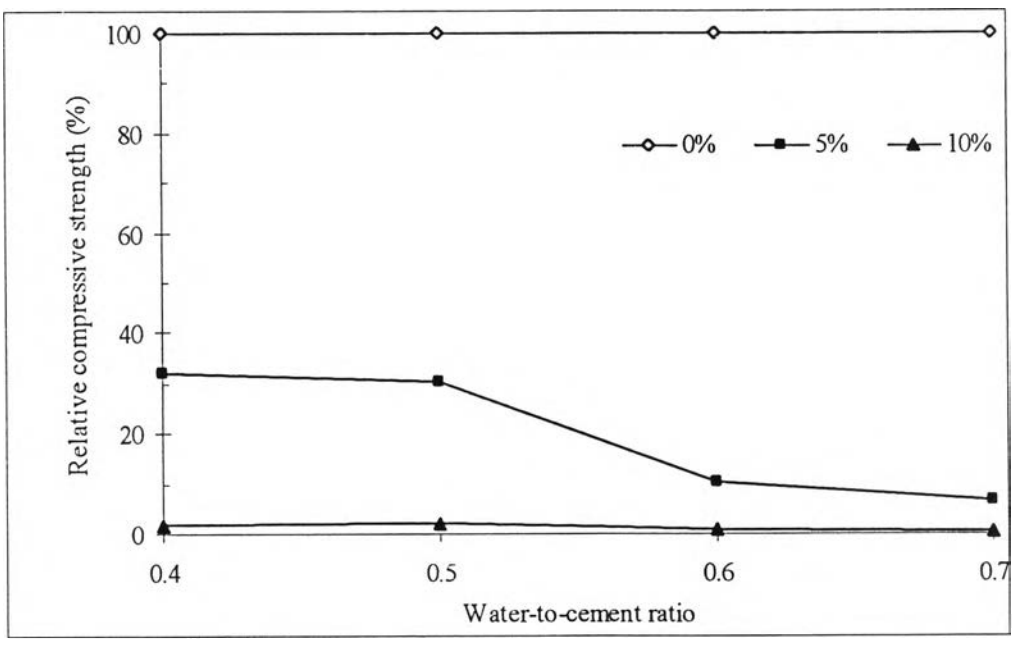

(b)

Figure 4.27 Development of (a) Compressive Strength and (b) Relative Compressive Strength of Bagasse-Cement Mortar at Different Percent Replacements and Water-to-Cement Ratios at 7-day Curing

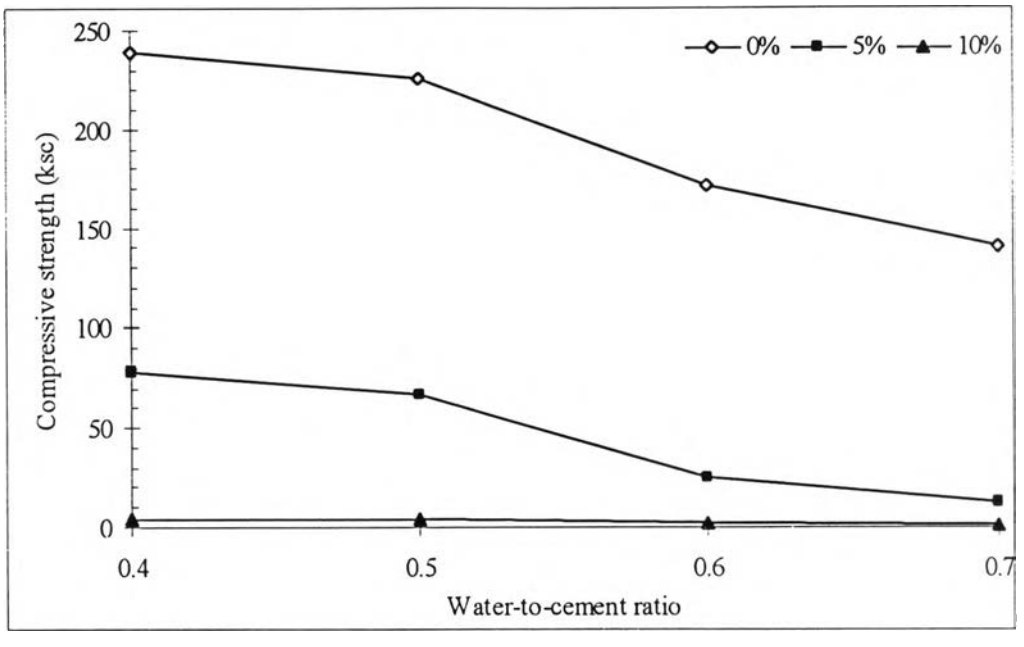

(a)

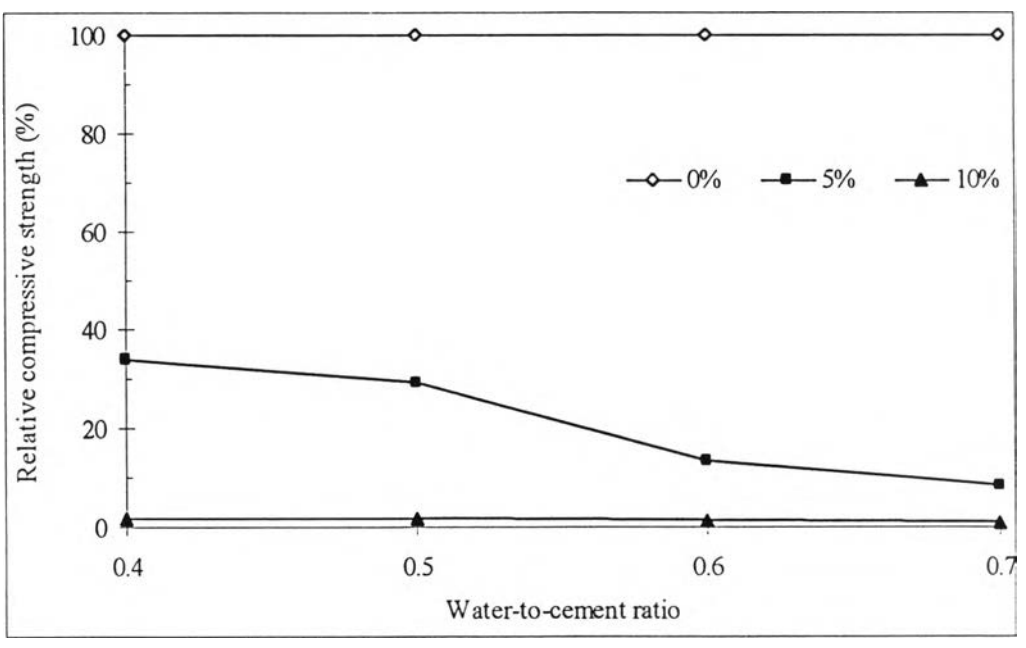

(b)

Figure 4.28 Development of (a) Compressive Strength and (b) Relative Compressive Strength of Pb adsorbed Bagasse-Cement Mortars at Different Percent Replacements and Water-to-Cement Ratios at 7-day Curing

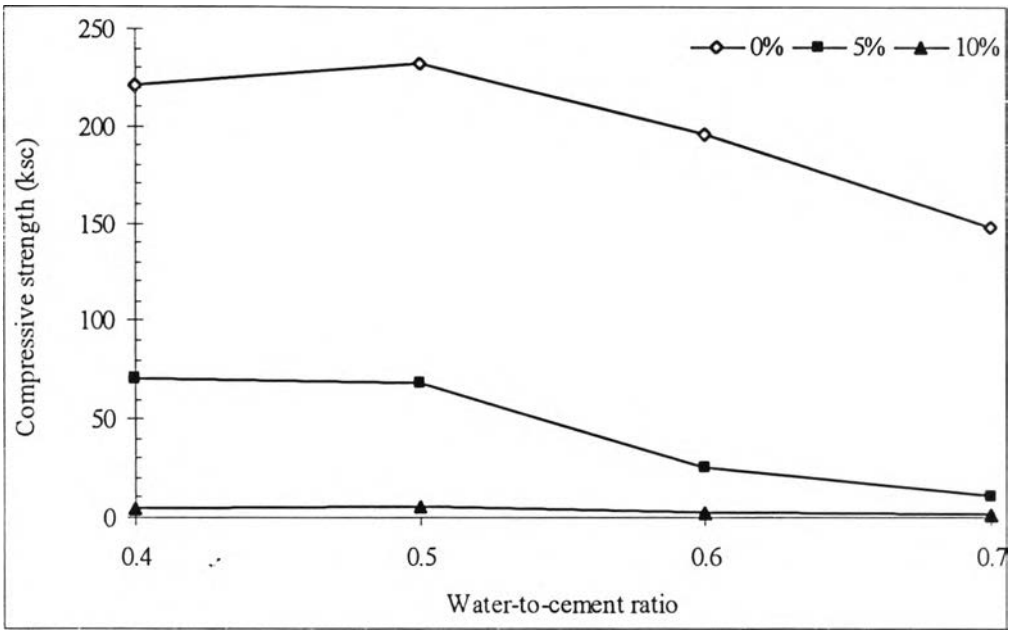

(a)

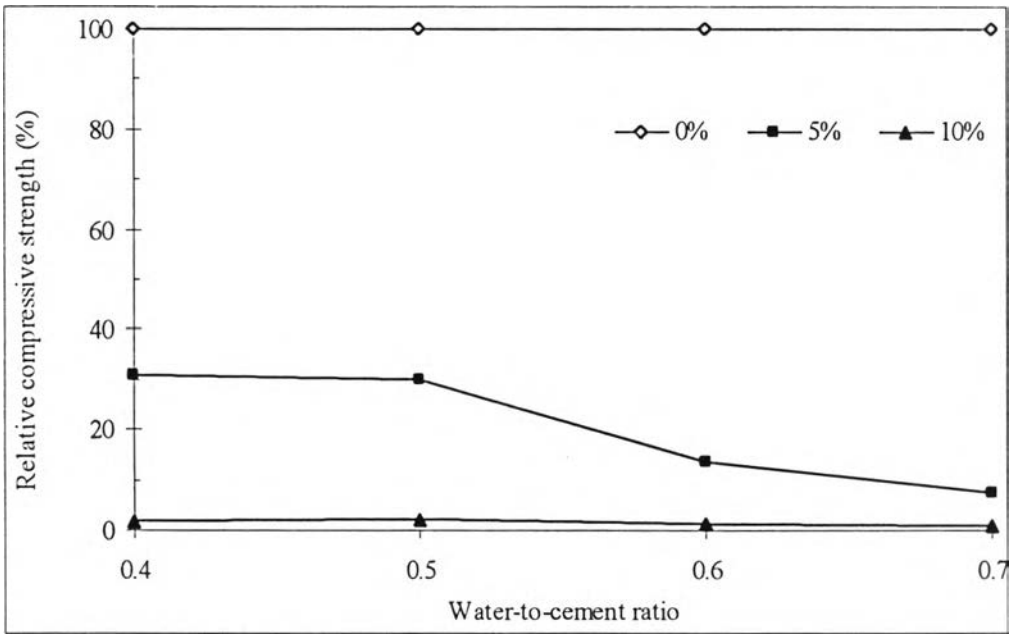

(b)

Figure 4.29 Development of (a) Compressive Strength and (b) Relative Compressive Strength of Cr adsorbed Bagasse-Cement Mortar at Different Percent Replacements and Water-to-Cement Ratios at 7-day Curing

4.4.1.4 Leachate characteristics

Leachate characteristics study focuses on concentrations of Pb and Cr that can leach from B-Pb and B-Cr, respectively, or their solidified matrices. The results of the leaching test are presented in Tables 4.15, 4.16 and 4.17 along with the limit values of Pb and Cr (5 mg/L) established by the Ministry of Industries No. 6, B.E. 2540 (1997).

The results of the test are expressed in three units namely, milligrams of contaminants (heavy metals) per litre of leachate which are detected by ICP-OES, milligrams of heavy metals per grams of B-Pb or B-Cr determined by calculation, and percent release of heavy metals which adsorbed onto bagasse which by calculation.

Pb and Cr concentrations in leachates from the solidified specimens were lower than 0.2 mg/L in all cases of replacement ratio (5, 10, and 15%), w/c ratio (0.40, 0.50, 0.60, and 0.70), and curing time (3, 7, 14, and 28 days). The results indicated that the concentrations of all cases were well below the limits established by the Ministry of Industries (1997). These showed that the cementitious solidification process is effective, even after a short curing time (3 days). The final pH value of the leaching solution was high (about 9) because of the concurrent release of calcium hydroxide and alkalies from the cementitious matrices. It indicated that this process was able to strongly immobilize Pb and Cr.

Pb and Cr concentrations from condition of with Portland cement were less than without Portland cement condition. This results show that the hydration reaction may improve the fixation of the heavy metals. When water is added to cement, a hydration reaction takes place. The hydration products crystallize and create a three-dimensional structure that binds together all the substances present into a hard mass. The three-dimensional structure formed, which comprises hydration products, water, small bubbles of air, and particles of sand or stone, can also include small particles (< 150 μm). Since bagasse particles have a small grain size they could fill these spaces and become encapsulated inside the concrete matrices.

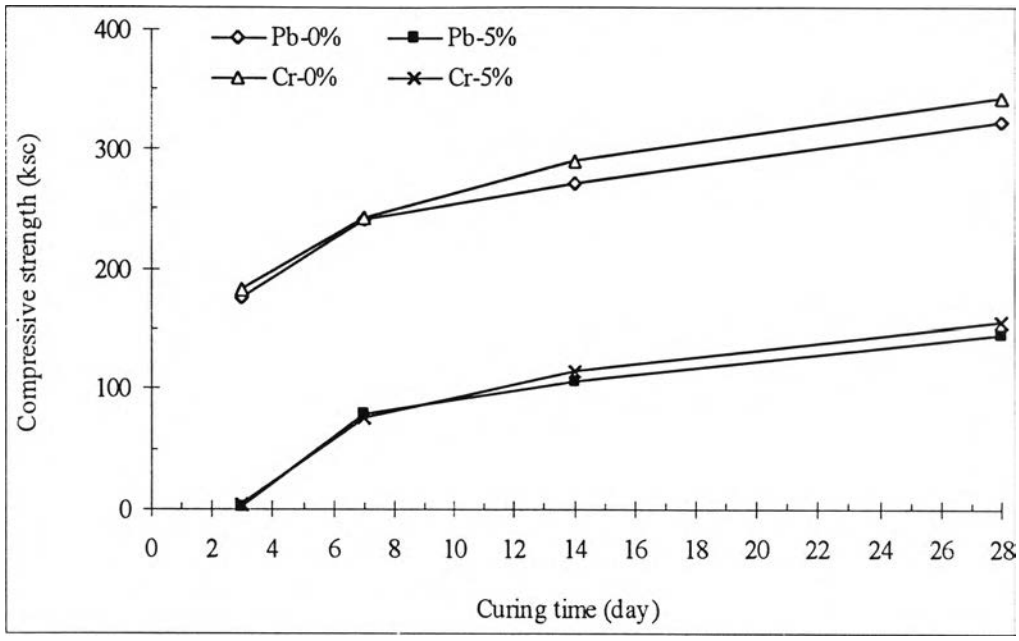

(a)

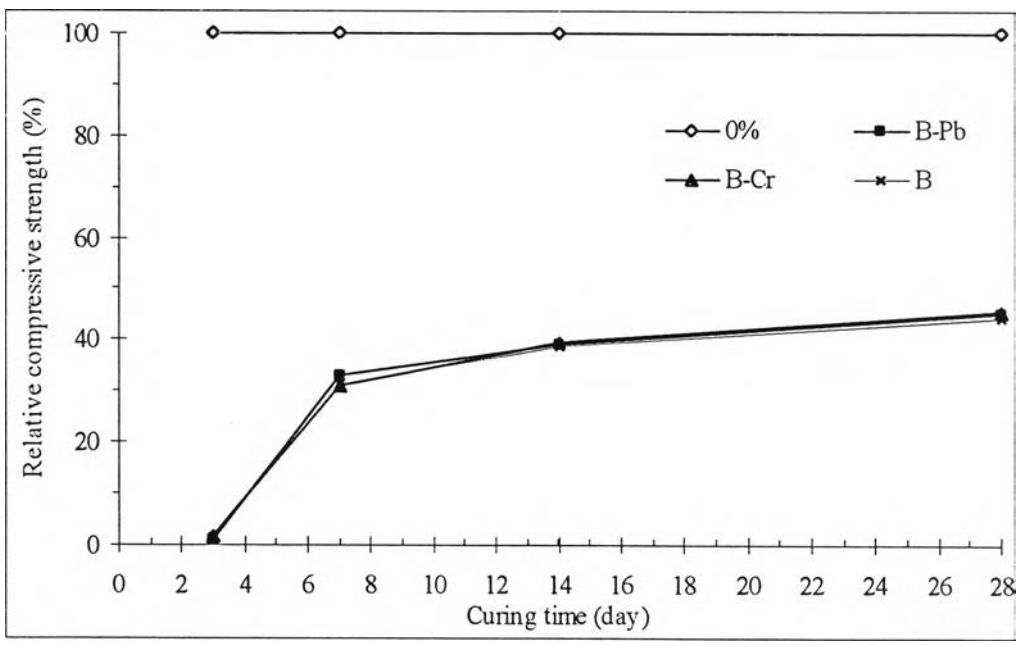

(b)

Figure 4.30 Development of (a) Compressive Strength and (b) Relative Compressive Strength at Different Curing Times of B, B-Pb, and B-Cr (w/c ratio of 0.50, 5% replacement)

Table 4.15 Amount of Released Pb from B-Pb, with and without Portland Cement at Different w/c ratios and Percentages of Replacement (%R)

Condition	w/c ratio	% R of Portland cement	Released Pb		
			mg/L	mg/g	% release
With Portland cement	0.40	5	ND	NC	NC
		10	ND	NC	NC
		15	0.01000	0.00054	0.01333
	0.50	5	ND	NC	NC
		10	ND	NC	NC
		15	0.00912	0.00049	0.01211
	0.60	5	ND	NC	NC
		10	ND	NC	NC
		15	0.01021	0.00054	0.01333
	0.70	5	0.00114	0.00016	0.00401
		10	0.01105	0.00089	0.02196
		15	0.19007	0.01027	0.25326
Condition	**Amount of B-Pb (g)**	**% R of Portland cement equivalent**	**Released Pb**		
			mg/L	**mg/g**	**% release**
Without Portland cement	12.3	5	0.09594	0.01560	0.38469
	24.7	10	0.19143	0.01550	0.38223
	37.0	15	0.29045	0.01571	0.38716

Notation; ND refered to can not be detected, below the detection limits of ICP-OES
NC refered can not calculation

Table 4.16 Amount of Released Cr from B-Cr, with and without Portland Cement at Different w/c ratios and Percentages of Replacement (%R)

Condition	w/c ratio	% R of Portland cement	Released Cr		
			mg/L	mg/g	% release
With Portland cement	0.40	5	0.09112	0.01484	2.07991
		10	0.10604	0.00858	1.20647
		15	0.09843	0.00530	0.74461
	0.50	5	0.08611	0.01398	1.96562
		10	0.08824	0.00713	1.00159
		15	0.09623	0.00519	0.72942
	0.60	5	0.09714	0.01577	2.21704
		10	0.10403	0.00842	1.18371
		15	0.09901	0.00535	0.75221
	0.70	5	0.09814	0.01593	2.23989
		10	0.11212	0.00907	1.27476
		15	0.12611	0.00681	0.95736
Condition	**Amount of B-Cr (g)**	**% R of Portland cement equivalent**	**Released Cr**		
			mg/L	**mg/g**	**% release**
Without Portland cement	12.3	5	0.22571	0.03671	5.15872
	24.7	10	0.44954	0.03644	5.11655
	37.0	15	0.61975	0.03351	4.70892

Table 4.17 Concentration of Pb and Cr from Solidified Matrices of B-Pb and B-Cr at Different Curing Times

Curing time (day)	Concentration (mg/L)	
	Pb	Cr
3	0.012	0.106
7	0.004	0.086
14	0.001	0.056
28	ND	0.027

4.4.2 Bagasse Fly Ash

The removal study results showed that the maximum adsorption capacity of bagasse fly ash adsorbing lead occurred at the following condition: solution pH 6, initial concentration approximately 80 mg/L, and bagasse dose 10 g/L. Adsorption capacity of bagasse in this condition was 7.9149 mg/g. In case of chromium, maximum adsorption capacity was 0.6547 mg/g at solution pH 1, initial concentration approximately 80 mg/L, and bagasse dose 20 g/L. As mentioned above, these conditions were used for subsequent works in this part because they could represent worst case of heavy metal leaching study.

4.4.2.2 Effect of percentage of replacement

Table 3.4 showed the conditions that were used in the experiments. The experimental results are summarized in Table 4.18 for four w/c ratios (0.40, 0.50, 0.60, and 0.70) and three replacement percentages (10, 20, and 30%). Mortar specimens which portions of cement were replaced by bagasse fly ash at 0 to 30% were shown in Figure 4.31.

The experimental results showing similar trend as those of bagasse, when BFA, BFA-Pb or BFA-Cr substituted aggregates, compressive strength lower than the controls were obtained. The compressive strength and relative compressive

strength decrease as the amount of BFA, BFA-Pb or BFA-Cr in the mix were increased. And replacement of 10% was finally selected for curing time tests.

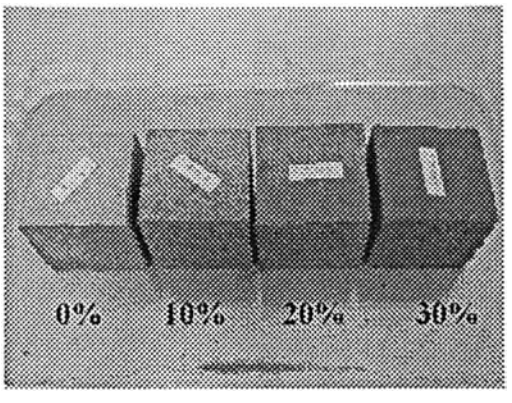

Figure 4.31 Mortar Specimens with Cement Replaced by Bagasse Fly Ash at 0, 10, 20, and 30%

XRD spectrum, Figure 4.32, indicated that bagasse fly ash inhibited cement hydration. The same results were obtained when bagasse was used. But, for bagasse fly ash, the hydration product $Ca(OH)_2$ was detected at higher intensities than in case of bagasse. Approximately, 1000 and 50 at 18.08° 2θ and 600 and 400 at 34.16° 2θ. The Portland cement hydration is inhibited by the addition of BFA, BFA-Pb, or BFA-Cr. The reasons for the poor compressive strength of the specimens containing them may be due to high free alkali metals oxides or MgO content in the BFA (Saikia, et al., 2002 and Kula, et al., 2002), or poor contact between the portlandite, or the low calcium content of BFA.

The analysis of variance (ANOVA) was shown in Table 4.19. The results have similar trend as those of bagasse, it was found that there was significant difference ($p<0.005$) among the w/c ratio and percent replacement, while there was no significant difference ($p>0.005$) among the types of bagasse (BFA, BFA-Pb, and BFA-Cr. It is concluded that type of bagasse fly ash was not effect on compressive strength. While, the value changed of w/c ratio and percent replacement were effect on compressive strength.

Table 4.18 Compressive Strength and Relative Compressive Strength at Difference Percent Replacements and Water-to-Cement Ratios of BFA, BFA-Pb and BFA-Cr at 7-day Curing Time

Percent replacement	w/c ratio	Compressive strength (ksc)			Relative compressive strength (%)		
0	0.40	263.00			100.00		
	0.50	298.86			100.00		
	0.60	236.77			100.00		
	0.70	184.80			100.00		
		BFA	**BFA-Pb**	**BFA-Cr**	**BFA**	**BFA-Pb**	**BFA-Cr**
10	0.40	149.32	152.87	143.40	56.77	58.12	54.53
	0.50	164.36	162.74	196.81	55.93	55.38	66.97
	0.60	123.63	123.58	132.24	52.22	52.20	55.85
	0.70	93.11	94.16	92.50	50.38	50.95	50.05
20	0.40	106.14	104.07	106.52	40.36	39.57	40.50
	0.50	117.40	113.75	136.06	39.95	38.71	46.30
	0.60	92.62	91.43	96.21	39.12	38.62	40.64
	0.70	65.95	67.30	63.04	35.69	36.42	34.11
30	0.40	87.98	99.30	93.64	33.45	37.76	35.61
	0.50	105.05	118.75	132.46	35.75	40.41	45.08
	0.60	80.43	73.68	83.86	33.97	31.12	35.42
	0.70	59.11	60.55	59.16	31.99	32.77	32.01

Table 4.19 Two-Way ANOVA Results of Bagasse Fly Ash at 99.50% Confidence Interval

w/c ratio	Between type of BFA		Between percent replacement	
	P-value	meaning	P-value	meaning
0.40	0.571	No difference	1.25E-08	Difference
0.50	0.009	No difference	3.94E-06	Difference
0.60	0.019	No difference	2.32E-08	Difference
0.70	0.020	No difference	3.89E-12	Difference
Percent replacement	**Between type of BFA**		**Between w/c ratio**	
	P-value	**meaning**	**P-value**	**meaning**
0	0.205	No difference	0.000661	Difference
10	0.475	No difference	0.000406	Difference
20	0.368	No difference	0.000152	Difference
30	0.289	No difference	0.000366	Difference

4.4.2.2 Effect of water-to-cement ratio

Figures 4.33, 4.34, and 4.35 demonstrate that the compressive strength of mortar is affected by w/c ratio at 0-30% replacement of BFA, BFA-Pb and BFA-Cr. Based on the results, the compressive strength for w/c ratio of 0.4, 0.5 and 0.6 was level. As mentioned above, water is essential to initiate hydration reactions but a broad range of water-to-cement ratio can be sustained. It can seen that at w/c ratio of 0.7, the lowest compressive strength values were obtained for all of specimens, then, w/c ratio of 0.7 is above an optimal value (0.4-0.6). Therefore, w/c ratio of 0.50 was finally selected for curing time tests.

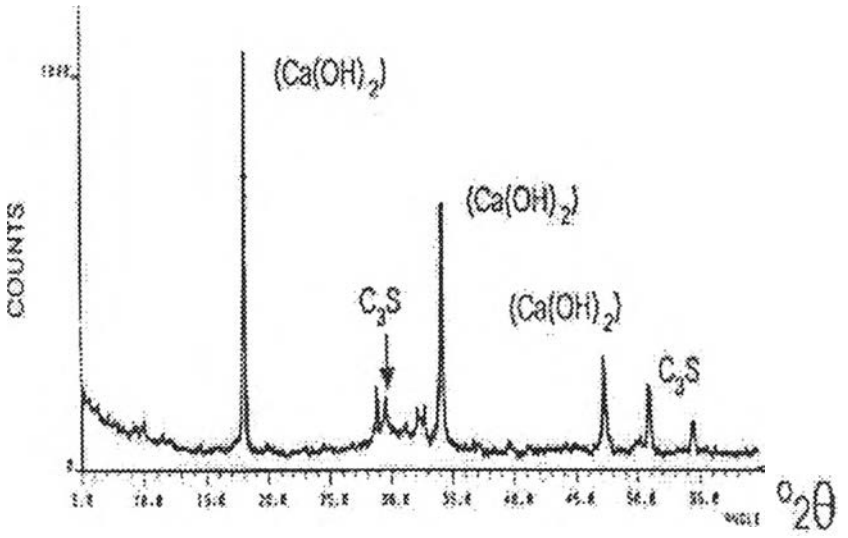

(a)

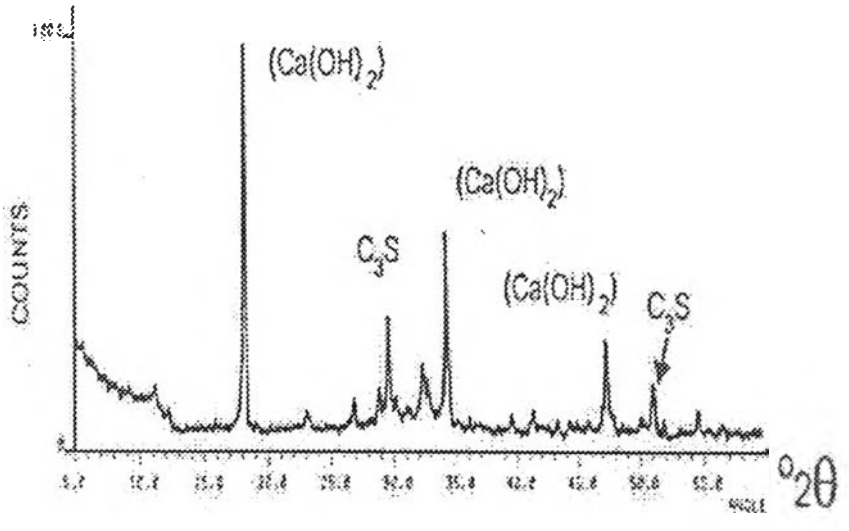

(b)

Figure 4.32 XRD Spectra of Mortars with (a) 0% replacement and (b) 15% replacement with Bagasse Fly Ash at w/c ratio of 0.50 and 7-day Curing Time

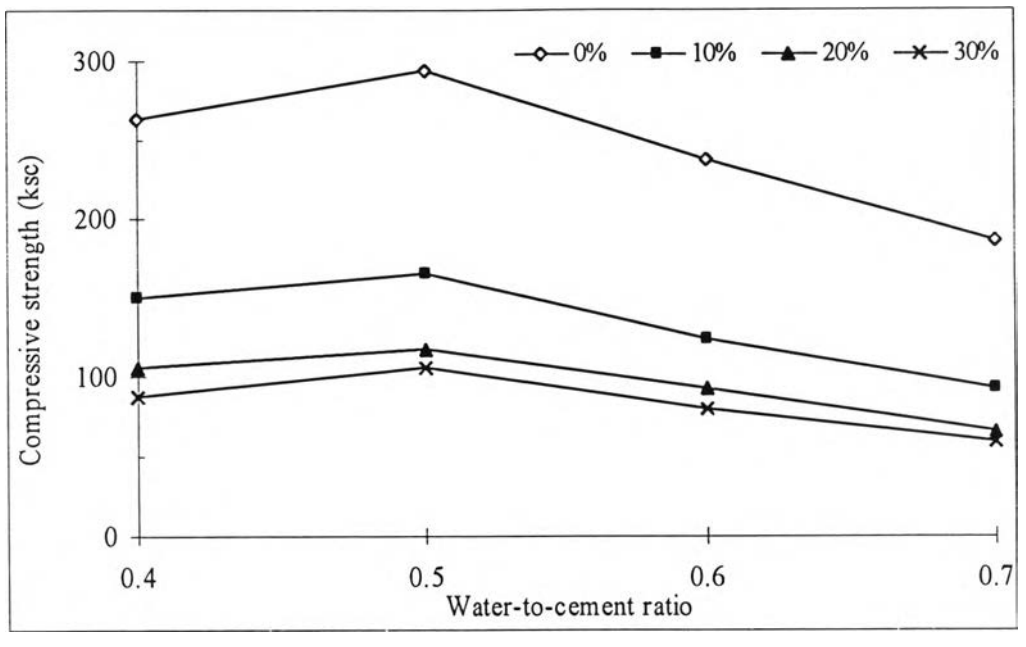

(a)

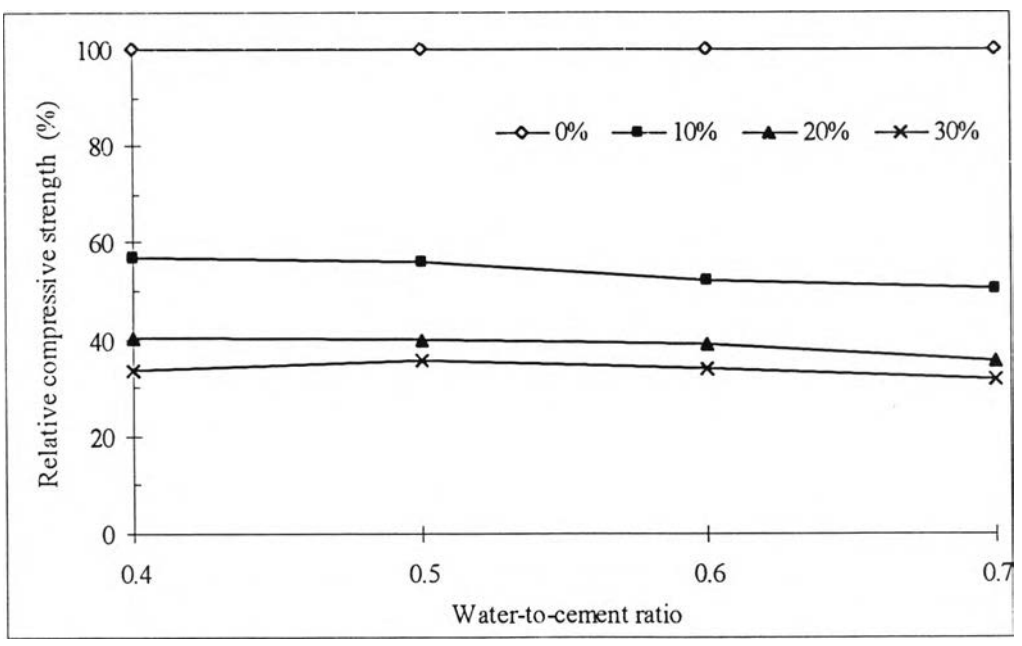

(b)

Figure 4.33 Development of (a) Compressive Strength and (b) Relative Compressive Strength of Bagasse Fly Ash-Cement Mortar at Different Percent Replacements and Water-to-Cement Ratios at 7-day Curing

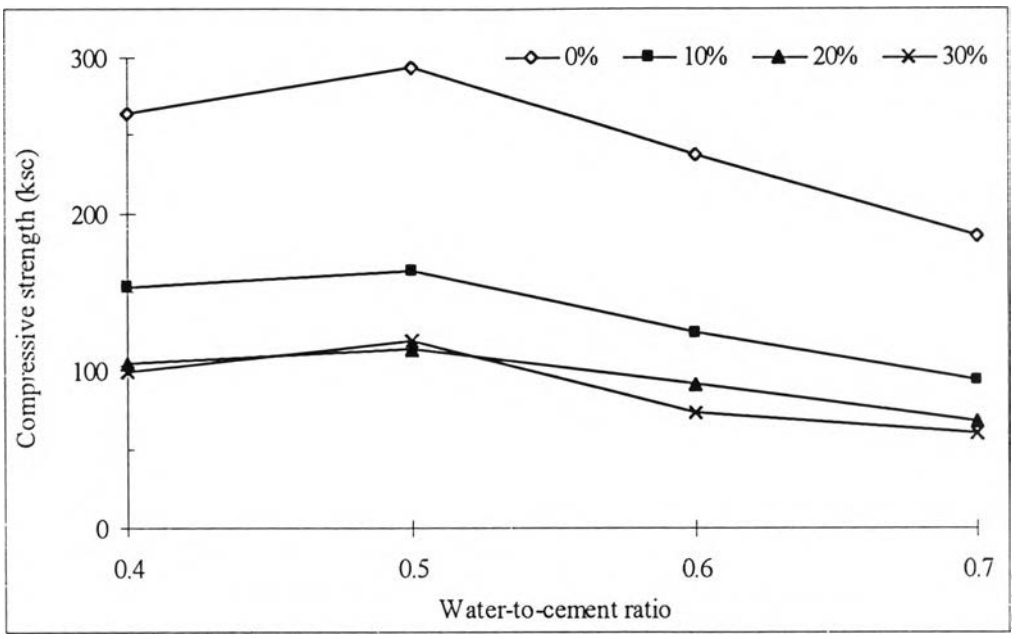

(a)

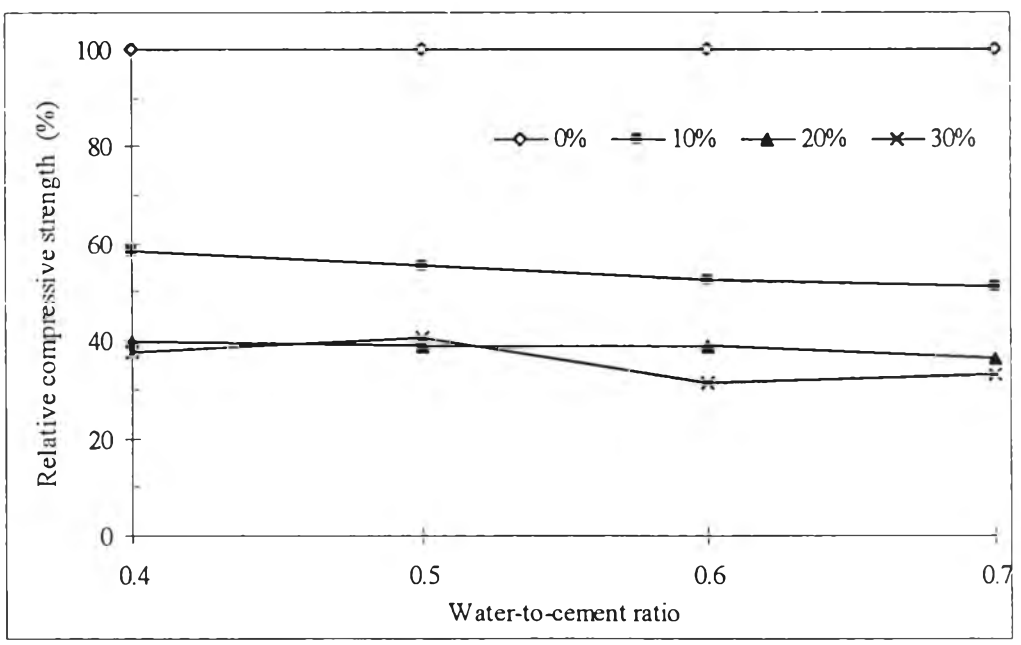

(b)

Figure 4.34 Development of (a) Compressive Strength and (b) Relative Compressive Strength of Pb adsorbed Bagasse Fly Ash-Cement Mortar at Different Percent Replacements and Water-to-Cement Ratios at 7-day Curing

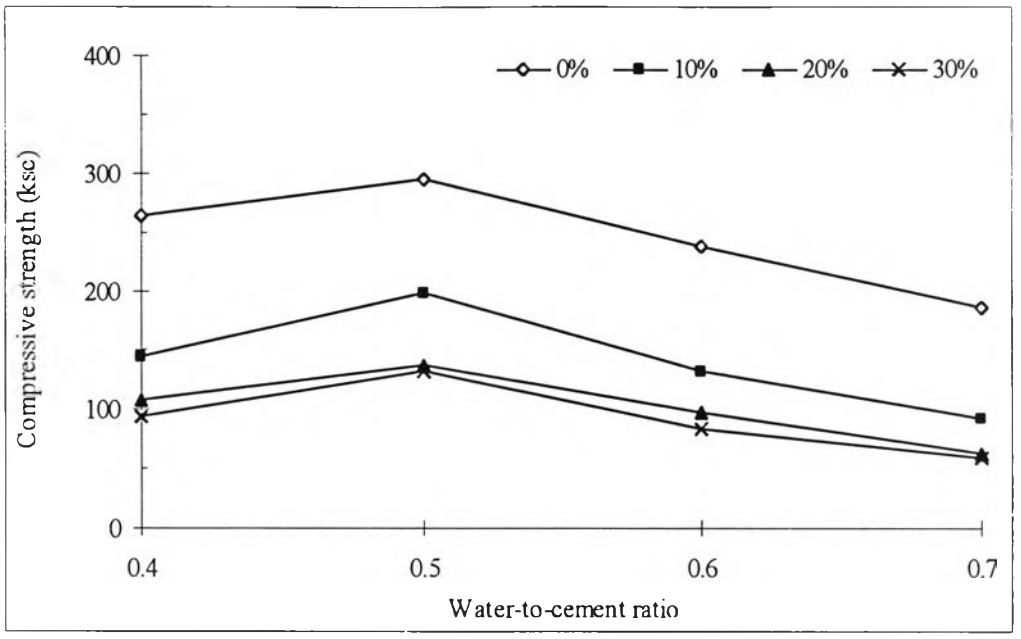

(a)

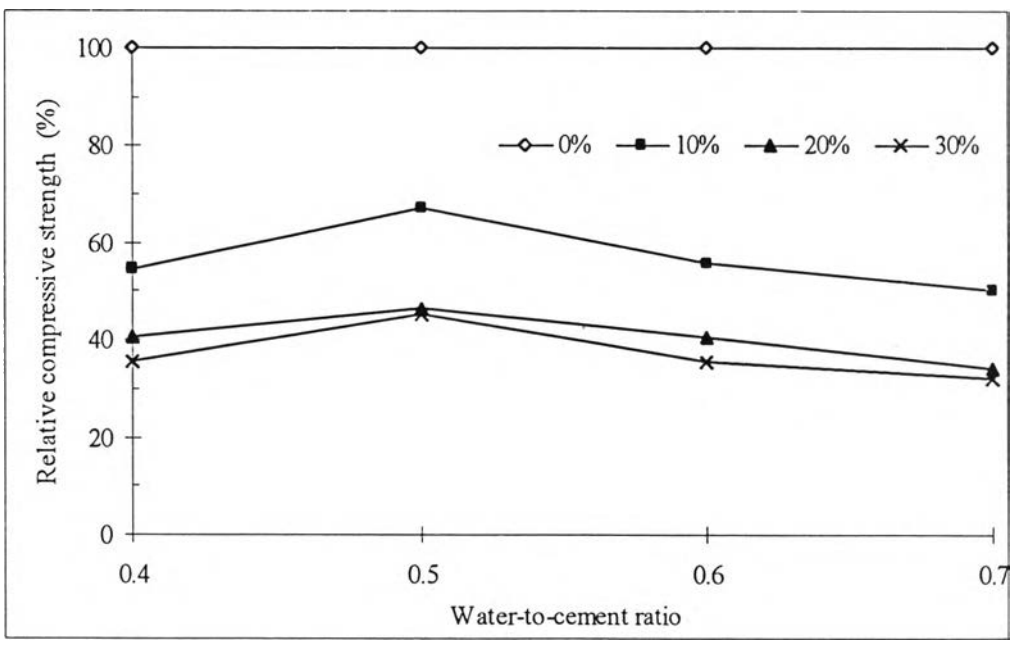

(b)

Figure 4.35 Development of (a) Compressive Strength and (b) Relative Compressive Strength of Cr Adsorbed Bagasse Fly Ash-Cement Mortar at Different Percent Replacements and Water-to-Cement Ratios at 7-day Curing

4.4.2.3 Effect of curing time

The change in compressive strength and relative compressive strength with age (up to 60 days) at w/c ratio of 0.50, replacement ratio of 0 and 10% were shown in Figure 4.36. Similar trends of those of bagasse were observed. That is, the compressive strength increased with hydration time. The compressive strength of specimens with cement replacement of 10% BFA showed, notable increases compared with control specimens at all ages.

Generally, silica will be responsible for increase in compressive strength brought about of pozzolanic reaction between calcium hydroxide and silica and the hydration of silica itself in the alkaline environment (Singh, et al., 2000). It was reported though that silica should be in an amorphous phase in order to be reactive (Rachakornkij, 2000 and Hernandez, et al., 1998). The results showed that BFA did not act like a reactive pozzalan, perhaps due to the presence of unburned materials and carbon (Hernandez, et al., 1998). Although BFA contain high content of silica, but it is present in form of quartz, a crystalline phase of silica, that is not available as active silica for pozzolanic reaction. However, in all cases, the values of compressive strengths of specimens after a 3-day curing were enough to meet the landfilling standard of (3.5 kg/cm^2) established by the Ministry of Industry No.6, B.E. 2540 (1997).

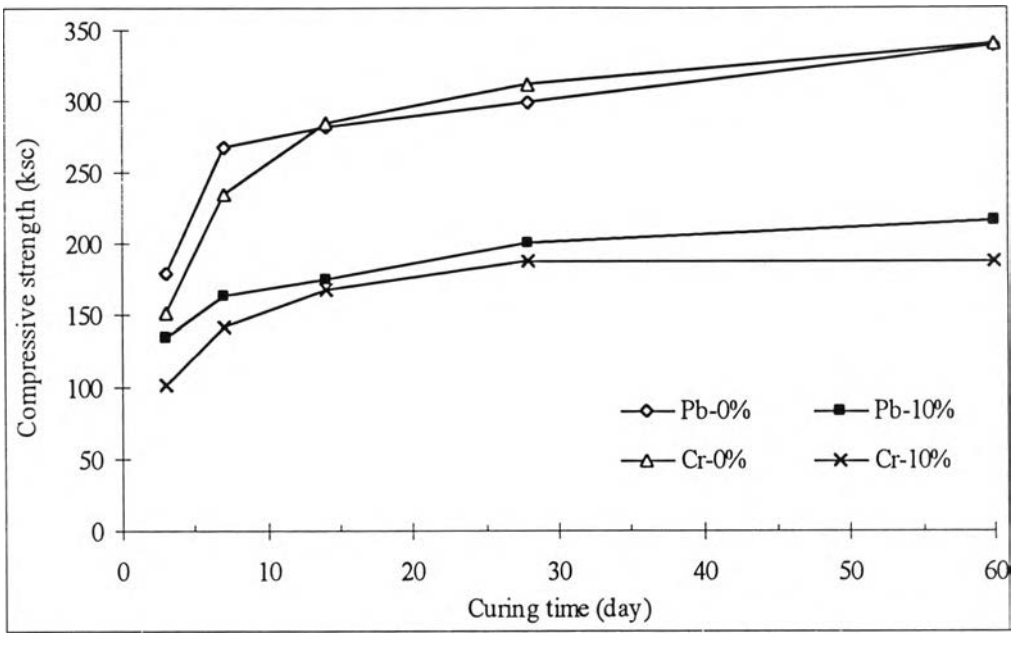

(a)

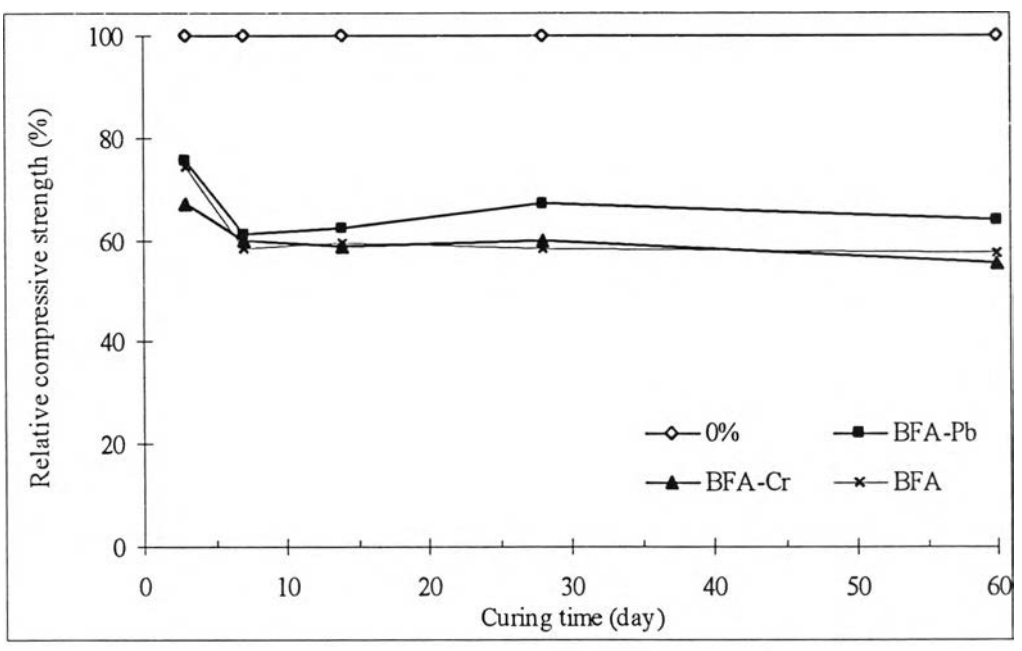

(b)

Figure 4.36 Development of (a) Compressive Strength and (b) Relative Compressive Strength at Different Curing Times of BFA, BFA-Pb, and BFA-Cr (w/c ratio of 0.50, 10% replacement)

4.4.2.4 Leachate characteristics

The results of the leaching test for the mortars incorporating of BFA-Pb and BFA-Cr are shown in Tables 4.20, 4.21, and 4.22. The results showed that Pb and Cr concentrations in leachates from the specimens is lower than 1.2 mg/L in all replacement ratios (10, 20, and 30%), w/c ratios (0.4, 0.5, 0.6 and 0.7), and curing periods (3, 7, 14, and 28 days). The final pH values of the leaching solutions were high (about 12) because of the concurrent release of calcium hydroxide and alkalis from the cementitious matrices.

It indicates that the concentrations of all cases are well below the limits established by the Ministry of Industries No. 6, B.E. 2540 (1997), as mentioned above. Like bagasse, these data showed that the cementitious solidification process was effective, even after a short curing time (3 days) and this process was able to strongly immobilized Pb and Cr. The results showed that the hydration reaction might improve fixation of heavy metals. Similar to bagasse, it was found that Pb and Cr concentrations leached from specimens with Portland cement were less than without Portland cement.

Table 4.20 Amount of Released Pb from BFA-Pb, with and without Portland Cement at Different w/c ratios and Replacement Ratios (%R)

Condition	w/c ratio	% R of Portland cement	Released Pb mg/L	Released Pb mg/g	Released Pb % release
With Portland cement	0.40	10	0.086	0.00696	0.088
		20	0.059	0.00239	0.030
		30	0.038	0.00103	0.013
	0.50	10	0.113	0.00915	0.116
		20	0.080	0.00324	0.041
		30	0.032	0.00086	0.011
	0.60	10	0.127	0.01028	0.130
		20	0.103	0.00417	0.053
		30	0.044	0.00119	0.015
	0.70	10	0.125	0.01012	0.128
		20	0.092	0.00372	0.047
		30	0.050	0.00135	0.017
Condition	**Amount of B-Pb (g)**	**% R of Portland cement equivalent**	**Released Pb mg/L**	**Released Pb mg/g**	**Released Pb % release**
Without Portland cement	24.7	10	0.378	0.03062	0.387
	49.4	20	0.778	0.03150	0.398
	74.1	30	1.128	0.03046	0.385

Table 4.21 Amount of Released Cr from BFA-Cr, with and without Portland Cement at Different w/c ratios and Replacement Ratios (%R)

Condition	w/c ratio	% R of Portland cement	Released Cr mg/L	Released Cr mg/g	Released Cr % release
With Portland cement	0.40	10	ND	NC	NC
		20	0.063	0.00255	0.390
		30	0.096	0.00259	0.396
	0.50	10	0.057	0.00462	0.705
		20	0.083	0.00336	0.513
		30	0.134	0.00362	0.552
	0.60	10	0.079	0.0064	0.977
		20	0.107	0.00433	0.662
		30	0.141	0.00381	0.581
	0.70	10	0.084	0.0068	1.039
		20	0.118	0.00478	0.730
		30	0.156	0.00421	0.643
Condition	**Amount of B-Cr (g)**	**% R of Portland cement equivalent**	**Released Cr mg/L**	**Released Cr mg/g**	**Released Cr % release**
Without Portland cement	24.7	10	0.123	0.00999	1.526
	49.4	20	0.253	0.01024	1.565
	74.1	30	0.373	0.01006	1.537

Notation; ND refered to cannot be detected (below the detection limit of ICP-OES)
NC refered to cannot calculated

Table 4.22 Concentrations of Pb and Cr from Solidified Matrices Incorporating BFA-Pb and BFA-Cr at Different Curing Periods

Curing time (day)	Concentration (mg/L)	
	Pb	Cr
3	0.135	0.097
7	0.113	0.057
14	0.039	0.023
28	0.028	0.021
60	0.022	0.021

4.5 Construction Material Study

The results of the S/S experiments indicated that bagasse fly ash is more suitable for use as construction material than bagasse. Therefore, in this section, construction material study, only bagasse fly ash was evaluated for the feasibility for use as a construction material.

4.5.1 Effect of Aggregate Proportion

Figure 4.37 shows compressive strengths at different five mixing proportions of Portland cement, river sand, and crushed stone. The experimental results showed that the proportion of 1 : 1.1 : 1.9 gave the highest compressive strength (400 kg/cm^2). Therefore, this ratio was finally selected for all of the next tests.

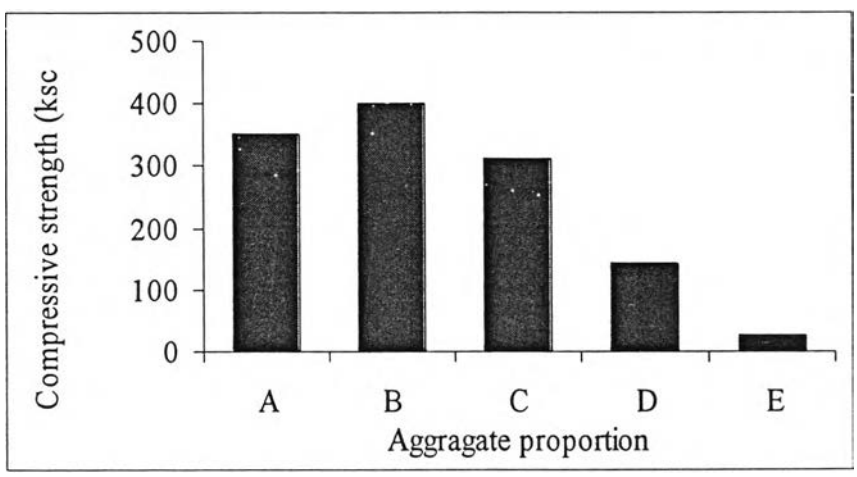

Figure 4.37 Effect of Aggregate Proportion; Cement : Sand : Crushed Stone as 1 : 1 : 2 (A), 1 : 1.1 : 1.9 (B), 1 : 1.5 : 2.5 (C), 1 : 2 : 3 (D), and 1 : 3 : 5 (E) on Compressive Strength (curing time 7 day, w/c ratio 0.5)

4.5.2 Effect of Replacement Ratio

Figure 4.38 showed concrete specimens which cement was replaced by bagasse fly ash at 0 to 30% and specimens after the compressive strength test. The experimental results are summarized in Figures 4.39 and 4.40, which showed similar trend as in the S/S study. When BFA-Pb or BFA-Cr substituted aggregates, compressive strength of lower than those of the controls were obtained. In addition, the compressive strength and relative compressive strength decreased as the percentage of BFA-Pb or BFA-Cr in the mix was increased. This may be due to the fact that these materials inhibited the hydration reaction, as mentioned above. However, compared with S/S study, compressive strength values of specimens in this experiment were higher than those in S/S study. This may be due to the fact that crushed stone was mixed added to make specimens.

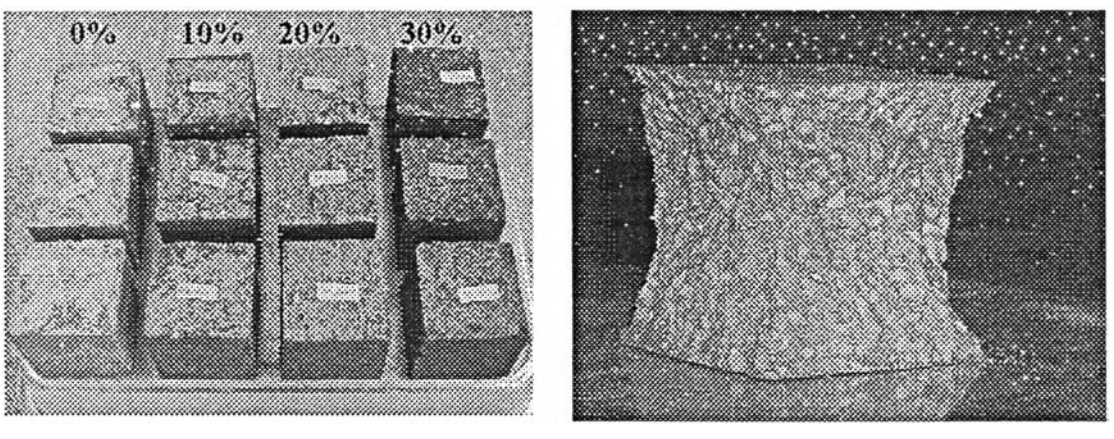

(a) (b)

Figure 4.38 Concrete Specimens with (a) Cement Replacement by Bagasse Fly Ash at 0, 10, 20, and 30% and (b) after Compressive Strength Test

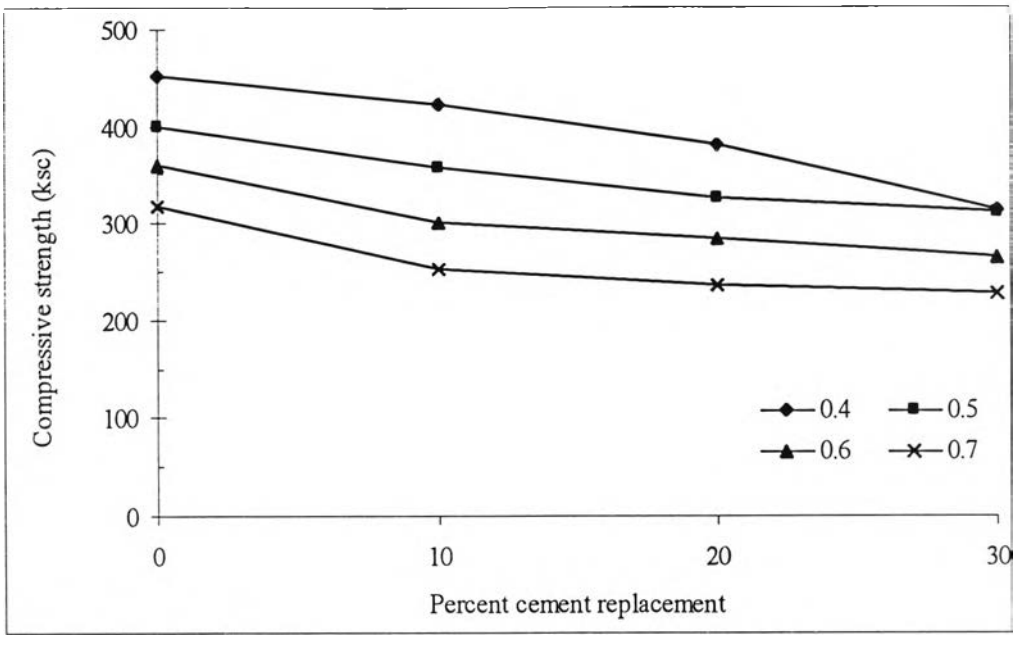

(a)

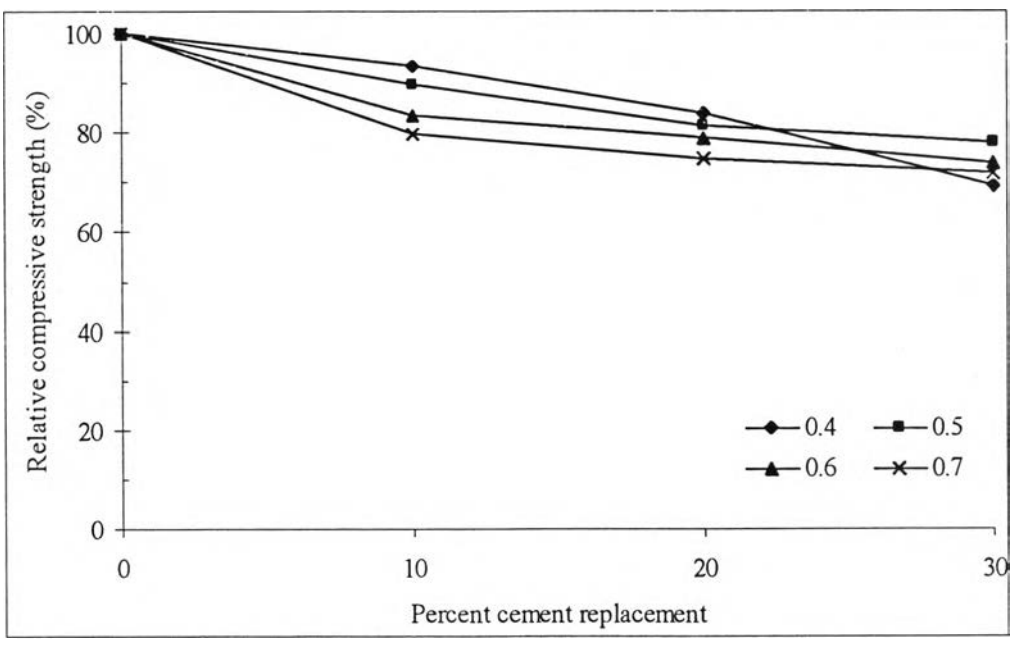

(b)

Figure 4.39 Development of (a) Compressive Strength and (b) Relative Compressive Strength at Different Percent Replacements of Pb Adsorbed Bagasse Fly Ash-Cement Mortar at 7-Day Curing Time, Cement : Sand : Crushed Stone of 1 : 1.1 : 1.9

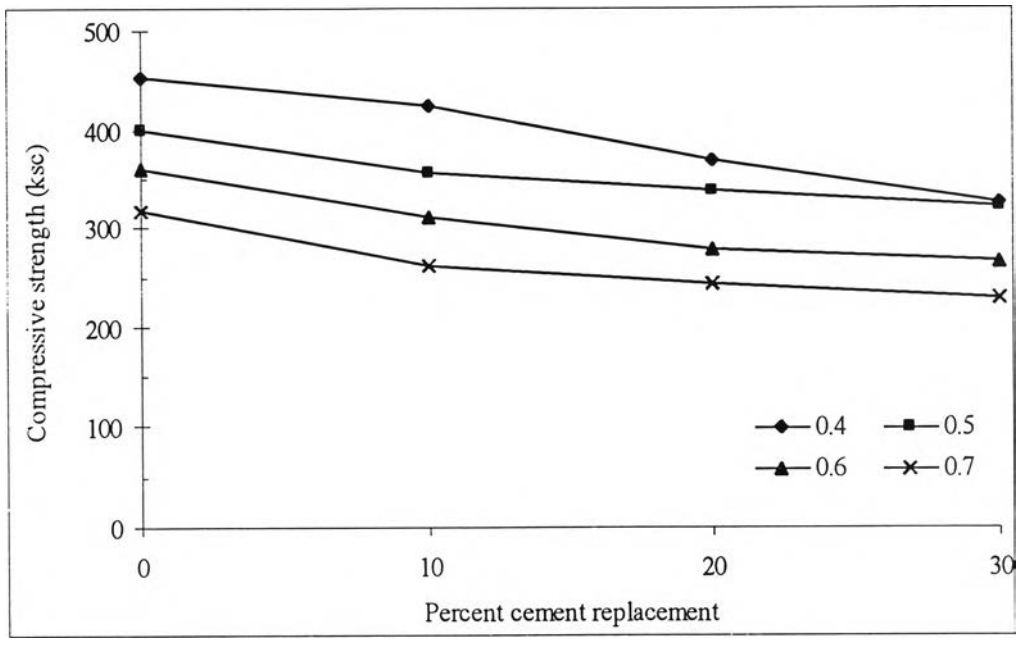

(a)

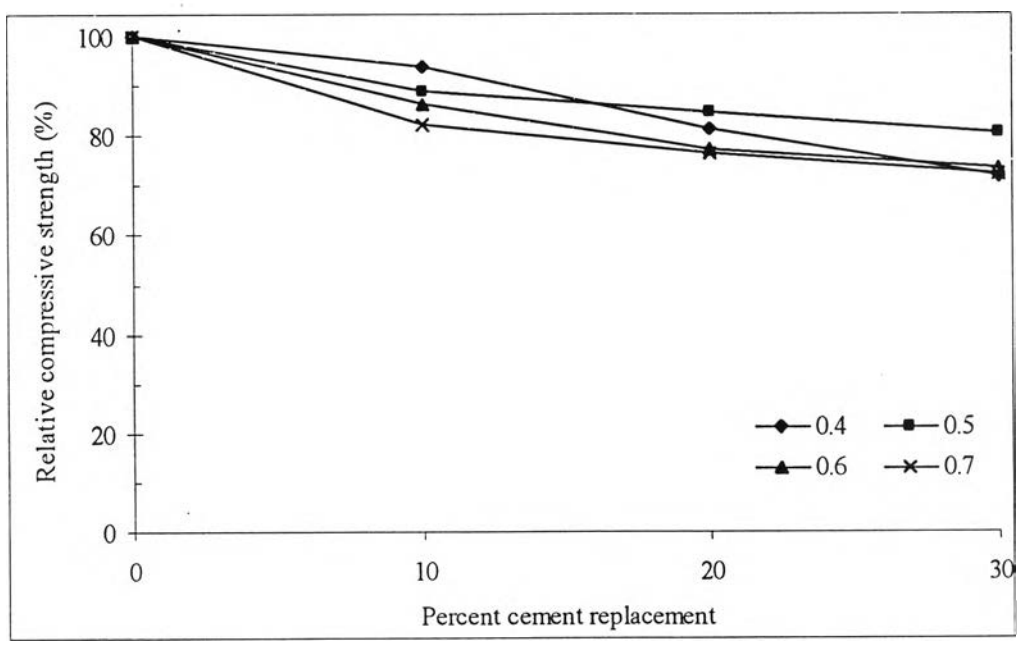

(b)

Figure 4.40 Development of (a) Compressive Strength and (b) Relative Compressive Strength at Different Percent Replacements of Cr Adsorbed Bagasse Fly Ash-Cement Mortar at 7-Day Curing Time, Cement : Sand : Crushed Stone of 1 : 1.1 : 1.9

4.5.3 Effect of Water-to-Cement Ratio

Based on the results shown in Figures 4.41 and 4.42 most of compressive strength values at w/c ratio of 0.4 were the highest. The compressive strengths and relative compressive strengths slightly decreased as the percentage of BFA-Pb or BFA-Cr in the mix increased. Therefore, w/c ratio of 0.40 was finally selected for curing time tests.

4.5.4 Effect of Curing Time

The changes in compressive strength and relative compressive strength with age (up to 60 days) at different replacement ratios, and w/c ratio of 0.40, were shown in Figures 4.43 and 4.44 for Pb adsorbed BFA and Cr adsorbed BFA, respectively. It was observed that, with trends similar to those of the S/S study, the compressive strength increased as hydration progressed. Additionally, the strengths of specimens were lower than those of the control specimens at all curing ages except at 3-days curing time of 10% replacement. The compressive strength of specimens at this condition were higher than those of the control, it may be due to packing effect. At early ages, the compressive strength of fly ash mortar due to packing effect is higher than that due to pozzolanic reaction (Tangpagasit, 2004). Insoluble material which has particle size smaller than sand and crushed stone, can insert into pore between sand and crushed stone, then decreased pore volume of concrete will occurred and compressive strength will increased.

4.5.5 Leachate Characteristics

The results of the leaching test for the mortars incorporating BFA-Pb and BFA-Cr are shown in Table 4.23. Pb and Cr concentrations in leachates from the specimens were lower than the limits established by the Ministry of Industry No.6 B.E. 2540 (1997), 5.0 mg/L for both metals in the leachate. Like the S/S study, these showed that the cementitious solidification process was effective, even after a short curing period (3 days) and that this process was able to strongly immobilize Pb and

Cr. The results indicated that the construction material developed form this study is should be safe for environment.

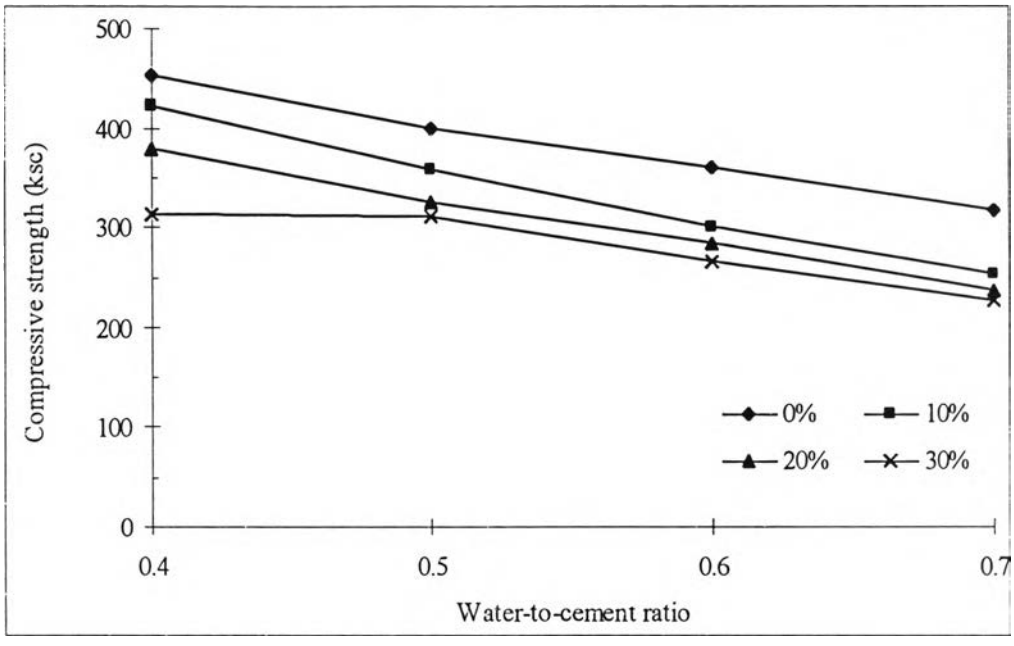

(a)

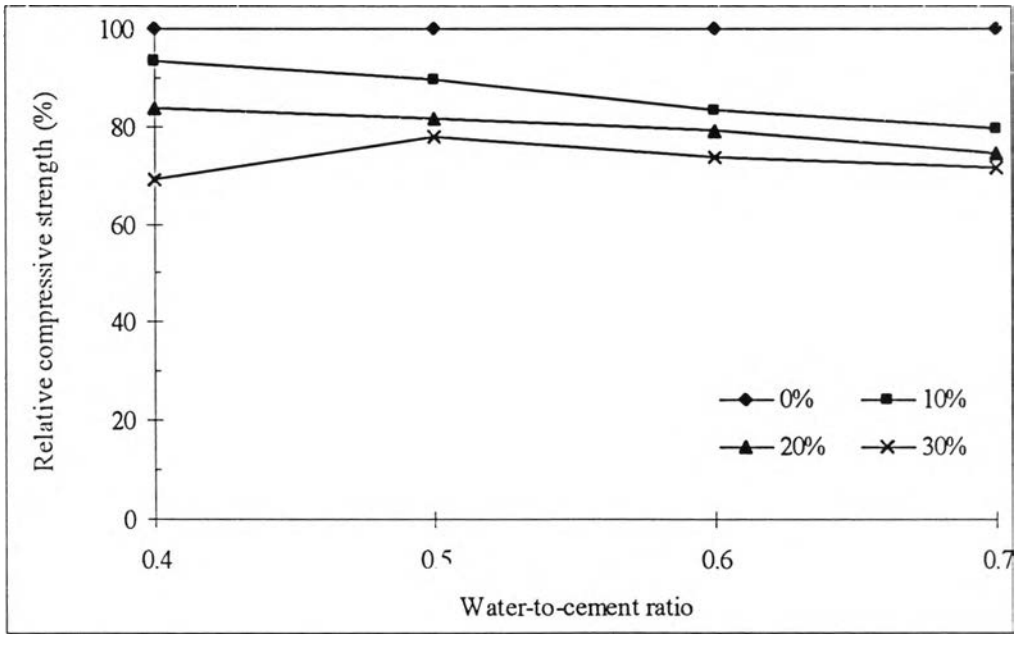

(b)

Figure 4.41 Development of (a) Compressive Strength and (b) Relative Compressive Strength at Different w/c ratios of Pb Adsorbed Bagasse Fly Ash-Cement Mortar at 7-Day Curing Time, Cement : Sand : Crushed Stone of 1 : 1.1 : 1.9

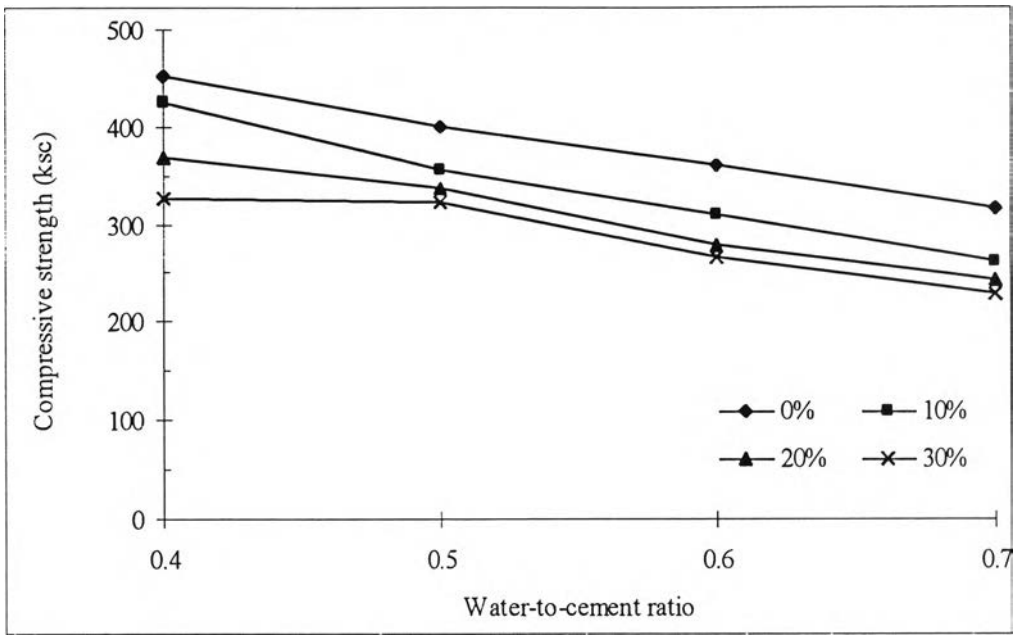

(a)

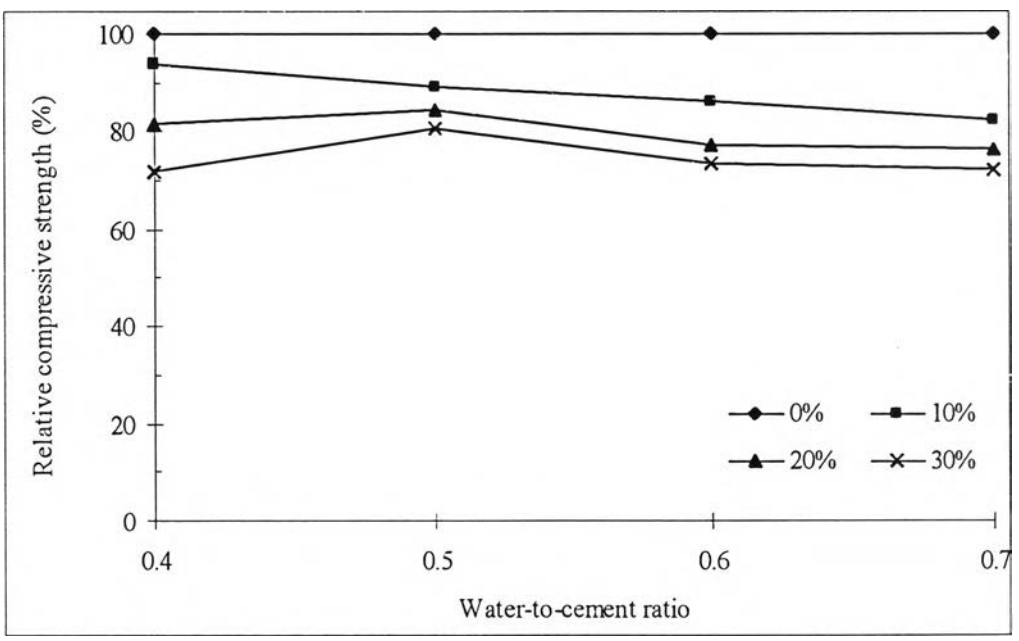

(b)

Figure 4.42 Development of (a) Compressive Strength and (b) Relative Compressive Strength at Different w/c ratios of Cr Adsorbed Bagasse Fly Ash-Cement Mortar at 7-Day Curing Time, Cement : Sand : Crushed Stone of 1 : 1.1 : 1.9

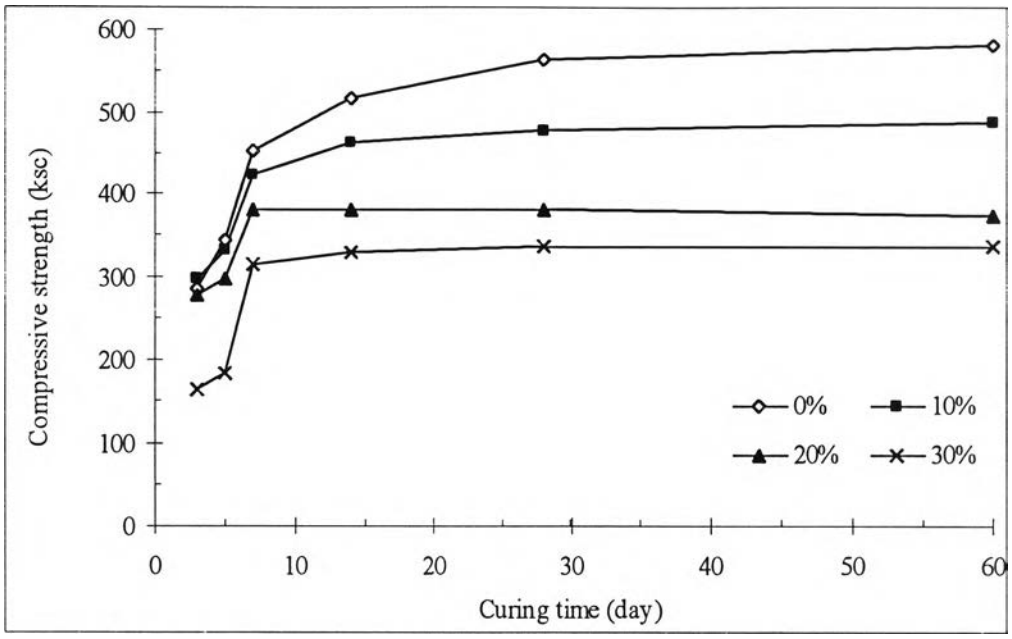

(a)

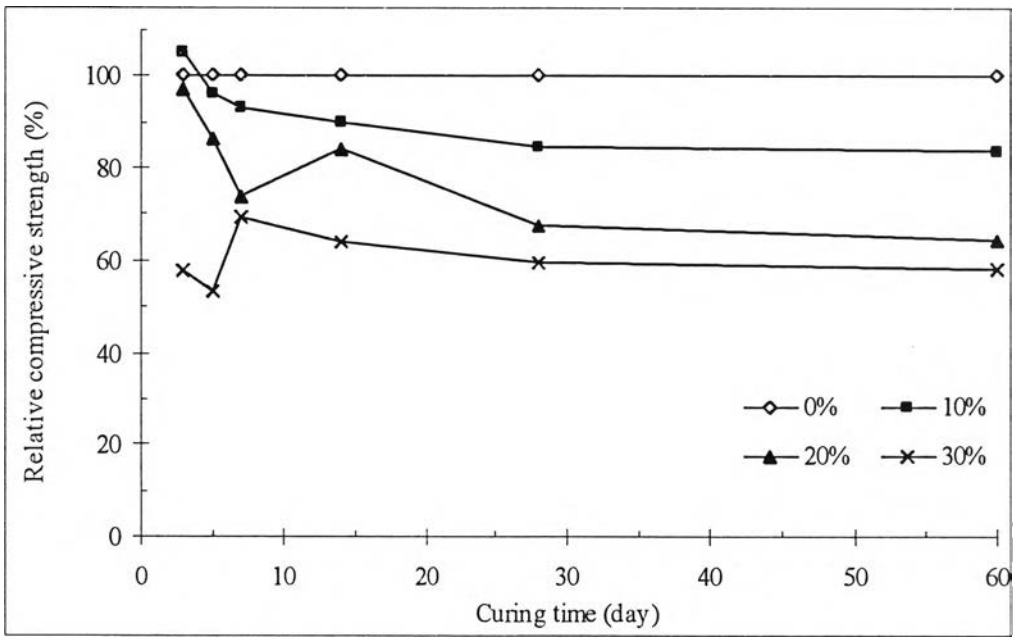

(b)

Figure 4.43 Development of (a) Compressive Strength and (b) Relative Compressive Strength at Different Curing Times of Pb Adsorbed Bagasse Fly Ash-Cement Mortar at 7-Day Curing Time, Cement : Sand : Crushed Stone of 1 : 1.1 : 1.9, w/c ratio : 0.4

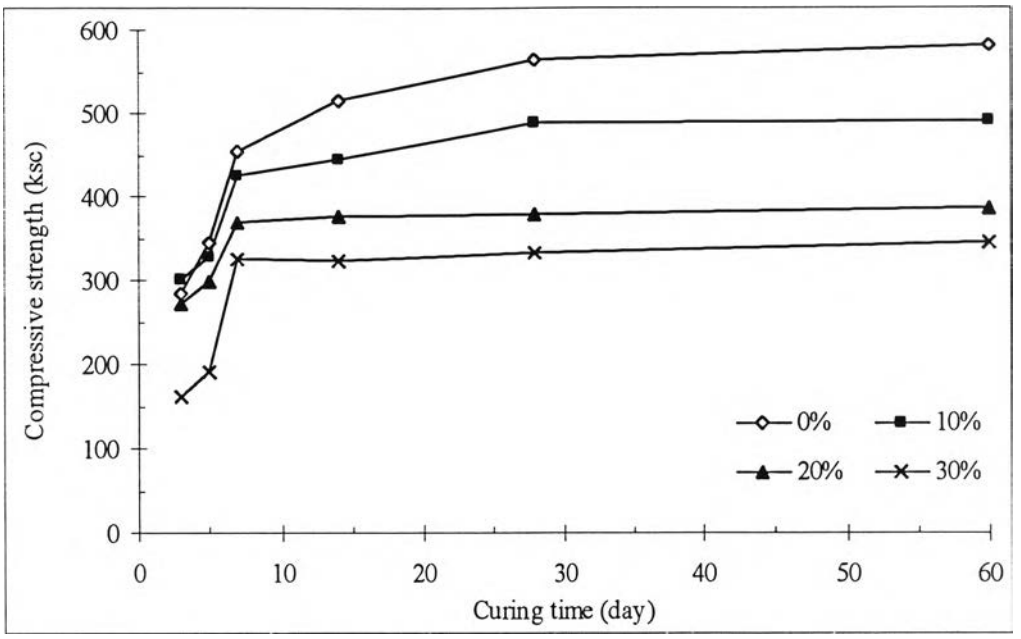

(a)

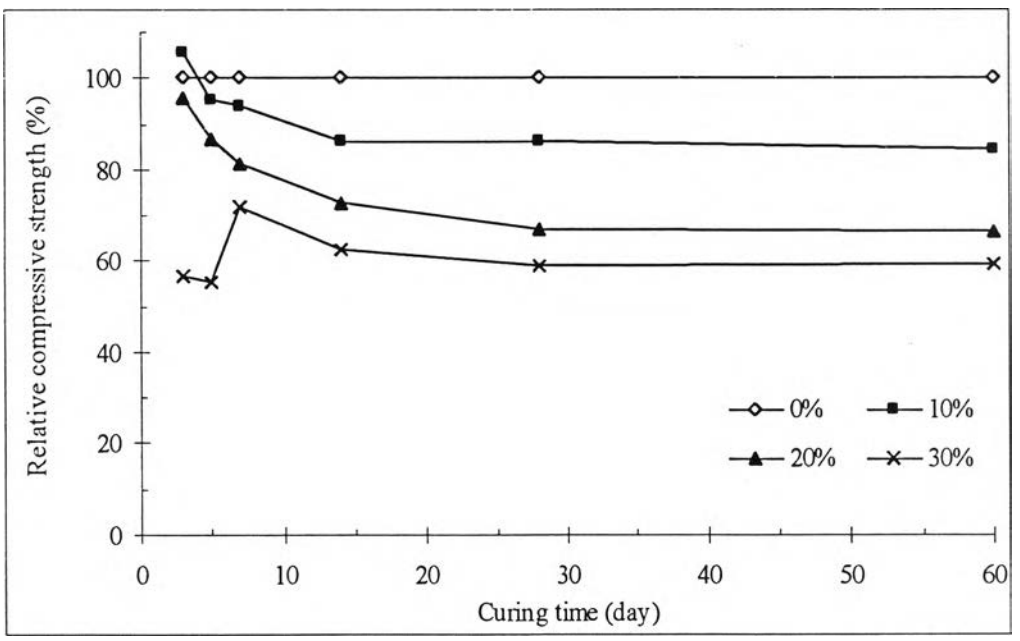

(b)

Figure 4.44 Development of (a) Compressive Strength and (b) Relative Compressive Strength at Different Curing Time of Cr Adsorbed Bagasse Fly Ash-Cement Mortar at 7-Day Curing Time, Cement : Sand : Crushed Stone of 1 : 1.1 : 1.9, w/c ratio : 0.4

Table 4.23 Concentrations of Pb and Cr in Leachate from Solidified Product of BFA-Pb and BFA-Cr in Construction Material Study at Different w/c Ratios

Curing time (days)	Concentration (mg/L)	
	Pb	Cr
3	0.210	0.179
7	0.156	0.115
14	0.101	0.065
28	0.006	0.007
60	0.005	0.005

4.5.6 Equation Development

Non-linear regression analyses of experimental data were performed with SigmaPlot Program version 6.1. This program plotted four difference types of equation namely; Plane, Paraboloid, Gaussian, and Lorentzian and showed in three-dimension graph. These graphs were plotted between replacement percentage, w/c ratio, and compressive strength at 3-day, 5-day, and 7-day curing times as shown in Figures 4.45, 4.46, and 4.47, respectively.

Coefficient of correlation value of each equation was used to identify the most suitable equation; which provided correlation coefficient value closest to 1. They presented in Table 4.24, showed that R^2 for each equation type was almost level, between 0.836-0.977. However, Gaussian equations showed the value closest to 1. Therefore, the recommended equations were presented in Gaussian equations as shown in Table 4.25.

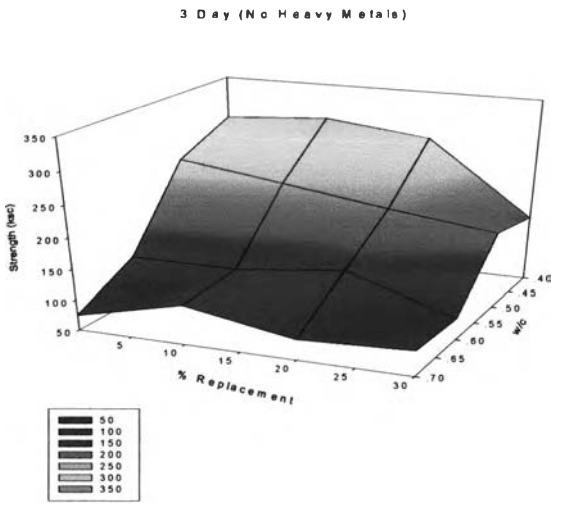

(a)

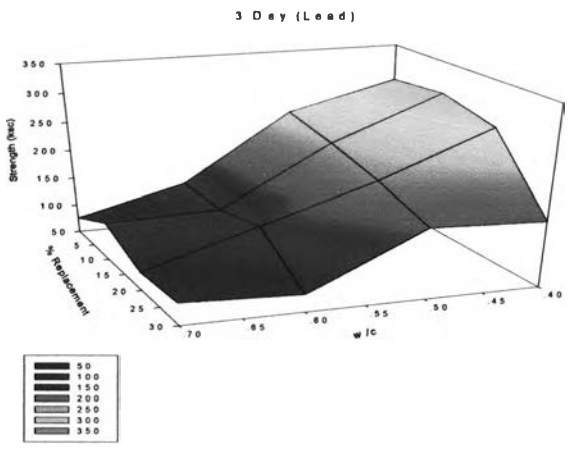

(b)

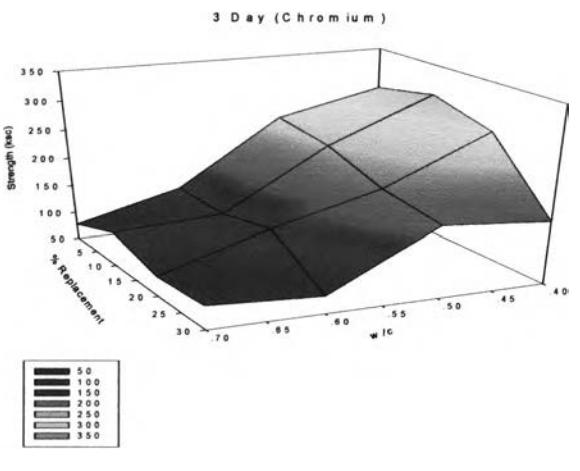

(c)

Figure 4.45 3D Graph Relationship between Compressive Strength, w/c ratio and Percent Replacement of (a) BFA, (b) BFA-Pb and (c) BFA-Cr at 3-day Curing Time

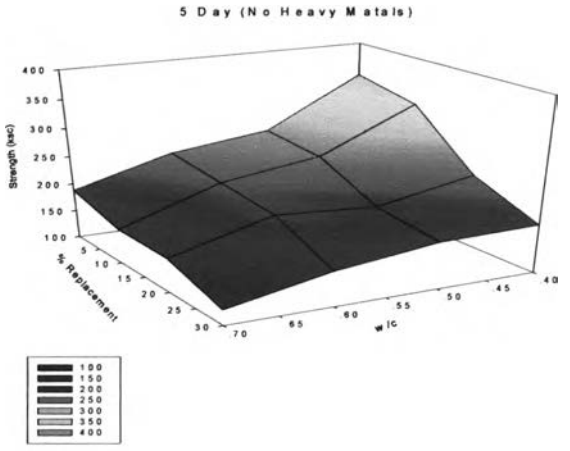

(a)

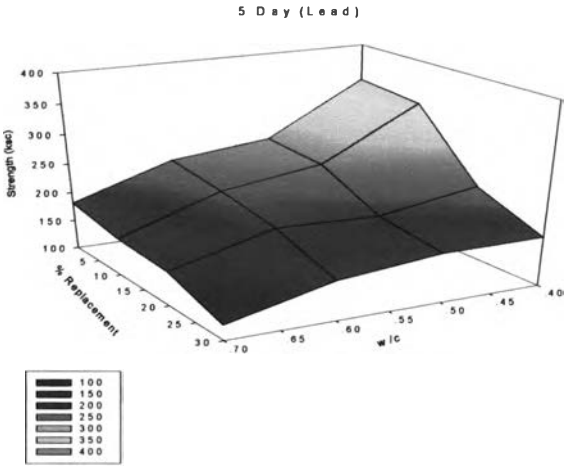

(b)

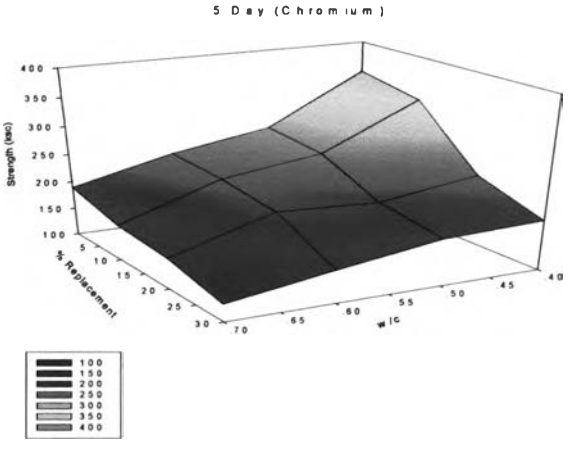

(c)

Figure 4.46 3D Graph Relationship between Compressive Strength, w/c ratio and Percent Replacement of (a) BFA, (b) BFA-Pb and (c) BFA-Cr at 5-day Curing Time

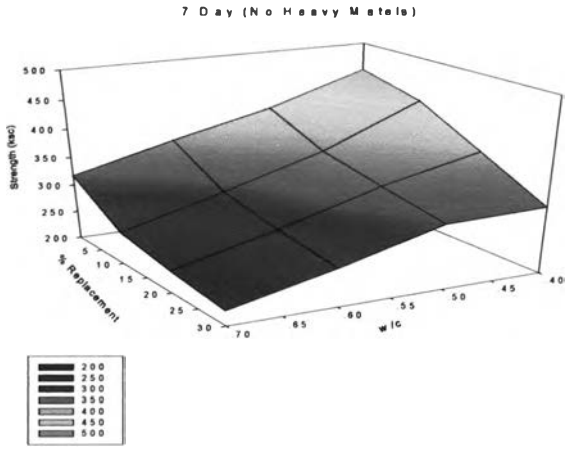

(a)

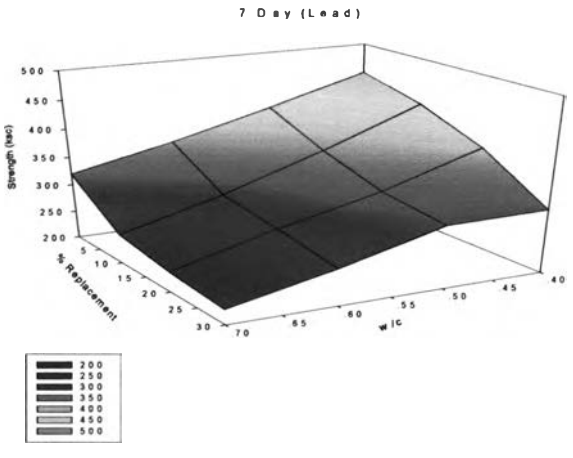

(b)

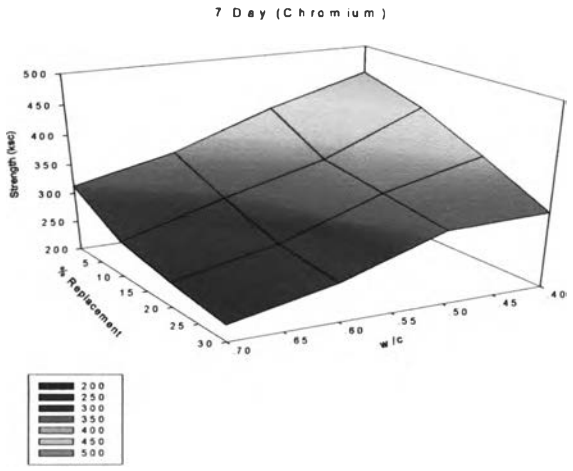

(c)

Figure 4.47 3D Graph Relationship between Compressive Strength, w/c ratio and Percent Replacement of (a) BFA, (b) BFA-Pb and (c) BFA-Cr at 7-day Curing Time

Table 4.24 Coefficient of Correlation (R^2) of Plane, Paraboloid, Gaussian, and Lorentian Equation

Curing time (day)	Condition	R^2 of Equation			
		Plane	Paraboloid	Gaussian	Lorentzian
3	BFA	0.836	0.873	**0.924**	0.908
	BFA-Pb	0.848	0.888	**0.936**	0.922
	BFA-Cr	0.841	0.878	**0.930**	0.916
5	BFA	0.865	0.870	**0.920**	0.892
	BFA-Pb	0.844	0.851	**0.905**	0.874
	BFA-Cr	0.863	0.869	**0.920**	0.893
7	BFA	0.961	0.967	**0.971**	0.962
	BFA-Pb	0.955	0.962	**0.966**	0.955
	BFA-Cr	0.966	0.975	**0.977**	0.971

Table 4.25 Recommended Equations

Curing time (day)	Condition	Recommended Equation
3	BFA	$f = 358.193*\exp^{(-0.5*((x-0.224)/0.290)^2 + ((y-7.663)/23.689)^2)}$
	BFA-Pb	$f = 365.930*\exp^{(-0.5*((x-0.210)/0.297)^2 + ((y-7.811)/23.241)^2)}$
	BFA-Cr	$f = 375.610*\exp^{(-0.5*((x-0.205)/0.296)^2 + ((y-7.669)/23.379)^2)}$
5	BFA	$f = 835.076*\exp^{(-0.5*((x+0.819)/0.900)^2 + ((y+9.451)/39.295)^2)}$
	BFA-Pb	$f = 828.342*\exp^{(-0.5*((x+0.773)/0.874)^2 + ((y+8.717)/38.636)^2)}$
	BFA-Cr	$f = 788.698*\exp^{(-0.5*((x+0.747)/0.865)^2 + ((y+6.059)/36.454)^2)}$
7	BFA	$f = 1554.84*\exp^{(-0.5*((x+0.104)/0.688)^2 + ((y+201.477)/145.149)^2)}$
	BFA-Pb	$f = 2471.00*\exp^{(-0.5*((x+0.169)/0.711)^2 + ((y+292.559)/176.864)^2)}$
	BFA-Cr	$f = 2450.59*\exp^{(-0.5*((x+0.185)/0.730)^2 + ((y+277.328)/167.836)^2)}$

Natation f = compressive strength (ksc)

x = w/c ratio

y = replacement percentage

4.5.7 Test of Equations

The recommended equations shown in Table 4.25 were tested for use by build construction materials namely; interlocking concrete paving blocks and hollow non-load-bearing concrete block as shown in Figure 4.48 and 4.49, respectively. The procedures for test were followed as mentioned in section 3.2.5.3.

Tables 4.26 and 4.27 presented the comparison of predicted strength and actual strength of the specimens with BFA-Pb and BFA-Cr, respectively. Table 4.28 showed percent of error of their comparison in which negative values mean that actual strength lower than predicted strength.

The percent of error showed a good agreement between predicted strength and actual strength with less than 10% error in range of 0-15% replacement. However, the recommended equation may not be suitable for replacement ratio of more than 35%, since, the error was more than 50%. In some conditions of 35% replacement, the compressive strength of the specimens were not be able to measured due to disintegration of specimens prior to loading.

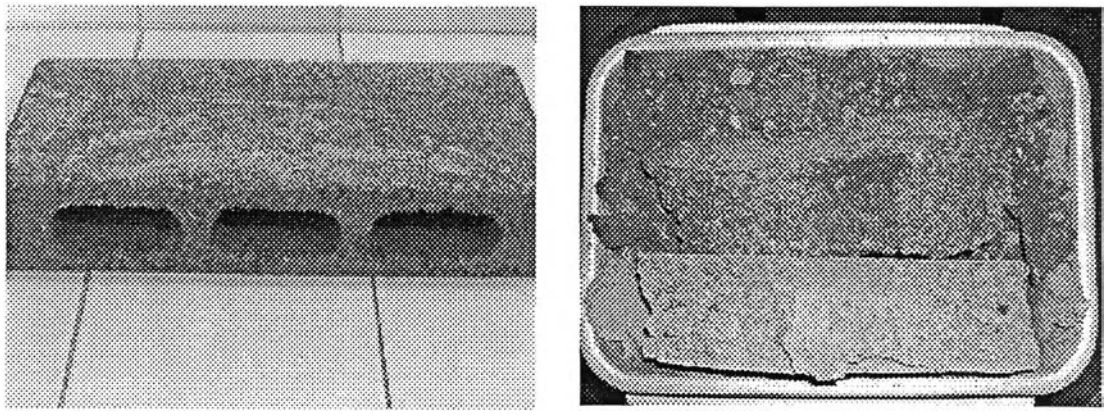

(a) (b)

Figure 4.48 Hollow Concrete Block (a) Before and (b) After Compressive Strength Test

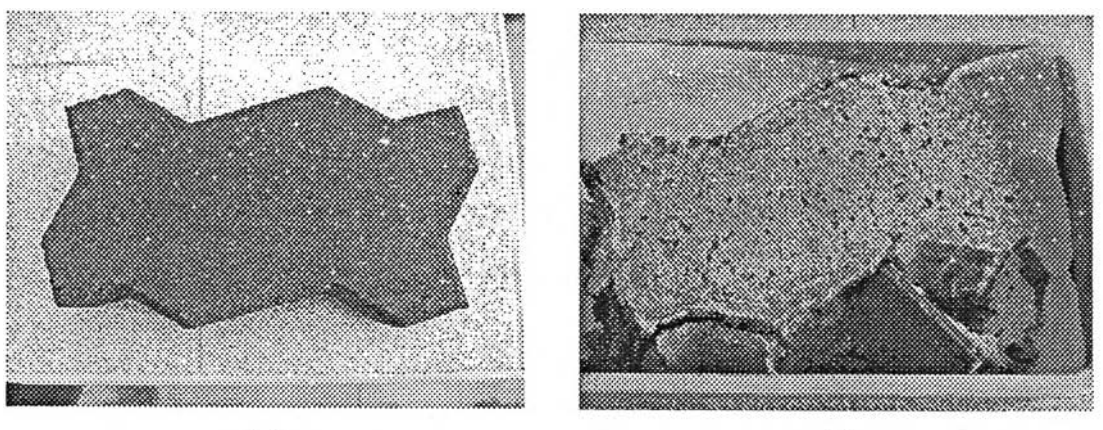

(a) (b)

Figure 4.49 Interlocking Paving Concrete Block (a) Before and (b) After Compressive Strength Test

Table 4.26 Comparison of Predicted Compressive Strength and Actual Compressive Strength of Interlocking Concrete Paving Blocks and Hollow Non-Load-Bearing Concrete Blocks with BFA-Pb at Different Curing Times and Replacement Ratios

Curing time (day)	Replacement (%)	Interlocking concrete paving blocks		Hollow non-load-bearing concrete block	
		Predicted strength (ksc)	Actual strength (ksc)	Predicted strength (ksc)	Actual strength (ksc)
3	0	200	202.9	200	210.2
	15	200	198.6	200	201.6
	35	160	ND	160	ND
5	0	200	201.8	200	196.9
	15	200	197.3	200	196.7
	35	160	26.2	160	ND
7	0	200	193.3	200	195.8
	15	200	199.3	200	194.5
	35	160	66.2	160	ND

Notation: ND referred to can not detection

Table 4.27 Comparison of Predicted Compressive Strength and Actual Compressive Strength of Interlocking Concrete Paving Blocks and Hollow Non-Load-Bearing Concrete Blocks with BFA-Cr at Different Curing Times and Replacement Ratios

Curing time (day)	Replacement (%)	Interlocking concrete paving blocks		Hollow non-load-bearing concrete block	
		Predicted strength (ksc)	Actual strength (ksc)	Predicted strength (ksc)	Actual strength (ksc)
3	0	200	201.4	200	208.7
	15	200	201.4	200	198.2
	35	160	ND	160	ND
5	0	200	200.8	200	200.6
	15	200	196.1	200	201.4
	35	160	25.8	160	ND
7	0	200	203.2	200	205.0
	15	200	209.9	200	203.3
	35	160	62.6	160	ND

Notation: ND referred to can not detection

Table 4.28 Errors between Predicted Compressive Strength and Actual Compressive Strength of Interlocking Concrete Paving Blocks and Hollow Non-Load-Bearing Concrete Blocks with BFA-Pb and BFA-Cr at Different Curing Times and Replacement Ratios

Curing time (day)	Replacement (%)	Percent of error (%)			
		Interlocking concrete paving blocks		Hollow non-load-bearing concrete block	
		BFA-Pb	BFA-Cr	BFA-Pb	BFA-Cr
3	0	1.47	0.70	5.08	4.35
	15	(-) 0.70	0.70	0.81	(-) 0.89
	35	NC	NC	NC	NC
5	0	0.91	0.42	(-) 1.50	0.33
	15	(-) 1.33	(-) 1.96	(-) 1.64	0.69
	35	(-) 83.56	(-) 83.86	NC	NC
7	0	(-) 3.37	1.61	(-) 2.11	2.52
	15	(-) 0.35	4.98	(-) 2.72	1.67
	35	(-) 58.60	(-) 60.88	NC	NC

Notation: NC referred to not calculated (specimens failed prior to loading)

(-) referred to actual strength lower than predicted strength

4.6 Economic Study

Bagasse, before being used as a removal material, is subject to a chemical treatment using acid. Since pH is one of the most important factors for Pb and Cr removal, pH adjustment was necessary in the experiment. Having removed Pb and Cr, the spent materials were mixed with cement for disposal by landfilling. As mentioned above, bagasse fly ash was effective as an ingredient in concrete blocks. Then cost of acid treatment for bagasse, pH adjustment, cement for solidification process and raw material of concrete blocks were considered in this section. In addition, this section included cost analyses of two case studies; namely, Case Study 1: Pb removal in wastewater from a hypothetical Factory A, and Case Study 2 sugar factory wastes from Factory AA.

4.6.1 Cost Analysis of Acid Treatment of Bagasse

Important factor for the determination of cost of acid treatment was chemical reagent namely; hydrochloric acid (HCl). One liter of 0.1 M HCl was used to treat 100 g of bagasse. The acid was prepared from diluting 8.33 mL of 37% HCl to one liter. The price of 37% HCl was 350 Baht/one 2.5-L bottle. The cost of chemical reagent can be calculated as follows.

$$\text{Cost (Baht/g)} = \frac{0.1\ \text{M}}{100\ \text{g}} \times \frac{1\ \text{L}}{0.1\ \text{M}} \times \frac{8.33\ \text{mL}}{1\ \text{L}} \times \frac{350\ \text{Baht}}{2500\ \text{mL}}$$

$$= 0.01161\ \text{Baht/g}$$

The operational cost of acid treated bagasse was 0.01161 Baht per 1 gram. It should be noted that HCl used in the experiments was analytical grade that was high in purity and price. However, in real practice, commercial-grade HCl may be used instead in order to save the cost of chemical. It is also important to note that this calculation excluded cost of energy, which was minimal.

4.6.2 Cost Analysis of pH Adjustment

The experimental results showed that maximum removal of Pb and Cr occurred at solution pH of 6 and 1, respectively. Therefore, pH adjustment was necessary for effective and efficient removal of both heavy metals. This is particularly so in the case of Pb removal because wastewater containing Pb must be kept acidic in order to avoid Pb precipitation (Zhan and Zhao, 2003). From laboratory experiments, it was found that 1.5 mL of 6 N NaOH was used to adjust the pH from 2 to 6 for 100 mL of wastewater. The price for 50% NaOH was 8 Baht/kg (equivalent to 16 Baht/kg of 100% NaOH). The pH adjustment cost can then be calculated as follows.

$$\text{Amount of NaOH} = \frac{6\ \text{mol}}{1\ \text{L}} \times 1.5\ \text{mL} \times \frac{1\ \text{L}}{1000\ \text{mL}} \times \frac{40\ \text{g}}{1\ \text{mol}}$$

$$= 0.36\ \text{g equivalent/100 mL wastewater}$$

$$= 3{,}600\ \text{g equivalent/m}^3\ \text{wastewater}$$

$$\text{Cost (Baht/m}^3\text{)} = \frac{16\ \text{Baht}}{1\ \text{kg}} \times \frac{3600\ \text{g}}{1\ \text{m}^3} \times \frac{1\ \text{kg}}{1000\ \text{g}}$$

$$= 57.6\ \text{Baht/m}^3$$

The cost of pH adjustment of 1 m^3 wastewater from pH 2 of to pH 6 was 57.6 Baht. If other basic reagents were to be used to adjust the pH, calculations could be done in the like manner.

4.6.3 Cost Analysis of Spent Material Disposal by Landfilling

The results from the S/S study showed that optimal cement replacement ratios of bagasse and bagasse fly ash were 10 and 30%, respectively. With these ratios, the solidified products should be acceptable for disposal via landfilling since compressive strength more than 3.5 ksc. Therefore, cement is required in the amounts of 9 and 2.3

kg to mix with bagasse and bagasse fly ash 1 kg, respectively. The price of Portland cement was 102 Baht per 50-kg bag at the time of this study. The cost can then be determined as shown below:

Bagasse:

$$\text{Cost (Baht/kg)} = \frac{102 \text{ Baht}}{1 \text{ bag}} \times \frac{1 \text{ bag}}{50 \text{ kg}} \times 9 \text{ kg}$$

$$= 18.36 \text{ Baht/kg of bagasse}$$

Bagasse fly ash:

$$\text{Cost (Baht/kg)} = \frac{102 \text{ Baht}}{1 \text{ bag}} \times \frac{1 \text{ bag}}{50 \text{ kg}} \times 2.3 \text{ kg}$$

$$= 4.70 \text{ Baht/kg of bagasse fly ash}$$

The cost of cement was 18.36 and 4.70 Baht for mix with bagasse and bagasse fly ash 1 kg, respectively. Cost calculation in the same way, if Portland cement price was changed and cement price was difference in difference type and brand.

4.6.4 Cost Analysis of Partial Cement Replacement in Concrete Blocks

The experimental results of construction material study showed that it was feasible to use bagasse fly ash to partially replace cement in the production of concrete blocks, such as hollow non-load-bearing concrete blocks and interlocking concrete paving blocks. Unit costs of the materials for production of concrete blocks were shown in Table 4.2.9. The best mix proportion at the ratio of cement : sand : crushed stone as 1 : 1.1 : 1.9 and w/c ratio of 0.5 were used. The construction cost of interlocking concrete paving blocks and hollow non-load-bearing concrete blocks in comparison between 0, 15, and 30% cement replacement with bagasse fly ash were shown in Tables 4.30 and 4.31, respectively.

Table 4.29 Price of Construction Material

Material	Price (Baht/unit)	Weight/Unit (kg)	Price (Baht/kg)
Portland cement	102 Baht/bag	50	2.04
Sand	350 Baht/m^3	2650	0.13
Crushed stone	380 Baht/m^3	2700	0.14
Water	10.50 Baht/m^3	1000	0.01
BFA	0	-	0

Note: Price as of April 2005
Transportation and labor cost are not included

Table 4.30 Comparative Costs of One Interlocking Concrete Paving Blocks Construction at Different Mix Proportions

Material	0% Replacement		15% Replacement		30% Replacement	
	Amount (kg)	Price (Baht)	Amount (kg)	Price (Baht)	Amount (kg)	Price (Baht)
Portland cement	0.88	1.79	0.75	1.53	0.62	1.25
Sand	0.96	0.12	0.96	0.12	0.96	0.12
Crushed stone	1.66	0.23	1.66	0.23	1.66	0.23
Water	0.44	0.004	0.44	0.004	0.44	0.004
BFA	0	0	0.13	0	0.26	0
Total price (Baht)		**2.14**		**1.88**		**1.60**

Note: Weight of interlocking concrete paving blocks approximately 3.5 kg/unit
Energy cost is not included

Table 4.31 Comparative Costs of One Hollow Non-Load-Bearing Concrete Blocks Construction at Different Mix Proportions

Material	0% Replacement		15% Replacement		30% Replacement	
	Amount (kg)	Price (Baht)	Amount (kg)	Price (Baht)	Amount (kg)	Price (Baht)
Portland cement	1.88	3.84	1.60	3.26	1.32	2.69
Sand	2.06	0.27	2.06	0.27	2.06	0.27
Crushed stone	3.56	0.50	3.56	0.50	3.56	0.50
Water	0.94	0.009	0.94	0.009	0.94	0.009
BFA	0	0	0.28	0	0.56	0
Total price (Baht)		**4.62**		**4.04**		**3.47**

Note: Weight of interlocking concrete paving blocks approximately 7.5 kg/unit
Energy cost is not included

The cost of concrete block decreased with increasing amount of bagasse fly ash, because bagasse fly ash is a waste from sugar factory obtained at no cost. However, practically transportation and labor cost should be included in the calculations.

4.6.5 Case Study 1: Cost Analysis for Pb Removal in Wastewater from Factory A

It is assumed that industrial activity of Factory A involved electroplating process that produced wastewater with characteristic as shown in Table 4.32. This section shows analysis of treatment costs between conventional process (precipitation by pH adjustment) and alternative process (adsorption by bagasse or bagasse fly ash) and it considers only lead in wastewater. Pb removal processes of conventional and alternative process are as shown in Figures 4.50 and 4.51, respectively.

Table 4.32 Characteristic of Wastewater from Factory A

Parameter	Pb Concentration	
	Wastewater	**Effluent Standards ***
Concentration of Pb	30 mg/L	< 0.2 mg/L
Solution pH	2	5-9

Note: * from http//www.pcd.go.th

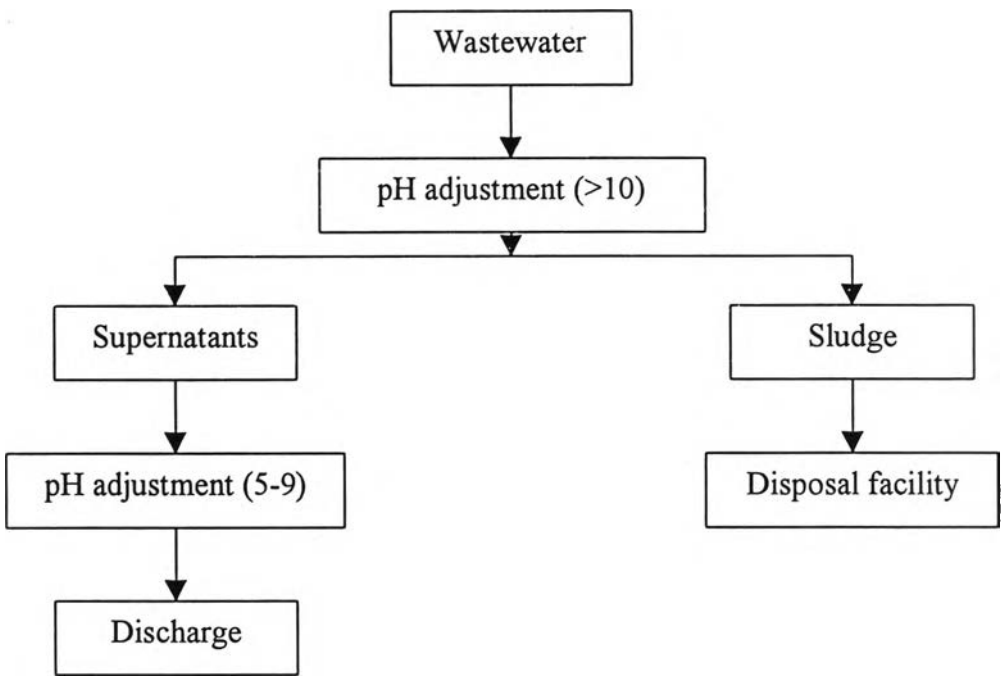

Figure 4.50 Conventional Pb Removal Process of Factory A

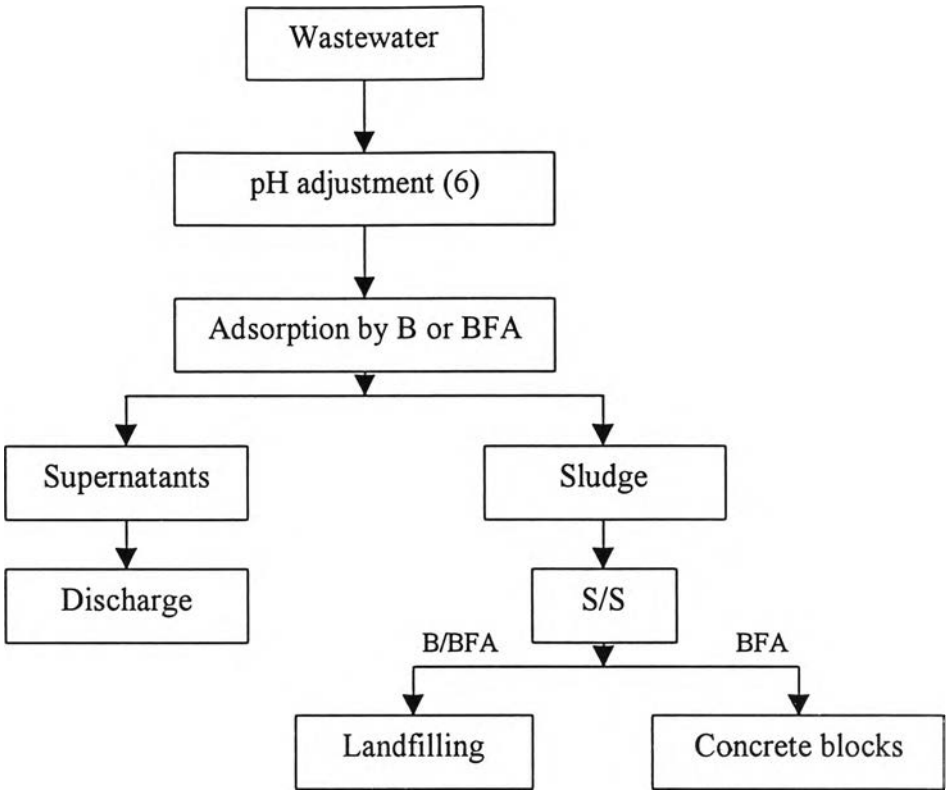

Figure 4.51 Alternative Pb Removal Process of Factory A

4.6.5.1 Cost Analysis of Conventional Pb removal Process

4.6.5.1.1 Cost of pH adjustment from 2 to 10

From the laboratory experiments, it was found that 2.0 mL of 6N NaOH was used to raise the pH from 2 to 10 for 100 mL of wastewater. The price of 50% NaOH was 8 Baht/kg (equivalent to 16 Baht/kg for 100% NaOH). The cost of chemical reagent can be calculated as follows.

$$\text{Amount of NaOH} = \frac{6\ \text{mol}}{1\ \text{L}} \times 2.0\ \text{mL} \times \frac{1\ \text{L}}{1000\ \text{mL}} \times \frac{40\ \text{g}}{1\ \text{mol}}$$

$$= 0.48\ \text{g equivalent/100 mL wastewater}$$

$$= \quad 0.48 \text{ g/100 mL wastewater}$$

$$= \quad 4{,}800 \text{ g equivalent/m}^3 \text{ wastewater}$$

$$\text{Cost (Baht/m}^3) = \quad \frac{16 \text{ Baht}}{1 \text{ kg}} \times \frac{4800 \text{ g}}{1 \text{ m}^3} \times \frac{1 \text{ kg}}{1000 \text{ g}}$$

$$= \quad 76.80 \text{ Baht/m}^3$$

The cost of pH adjustment of 1 m^3 wastewater from pH 2 to pH 10 by 50% NaOH was 76.80 Baht.

4.6.5.1.2 Cost of pH adjustment from 10 to 6

From laboratory test, it was found that 2.0 mL of 0.1N H_2SO_4 and 0.23 mL of 6N H_2SO_4 were used to adjust the pH from 10 to 6 for 100 mL wastewater. The price of 80% H_2SO_4 was 6.70 Baht/kg (equivalent to 8.40 Baht/kg of 100% H_2SO_4). The cost of chemical reagent can be calculated as follows.

$$\text{mol of 0.1N } H_2SO_4 \text{ 2.0 mL} = \frac{0.05 \text{ mol}}{1 \text{ L}} \times 2.0 \text{ mL} \times \frac{1 \text{ L}}{1000 \text{ mL}}$$

$$= \quad 0.0001 \text{ mol}$$

$$\text{mol of 6N } H_2SO_4 \text{ 0.23 mL} = \frac{3 \text{ mol}}{1 \text{ L}} \times 0.23 \text{ mL} \times \frac{1 \text{ L}}{1000 \text{ mL}}$$

$$= \quad 0.00069 \text{ mol}$$

$$\text{Total mol of } H_2SO_4 = \quad 0.00079 \text{ mol}$$

$$\text{Weight of } H_2SO_4 = \quad 0.00079 \text{ mol} \times \frac{98 \text{ g}}{1 \text{ mol}}$$

$$= \quad 0.0774 \text{ g equivalent/100 mL wastewater}$$

$$= \quad 774 \text{ g equivalent/m}^3 \text{ wastewater}$$

$$\text{Cost (Baht/m}^3) = \quad \frac{8.4 \text{ Baht}}{1 \text{ kg}} \times \frac{774 \text{ g}}{1 \text{ m}^3} \times \frac{1 \text{ kg}}{1000 \text{ g}}$$

$$= \quad 6.50 \text{ Baht/m}^3$$

The cost of pH adjustment of 1 m^3 wastewater from pH 10 to pH 6 by 80% H_2SO_4 was 6.50 Baht.

4.6.5.1.3 Cost of sludge disposal

$$Pb^{2+} + 2OH^- \leftrightarrow Pb(OH)_{2(s)}$$

From the equation mentioned above, 1 mol of Pb(II) would generate 1 mol of sludge ($Pb(OH)_2$). Then, initial concentration of Pb(II) of 30 mg/L (0.145 mmol/L) would generate 0.145 mmol/L of sludge. Sludge 0.145 mmol/L was equal to 35 mg/L or 0.035 kg/m^3. It was assumed that the sludge contained 10% solid content; therefore, amount of total sludge was equal to 0.35 kg/m^3. Cost of sludge disposal by a Treatment Storage and Disposal facility (General Environmental Conservation Public Company Limited, GENCO) was 30,000 Baht/ton or 30 Baht/kg. Then the cost for disposal of this sludge was equal to 10.5 Baht/m^3. Total cost for removal of Pb in the wastewater and disposal of the sludge was approximately 94 Baht/m^3 as shown in Table 4.33.

Table 4.33 Cost of Conventional Pb removal Process of Factory A

Step	Detail	Cost (Baht/m^3)
pH adjustment	From 2 to 10	76.80
pH adjustment	From 10 to 6	6.50
Sludge disposal	By disposal facility	10.50
Total cost		**93.80**

4.6.5.2 Cost Analysis of Alternative Process

This research proposed an alternative lead-containing wastewater treatment process that uses wastes from sugar factory as an adsorbent. Management of the spent adsorbents can be done in four ways; namely; mixing spent bagasse with cement for landfill disposal, mixing spent bagasse fly ash with cement for landfill disposal, producing Hollow block using spent bagasse fly ash, and producing Paving blocks using spent bagasse fly ash. Final concentration of Pb was less than 0.2 mg/L, using bagasse and bagasse fly ash were 30 and 20 kg/m^3, respectively. Operational costs of each alternative were shown in Table 4.34. It can be seen that, when the materials were used as adsorbent, solidified and stabilized, and disposed of in landfill, total cost of waste treatment were 1567 and 152 Baht/m^3 for bagasse and bagasse fly ash, respectively. However, if use bagasse fly ash was to be used as adsorbent and consequently used to produce Hollow block and Paving block, total cost of waste treatment were significantly lower at 17 and 16 Baht/m^3, respectively.

Table 4.34 Cost of Alternative Pb removal Process of Factory A

Process	Detail	Cost (Baht/m^3)
B / Landfilling	pH adjustment from 2 to 6	57.60
	acid treatment (0.01161 Baht/g of bagasse)	348.30
	cost of cement (18.36 Baht/kg)	550.80
	Total cost	**956.70**
BFA / Landfilling	pH adjustment from 2 to 6	57.60
	cost of cement (4.7 Baht/kg)	94
	Total cost	**151.60**
BFA / Hollow block	pH adjustment from 2 to 6	57.60
	save cost of cement for 35 unit, 30% replacement (0.56 kg/unit, 1.15 Baht/unit)	(-) 40.25
	Total cost	**17.35**
BFA / Paving block	pH adjustment from 2 to 6	57.60
	save cost of cement for 77 unit, 30% replacement (0.26 kg/unit, 0.54 Baht/unit)	(-) 41.58
	Total cost	**16.02**

4.6.5.3 Comparison of Costs between Conventional and Alternative Process

From Tables 4.33 and 4.34, it indicated that the cost of utilization of bagasse fly ash as adsorbent and the subsequent use of the spent material in Hollow block or Paving block was significantly lower than that of the conventional process. In addition, the simple process does not require rigorous control. There is no toxic or flammable chemical involved in the process as compared to other adsorbents. Challenge and sustainable development should be occurrence, if treat waste by using other waste. However, the cost analysis on the alternative process excludes investment cost and labor cost.

4.6.6 Case Study 2: Cost Analysis of Sugar Factory Waste from Factory AA

The amounts of waste from sugar factory AA including lead acetate from Pol measurement, bagasse fly ash, and wastewater from evaporator, amount of these wastes were shown in Table 4.35. (Pol is the apparent sucrose content of any substance expressed as a percentage by mass and determined by the single or direct polarization method). This section shows analysis of treatment cost between conventional process (Figure 4.52) and alternative process (Figure 4.53). For Factory AA, bagasse was not as waste, all of it was used as fuel in plant boilers. Other sugar factories may sell bagasse to paper producing factory at 200-300 Baht/ton. Most sugar factories in Thailand burn all bagasse as fuel in boiler to produce stream and electricity, as previously mentioned.

Table 4.35 Information on Sugar Factory AA

Parameter	Amount	Unit
Sugar production rate	60,000-100,000	Ton/year
Sugarcane input	600,000-1,000,000	Ton/year
Bagasse	150,000-250,000	Ton/year
Bagasse fly ash	15,000-25,000	Ton/year
Wastewater from evaporator cleaning	6,000	m^3/year
Lead acetate from sweet test	3,000	kg/year

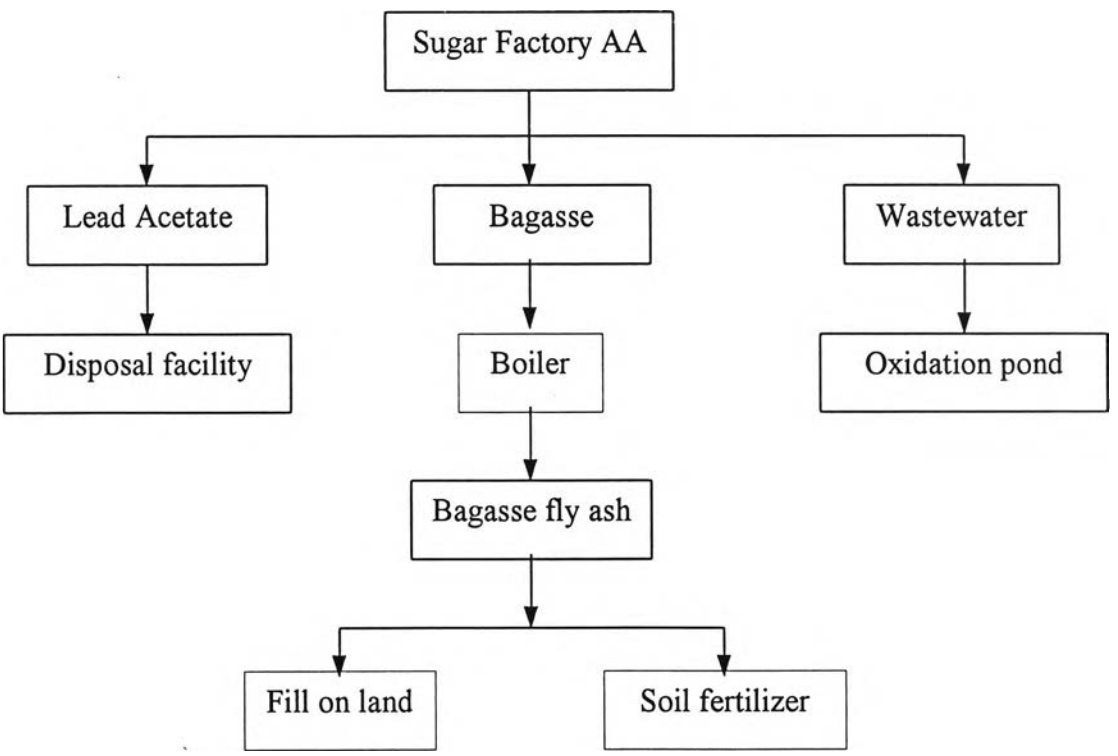

Figure 4.52 Conventional Waste Management Process of Sugar Factory AA

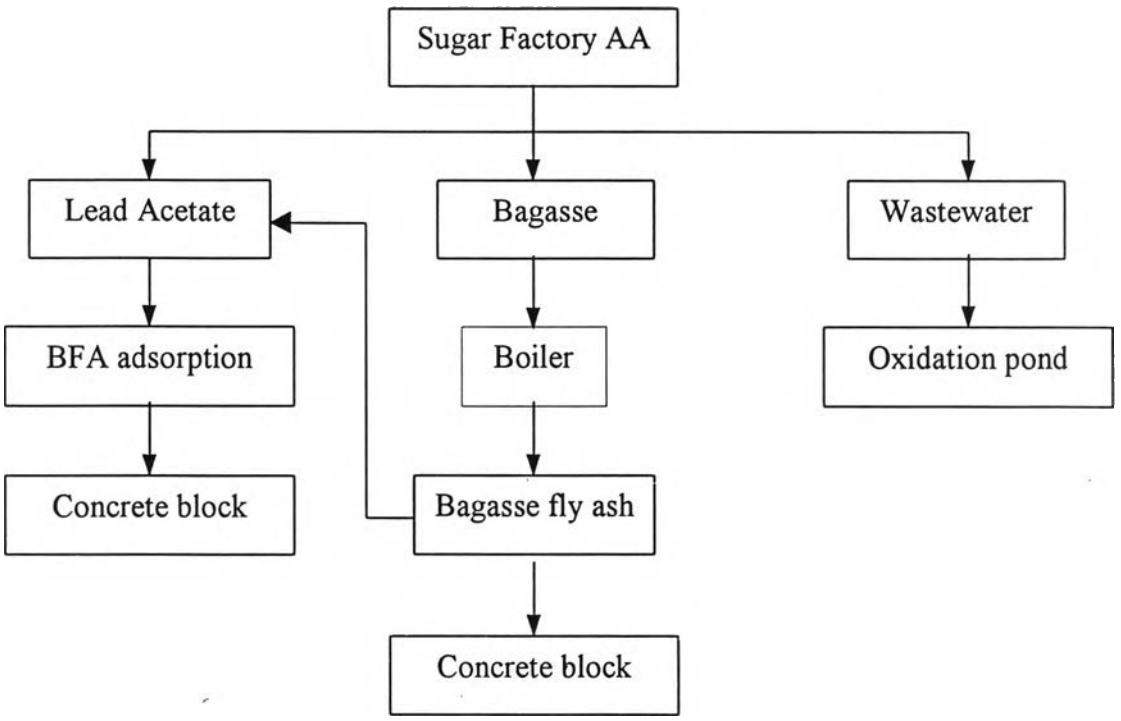

Figure 4.53 Alternative Waste Management Process of Sugar Factory AA

4.6.6.1 Cost Analysis of Conventional Waste Removal Process

As mentioned above, the waste from sugar Factory AA included lead acetate from Pol test, bagasse fly ash, and wastewater from evaporator. Factory AA did not need to pay for treatments of wastewater from evaporator because evaporation caused by the sun was enough to keep amount of wastewater minimal. Evaporator was cleaned 2 times a year and wastewater did not contain heavy metals. Therefore, Factory AA paid for 3 activities; namely, disposal of lead acetate from Pol test, transfer of bagasse fly ash to be landfilled which created dust problem, and transfer of bagasse fly ash to plantation for use as soil conditioner. These costs were shown in Table 4.36.

Table 4.36 Cost of Conventional Waste Management Process of Sugar Factory AA

Step	Detail	Cost (Baht/year)
Lead acetate	Disposal facility	33,250
Landfilling of BFA	Transportation cost	1,000
	Car maintaining cost	2,500
Soil conditioner of BFA	Transportation cost	1,000
	Car maintaining cost	2,500
Total cost		**40,250**

4.6.6.2 Cost Analysis of Alternative Waste Removal Process

The alternative process, bagasse fly ash was used as adsorbent for lead acetate and used the spent material as concrete blocks which partial cement replacement up to 30%. In addition, residual bagasse fly ash was not transfer to fill on earth or plantation; they were used as concrete blocks. Therefore, Factory AA will not pay 40,250 Baht/year.

From Table 4.35, amount of bagasse fly ash approximately 20,000 Ton/year or 20,000,000 kg/year. Utilization of Pb-BFA as 15% replacement for Hollow block and Paving block would produce about 71,428,571 and 153,846,153 units a year, respectively (0.28 and 0.13 kg BFA/unit of Hollow block and Paving block, respectively). This could save the cost of cement 41,428,571 and 36,923,076 Baht/year for Hollow block and Paving block, respectively (cost saving of 0.58 and 0.24 Baht/unit for Hollow block and Paving block, respectively). However, the investment cost and labor cost were not addressed in the calculations.